

# ON THE ORIGIN OF HIPPOCAMPAL ENSEMBLE ACTIVITY

*Neural Mechanisms for Sharp-Wave Ripples and Place Cell Responses*

by  
Heydar Davoudi

A dissertation submitted to Johns Hopkins University in conformity with the  
requirements for the degree of Doctor of Philosophy

Baltimore, Maryland  
March, 2017

© 2017 Heydar Davoudi  
All Rights Reserved

## **Abstract**

Our cognition is heavily dependent on our ability to form memories out of our experiences. The hippocampus is necessary for the formation of new memories and their retrieval for planning our future behavior. Hippocampal area CA1 local field potential (LFP) exhibits high frequency (100- 250 Hz) events known as sharp-wave ripples (SWRs). These events that occur during slow-wave sleep and awake restfulness have been shown to be important for the consolidation of spatial memory. During exploration, CA1 pyramidal cells, which receive excitatory inputs from entorhinal cortex (EC) and hippocampal area CA3, show location-specific activity known as place fields. However, the mechanism of formation of SWRs and place fields in the presence of these two inputs is not yet well understood. Using high-density multi-tetrode recording and reversible optogenetic manipulation, I found that the silencing of hippocampal area CA3's Schaffer collateral (SC) projections to CA1 decimates SWRs. Furthermore, SC silencing substantially suppresses hippocampal place cell activity during exploration but does not change the position of place fields. Moreover, temporal coding in CA1 place cells, as reflected in their theta phase precession ability, remains intact without CA3 input. These findings shed light on the functional

interconnections between hippocampal subregions that support episodic memory.

Hippocampal structure and function is disrupted in several psychiatric disorders such as schizophrenia. The calcineurin mouse model of schizophrenia whose synaptic activity is impaired by deleting the calcineurin phosphatase gene in its forebrain shows behavioral and cognitive abnormalities recapitulating symptoms of schizophrenia and is therefore a good candidate for examining hippocampal neural circuit dysfunctions. Using multi-tetrode recording, we found that CA1 SWRs in these mice become overabundant and the reactivation of place cells during SWRs is abolished. However, place cells preserve their normal activity during exploration. This selective disruption in SWRs provides a mechanism for underlying impairments in information processing that may contribute to the cognitive impairments in schizophrenia. Overall, the research and technical advances described in this dissertation represent a step towards understanding hippocampal neural ensemble activity as is reflected in SWRs and place cell responses.

**Thesis Committee:**

David J. Foster, Ph.D. (Department of Neuroscience, advisor, first reader)

James J. Knierim, Ph.D. (Department of Neuroscience, committee chair, second reader)

Marshall G. Hussain Shuler, Ph.D. (Department of Neuroscience)

Ke Chen Zhang, Ph.D. (Department of Biomedical Engineering)

To four women who show me the beauty of life:

Zeinab, my wife,

Aghdas, my mother,

Parisa, my sister, and

Kimia, my niece.

## **Acknowledgements**

I am very grateful of Allah, Prophet Muhammad, and the Twelve Imams from his Household who without their support accomplishing this life milestone was not possible for me. I am also thankful of all people who influenced me in the pursuit of knowledge, especially in the fascinating field of neuroscience. I thank my friend and advisor, Dr. David Foster, who besides providing a creative research environment taught me how to think critically and gradually develop an independent perspective in our field. His hope and patience grew a confidence within me to have perseverance in confrontation with unexpected challenges of a research project. I also thank my thesis committee, Dr. James Knierim, Dr. Marshall Hussain Shuler, and Dr. Kechen Zhang, for their insightful and constructive feedbacks which kept me on track.

Also, I am grateful of the rest of the Foster lab whom I have a vivid memory about happy times I spent with each of them. They taught me how to do animal experiments, a pivotal phase in my transition from engineering to science. In particular, I thank my friend and labmate Dr. Matthew Kleinman for editing this dissertation. I also thank Biomedical Engineering and Neuroscience graduate program coordinators, Hong Lan, Rita Ragan, and Beth Wood-Roig who strive to

make student life a delightful experience. I also thank my fantastic instructors, classmates, and friends at Johns Hopkins.

Last but not least, I am appreciative of my parents, Mohammad and Aghdas, who the sight of hope and trust in their eyes have been transforming my life. I am thankful of my wife, Zeinab, whose unconditional love, wholehearted help and positive attitude actualized my graduation. And finally, I thank my sister and three brothers, my brother and sister in law, and my niece and nephews for their emotional support.

## Table of Contents

Chapter 1: Introduction .....	1
The hippocampus and episodic memory .....	5
The hippocampal circuitry .....	9
The hippocampus and psychiatric disorders .....	14
Place cells .....	18
Sharp-wave ripples .....	27
Unanswered questions .....	34
Chapter 2 : General Methods.....	41
Animal Training .....	41
Optogenetic setup .....	42
LFP and cellular unit recording .....	49
Task Design.....	52
Analysis .....	53
Chapter 3 : The role of CA3 in neural ensemble activity in CA1 .....	61
Introduction.....	61
CA3 input is necessary for SWRs in CA1 during sleep .....	68
CA3 input is necessary for awake SWRs in CA1 during explorative behavior .....	78
CA3 input is necessary for normal place cell responses.....	83
SC silencing increases theta power and place cell theta locking.....	95



Discussion.....	104
Chapter 4 : Impaired hippocampal ensemble activity in a mouse model of schizophrenia.....	113
Introduction.....	114
Experimental Procedures .....	118
Results .....	125
Overabundance of SWR in calcineurin KO mice.....	125
Normal place fields in calcineurin KO during exploratory behavior.....	129
Overactivity of place cells in calcineurin KO during SWRs .....	132
Abolished spatial information content of reactivation events in calcineurin KO .....	135
Discussion.....	140
Chapter 5 : General Discussion .....	146
Implications.....	152
Future work.....	155
References .....	161

## List of Figures

Figure 2.1: Schematic of research design. ....	42
Figure 2.2: eNpHR3.0 expression in CA3.....	43
Figure 2.3: Injection sites in dorsal and intermediate CA3.....	45
Figure 2.4: eArch3.0 is expressed in CA3 but not CA1 pyramidal cells. ....	47
Figure 2.5: The designed optetrode outperforms existing designs. ....	49
Figure 2.6: Experimental design and stimulation paradigm. ....	51
Figure 2.7: SWR detection algorithm. ....	53
Figure 3.1: Strategy for control of CA3 input to CA1 during recording of CA1 activity. ....	69
Figure 3.2: CA3 input is necessary for SWRs in CA1. ....	73
Figure 3.3 Effect of light on rest-state CA1 activity in individual rats.....	74
Figure 3.4: SWR modulation correlates with the tetrodes distance to optical fiber .....	75
Figure 3.5: Effect of light on SWR characteristics.....	77

Figure 3.6: CA3 input is necessary for awake SWRs in CA1 in exploratory behavior.....	81
Figure 3.7: SC silencing effect on CA1 activities of individual explorative rats .....	82
Figure 3.8: Subtle abnormalities in awake SWRs .....	83
Figure 3.9: SC silencing suppresses place fields in CA1. ....	85
Figure 3.10: Place cell firing in CON and EXP rats. ....	86
Figure 3.11: Examples of CON place fields .....	87
Figure 3.12: Examples of suppressed EXP place fields.....	88
Figure 3.13: Examples of emerged and enhanced EXP place fields .....	89
Figure 3.14: SC silencing suppresses CA1 place cell activity. ....	92
Figure 3.15: Cumulative density analysis depicts remapping-like effects in CA1 place fields.....	93
Figure 3.16: Place fields undergo subtractive suppression and resemble rate remapping.....	94

Figure 3.17: SC silencing increases theta power during explorative behavior	95
Figure 3.18: Examples of place cell theta locking .....	98
Figure 3.19: SC silencing increases place cell theta locking and diminishes population phase preference. ....	100
Figure 3.20: Examples of place cell theta phase precession .....	103
Figure 3.21: SC silencing does not affect phase precession slope .....	104
Figure 3.22: A possible model explaining E/I imbalance. ....	107
Figure 4.1: Increased hippocampal ripple activity in calcineurin KO mice during awake resting periods. ....	127
Figure 4.2: Cluster robustness is preserved in KO. ....	128
Figure 4.3: Similar basic properties of place cells in CT and KO mice in run periods. ....	130
Figure 4.4: Increased spike activity of place cells in calcineurin KO mice during ripple events. ....	134

Figure 4.5: Impaired reactivation of spatial experience on the linear track during awake resting periods on the linear track in calcineurin KO mice..... 138

# Chapter 1: Introduction

In our daily life, to take our best decisions and actions we need to recruit many essential cognitive processes. Recalling memory of our past experiences is one such crucial cognitive process to achieve these goals. The scientific community has uncovered several distinct memory systems, including declarative memory, which is memory of events and facts which can be explicitly recalled, and non-declarative memory, which is memory of skills, e.g. how to ride a bike, an classical and operant conditioning which are not explainable in words (Schacter, 1996). A particular type of declarative memory is called episodic memory, which is the memory of specific events which are vividly recalled as a personal experience rather than as a learned fact, like where a person parked his car (Tulving, 1972). It is a mental imagery which may contain temporal and spatial components. Study into the neural basis of episodic memory was sparked several decades ago, when neurosurgeons discovered that lesions in the medial temporal lobe (MTL) meant to alleviate severe epilepsy had the side effect of amnesia, later defined as a dramatic impairment in episodic memory (Scoville and Milner, 1957). In a separate line of work, neurologists and psychiatrists also found that the MTL is one of the severely damaged brain

regions in patients of Alzheimer's disease and to a lesser degree schizophrenia, two disorders with known memory impairments (Bäckman et al., 2004; Paul and Harrison, 2004). These findings, and others, have implicated the MTL in the neural basis of episodic memory, and sparked interest in understanding how this circuitry is disrupted in psychiatric disorders.

The MTL is the home for a deep seahorse-shaped brain structure called the hippocampus. Psychologists had theorized that the brain builds a "cognitive map" of the spatial environment (Tolman, 1948), and the hippocampus became a candidate structure for this cognitive map. Because the hippocampus is highly conserved across species and detailed in vivo study of it necessitates invasive experimental techniques, researchers turned to rodents as a model system. However, how this cognitive map was represented by neurons in the hippocampus was still not known.

Clues about the neural basis of a cognitive map were discovered when researchers probed the hippocampus while rodents explored spatial environments (O'Keefe and Nadel, 1978). In vivo extracellular recording from hippocampal neurons found that each cell only gets activated when the animal is in a particular location in the environment, dubbed a neuron's place field, as if

each neuron was encoding one particular spatial position. Because each cell with a place field, called a place cell, could represent any position in the environment, together as a population place cells in the hippocampus encode the entire spatial environment. Indeed, later work found that lesions of the hippocampus in rodents caused selective impairments in memory-guided spatial navigation tasks (Morris et al., 1982). These surprising discoveries provided some evidence for the existence of a neural substrate for a cognitive map.

Besides this place-related activity during active locomotion through an environment, when rodents groom, are quietly resting, or asleep, the extracellular hippocampal electrophysiological activity shows unique high-frequency events known as sharp-wave ripples (SWRs) (Buzsáki, 2015). Pharmacological or electrophysiological suppression of SWRs results in impairments in memory-guided navigation tasks (Girardeau and Zugaro, 2011). To find the link between the sequential activation of place cells when animals actively run and SWR burst activity during rest, the activity of place cells during SWR events was examined more closely. Researchers found that simultaneously with SWRs, ensembles of place cells were sequentially reactivated in the same order as during running through positions (Foster and Knierim, 2012). This reactivation was proposed to be a mechanism for consolidation of the recent



experience and a contributing factor to future decision making. Together, these signature hippocampal activities during run and rest may be a neural substrate for the cognitive map and the formation of episodic memories.

However, the neural mechanisms for expression of place cell responses and generation of these information-rich SWRs are not yet well understood.

Spatially-modulated responses in hippocampus are hypothesized to arise from the extrahippocampal flow of spatial information to the structure, with place cell responses during locomotion in hippocampal output area CA1 are hypothesized to be generated by inputs from the extrahippocampal medial entorhinal cortex (MEC) input (Brun et al., 2002). Meanwhile, SWRs, observed across the extent of the hippocampus, are thought to be generated within the hippocampus, likely generated in the highly recurrent neural network of intermediate hippocampal area CA3 and then propagated to hippocampal area CA1 (Buzsáki, 1984, 2015). However, previous work using lesioning and genetic methods has found that suppressing EC input to CA1 did not eliminate place cell response in CA1 and, on the other hand, removing CA3 inputs to CA1 did not greatly suppress the incidence of SWRs (Brun et al., 2002; Nakashiba et al., 2009). One explanation for these unexpected results may be the chronic nature of these lesioning and genetic

techniques, which can provide a long time frame for compensatory neural mechanisms to recover the function.

In my doctoral research, I used optogenetics, an acute silencing technique with a higher temporal resolution, to explore the effect of suppressing CA3 inputs to CA1 on the formation of SWRs and expression of place cell responses. I also investigated whether SWRs and place cell responses can be considered cognitive biomarkers for psychiatric diseases, using a rodent model of schizophrenia. In the rest of this chapter, the background for the problems will be presented in further detail. In Chapter 2, in addition to general methodology, I describe the method development I did for simultaneous axon silencing and cell body recording in the hippocampus. Chapter 3 describes the findings on the mechanisms of SWR generation and place cell responses. Chapter 4 shows the extent of disruption in SWRs and place cell responses in an animal model of schizophrenia. Chapter 5 concludes this dissertation with a general summary, implications, and potential future work.

## **The hippocampus and episodic memory**

Early hints that the hippocampus is critical for episodic memory were discovered as an unexpected memory deficit side effect presented following neurosurgical intervention for severe epilepsy. On September 1st, 1953, an

epilepsy patient named Henry Molaison, later known as patient H.M. (1926–2008), underwent a bilateral medial temporal lobectomy that removed significant parts of both MTLs, including hippocampus, parahippocampal cortices, and EC, with the hope of alleviating his seizures. This resection rendered his entire anterior hippocampus and EC non-functional. Although his seizures abated, H.M. developed severe anterograde amnesia and mild retrograde amnesia. He was unable to form new memories of events or to remember some life events that had happened only a few years before the surgery (Scoville and Milner, 1957; Hasselmo, 2012). For example, he was able to meet and have conversations with someone he had not met before, but did not recognize or remember the earlier meeting if he met the same person even just a few minutes later. However, H.M. was able to learn new motor skills, without remembering his past practice sessions, and to recognize words he had seen previously as more familiar than words he had not seen (Corkin, 2002). This early work with H.M. spurred decades of subsequent research and helped transform the field of cognitive neuropsychology and the neuroscience of memory (Squire and Zola-Morgan, 2011).

Human memory is often divided into short-term, at the scale of seconds to minutes and largely spared in H.M., and long-term, which can be retrieved during the entire lifespan of an individual but was unable to be formed by H.M.

after his surgery (Squire and Zola-Morgan, 2011). Long-term memory may be further divided into implicit, or non-declarative, and explicit, or declarative. Procedural memory, one form of implicit memory, is the unconscious development of motor skills, such as how to ride a bicycle. This memory was intact in patient H.M., suggesting evidence for its independence from the MTL.

The selective deficit in explicit memory following MTL removal led to more sophisticated examination of this distinct memory system (Hasselmo, 2012). Psychologist Endel Tulving categorized distinct components of explicit memory into the knowledge of facts (semantic memory) and the memory of past experiences and autobiographical events occurred in specific times and places (episodic memory, Tulving, 1972). He further speculated episodic memory as a mental trace through an already-shaped mental framework of the external world (Tulving, 1972). The case of patient H.M. and later patients showed that episodic memory is MTL-dependent. The hippocampus was hypothesized to be responsible for formation of new long-term memories and these memories will gradually be transferred from hippocampus and stored in cortical areas such as prefrontal cortex for later memory retrievals, a process called memory consolidation (Marr, 1971). Therefore, while memory formation is MTL-dependent memory retrieval is independent of hippocampus, only after

consolidation period. Cognitive psychologist Edward Tolman called the spatial representation of the surrounding environment in humans and rodents a “cognitive map” (Tolman, 1948). Researchers thus hypothesized that the deficits seen in episodic memory following lesions to the MTL may have resulted from an obliteration of the cognitive map, as the foundation upon which episodic content was built had been removed (O’Keefe and Nadel, 1978).

In addition to formation of episodic memories, the hippocampus has also been shown to be crucial for the prediction and imagination of future events (Buckner, 2010). Episodic memory and imagining new events share common psychological processes, such as visualization of an event within a rich spatial context, retrieval of multisensory information, and a narrative structure with a sense of presence (Schacter, 1996; Rubin et al., 2003). Patients with hippocampal damage show impairments not only in episodic memories but also when imagining new experiences (Hassabis et al., 2007). The patients’ imagined experiences particularly lacked a coherent spatial setting and were instead composed of only a few fragmented images. Therefore, the hippocampus is essential for envisioning both past and future experiences.

Functional magnetic resonance imaging (fMRI) studies have demonstrated that there is a “default-mode network” (DMN), comprised brain regions such as the hippocampus and prefrontal cortex, that is activated when individuals are in an awake rest state but not focusing on any specific, demanding task (Buckner, 2013). The DMN, which is essential for successful episodic memory retrieval and imagination, is hyperactive in individuals with schizophrenia, autism-spectrum disorders, and Alzheimer disease (Buckner et al., 2008; Rugg and Vilberg, 2012). The mechanisms for simultaneous DMN network activity, especially at neural ensemble level, are not well understood. Therefore, examining hippocampal ensemble activity may shed light on the mechanisms and functions of this rest-state brain activity.

### **The hippocampal circuitry**

The hippocampal formation is a deep structure receiving inputs from entorhinal cortex (EC) and subcortical structures (Andersen et al., 2009). Its output projections target numerous regions, including the parahippocampal gyrus, consisting of EC and perirhinal cortex, and areas in prefrontal cortex (Strange et al., 2014). Distinct inputs, outputs, and interconnections of excitatory pyramidal neurons and a wide variety of inhibitory interneurons form a versatile information processing circuit in the hippocampus, as well as maintain the

balance between excitation and inhibition that can generate stable state-dependent oscillations.

Neuromodulators also play crucial role in hippocampal circuitry. Hippocampus receives a variety of neuromodulatory inputs, such as cholinergic, dopaminergic, and serotonergic, from subcortical structures that influence hippocampal activity in a state-dependent manner (Hasselmo, 1999; Thomas, 2015; Wang et al., 2015). For example, lesioning medial septum, the source of cholinergic projections to hippocampus, impairs spatial memory as well as theta (5-10 Hz) rhythm in hippocampus and EC during run (Lee et al., 1994; Brandon et al., 2014). However, the selective contributions of neuromodulatory inputs to the EC-hippocampus system requires further investigations.

Behavioral studies in rodents following lesions to hippocampus, especially using tasks that rely on spatial memory, shed light on the function of this brain region. Lesions to dorsal hippocampus result in impairments in both spatial reference memory, the ability to learn a constant association between a fixed spatial location and a reward outcome, and spatial working memory, the ability to maintain trial-specific spatial information for a limited time, while lesions in ventral hippocampus do not cause a significant impairment (Morris et al., 1982;

Moser et al., 1993; Pothuizen et al., 2004). This and similar work suggests dorsal hippocampus is crucial for spatial learning and memory, while other work has implicated ventral hippocampus in affective processes such as fear conditioning (Cenquizca and Swanson, 2007). Similarly, lesions of EC, a prominent input to the hippocampal formation, causes distinct spatial and non-spatial deficits depending on the site of injury: lesions of MEC impair spatial memory, while lesions of lateral entorhinal cortex (LEC) affect non-spatial learning such as object recognition (Van Cauter et al., 2013). In other words, MEC and LEC provide the spatial “context” and “content” of an experience to the hippocampus, respectively (Knierim et al., 2013; Knierim and Neunuebel, 2016). These findings implicated dorsal hippocampus and EC together as the crucial substrate for spatial information processing. This resulted in further research on these two regions, the interactions between them, and the contribution of modulatory inputs to them. The neural substrate of these components of memory system at single cell level will be discussed in the section “Place cells” of this chapter.

To better understand the functional organization of the dorsal hippocampus, a detailed knowledge of its subregions and their inputs and outputs is required. The hippocampus is composed of the dentate gyrus (DG) and areas CA3, CA2, and CA1 (Andersen et al., 2009). EC communicates with all of these hippocampal



subregions through the projections of the perforant path. EC layer II neurons send axons to DG, CA3 and CA2, while EC layer III projects specifically to CA1 via the temporoammonic branch of the perforant path (TA). Lesions of the TA have demonstrated that direct EC input to CA1 is necessary for consolidation of memory in rats (Remondes and Schuman, 2004).

The first stage of the EC-hippocampal information processing occurs in DG. Excitatory neurons there, known as granule cells, show divergent responses in partially-similar environments to potentially establish non-overlapping sets of neural ensembles in downstream area CA3, a phenomenon known as spatial pattern separation and crucial for episodic memory (Marr, 1971; Leutgeb et al., 2007; Knierim and Neunuebel, 2016) . Granule cells send their axons, known as mossy fibers, to CA3.

CA3 is a highly recurrent circuit composed of subregions CA3c (adjacent to DG), CA3b, and CA3a (adjacent to CA2). Due to their dense recurrent axon collaterals CA3 neurons are then able to strengthen synapses between each other, in a way that triggering a subset of neurons activates an already-established pattern in CA3 neural ensembles. This makes CA3 essential for accomplishing spatial memory tasks in the presence of partial environmental cues, a function

known as spatial pattern completion (Gold and Kesner, 2005; Leutgeb and Leutgeb, 2007; Knierim and Neunuebel, 2016). The dense recurrent axons in CA3 and direct inputs from EC layer II and mossy fibers may result in complex cellular dynamics in this hippocampal region. CA3 sends this information to CA1 through its Schaffer collaterals (SCs), completing a trisynaptic connection between EC and CA1. CA2 is a small area interposed between CA3 and CA1 that receives input from MEC and LEC and is important for memory of social interactions and priming of specific neural activity in CA3 and CA1 (Jones and Mchugh, 2011; Hitti and Siegelbaum, 2014; Oliva et al., 2016).

CA1, the principal output of the hippocampal formation, processes converging inputs from EC via the TA, CA3 via the SCs, and CA2 and then sends the output to cortical areas such as EC, subiculum, and prefrontal cortex. CA1 circuitry is under the combined influence of extrahippocampal sensory-driven cortical TA input and intrahippocampally-generated SC input. The firing patterns of both inputs are able to induce post-synaptic modifications in CA1 pyramidal cells, a phenomenon known as synaptic plasticity (Malenka and Bear, 2004; Bannerman et al., 2014) . Synaptic plasticity, found in the hippocampus and other brain regions, has become the dominant theory for the neural basis of learning and memory at the synaptic level and is the persistent, bi-directional,

input-triggered change in synapse efficacy, either strengthening of synapses, known as long-term potentiation (LTP), or weakening of synapses, known as long-term depression (LTD) (Malenka and Bear, 2004; Bannerman et al., 2014). However, it is still unknown exactly how activity patterns in hippocampal circuits seen during behavior facilitate learning and memory, though induction of synaptic plasticity is a proposed mechanism (Buzsáki, 1986, 1989).

### **The hippocampus and psychiatric disorders**

Memory disorders such as amnesia and Alzheimer's disease are often characterized by heavy damage to the hippocampus (Bäckman et al., 2004). Hippocampal cell death and concomitant reduction in hippocampal volume are early brain symptoms for Alzheimer's disease, and Alzheimer's patients have problem in forming new short-term memories (Small et al., 2011). Moreover, hippocampal structure and function is also disrupted in some major psychiatric disorders such as schizophrenia (Paul and Harrison, 2004; Heckers, 2010; Barch and Ceaser, 2012). Schizophrenia is a devastating neurodevelopmental disorder affecting 1% of human society with positive symptoms (e.g. hallucinations and delusions), negative symptoms (e.g. social withdrawal and anhedonia), and cognitive symptoms (problems in attention, executive function, and working memory) (Fatemi and Folsom, 2009; Mesholam-Gately et al., 2009). Although

positive and negative symptoms are key to diagnosis of this disease and may potentially be ameliorated by antipsychotic medications, cognitive deficits also interrupt patients' daily lives and are usually resistant to treatment.

Among the symptoms of schizophrenia, cognitive deficits may be the subject of systems-level study in genetic animal models of the disease (Fernando and Robbins, 2011; Jones et al., 2011; Kvajo et al., 2012; Sigurdsson, 2016). Mouse models of schizophrenia are usually produced by deleting or duplicating a gene or a locus in mouse corresponding to genes that are found mutated in families with severe schizophrenic and schizoaffective persons (Nestler and Hyman, 2010; Fernando and Robbins, 2011; Jones et al., 2011; Sigurdsson, 2016). In addition, mutant mice with cognitive impairments in learning and memory and symptoms such as isolation and anhedonia are sometimes considered as models for schizophrenia.

Given their roles in learning and memory, hippocampus and prefrontal cortex have been intensively studied in the context of memory and cognitive deficits in mouse models of schizophrenia (Toulopoulou et al., 2003; Boyer et al., 2007; Nestor et al., 2007; Bonner-Jackson et al., 2008; Leavitt and Goldberg, 2009; Sigurdsson, 2016). For example, a mouse model of schizophrenia which has

disrupted communication between hippocampus and prefrontal cortex, show deficits in a spatial working memory task with alternating reward locations (Sigurdsson et al., 2010). However, the majority of these mouse models of schizophrenia either fail to recapitulate the cognitive deficits of schizophrenia or their genetic mutations are not clearly relevant to genetic disruption of schizophrenia patients. Moreover, dysfunctions in the neural ensemble activity of hippocampus in rodent models of schizophrenia have not been comprehensively explored (Sigurdsson, 2016).

The calcineurin mouse model of schizophrenia may be a good candidate for examining hippocampal neural circuit dysfunctions and to some extent studying symptoms of this disease (Suh et al., 2013). Calcineurin is a  $\text{Ca}^{2+}$ -sensitive protein phosphatase important for synaptic plasticity and forebrain-specific calcineurin knockout (KO) mice with deleted calcineurin in their excitatory cells show behavioral and cognitive abnormalities recapitulating symptoms of schizophrenia (Zeng et al., 2001; Miyakawa et al., 2003). In comparison to other mouse models, these mice satisfy three compelling features. First, a profile of behavioral impairments recapitulating those seen in schizophrenia patients; second, adult-onset altered synaptic activity essential for learning and memory; and third, although not the major gene, reported association of this mutated

gene with schizophrenia (Zeng et al., 2001; Gerber et al., 2003; Miyakawa et al., 2003; Gerber and Tonegawa, 2004).

Calcineurin KO mice exhibit a comprehensive array of behavioral impairments characteristic of schizophrenia patients (Goldman-Rakic, 1994; Elvevåg and Goldberg, 2000), including impairments in latent inhibition, prepulse inhibition, and social interaction (Miyakawa et al., 2003), as well as a severe deficit in working memory (Zeng et al., 2001). Furthermore, although not a major gene in schizophrenia research, the mutated calcineurin gene (*PPP3CC*) has been shown to map to chromosomal loci previously implicated in schizophrenia by genetic linkage studies (Gerber et al., 2003; Eastwood et al., 2005; Liu et al., 2007; Yamada et al., 2007; Murata et al., 2008; Wada et al., 2012, 2017). Although, this linkage to schizophrenia was challenged by some other population studies (Kinoshita et al., 2005; XI et al., 2007; Sanders et al., 2008; Kyogoku et al., 2011). Moreover, hippocampal synapses in these mice are unable to normally weaken their activity during persistent stimulations (Zeng et al., 2001). Taken together, these features suggest that the calcineurin KO provides a unique opportunity to investigate the neural basis of dysfunction in a schizophrenia model (Suh et al., 2013).

## **Place cells**

As described previously, early researchers found that CA1 pyramidal neurons display spatially-restricted firing fields, and so were called “place cells” with their spatial receptive fields known as “place fields” (O’Keefe and Dostrovsky, 1971; O’Keefe, 1976). These place cells, which later were also found in CA3 and DG, together cover a whole environment, and can therefore as a population represent any location in the local environment. Place cells do not show a topographic map, unlike, for example, retinotopic maps found in the visual system; physically adjacent cells do not have adjacent fields, which is hypothesized to potentially increase the capacity of the hippocampus to save arbitrary associations (Redish et al., 2001; Smith and Häusser, 2010). Place cells were proposed to be a neural building block of the cognitive map in the brain, robustly representing allocentric spatial relationships in an environment, as well as the animal’s own position in that environment (Moser et al., 2008). In addition to spatial information processing, hippocampal place cells were later shown to represent temporal aspects of extended experiences, another component of episodic memory (MacDonald et al., 2011).

While searching for upstream sources of spatial coding that might contribute spatial information to the hippocampal circuit, researchers found that MEC

pyramidal cells depict multiple firing fields forming a periodic triangular grid covering the whole environment, and such cells were named grid cells (Fyhn et al., 2004; Hafting et al., 2005). Some other MEC pyramidal cells responded selectively to boundaries of explored environments, the animal's head direction in terms of compass coordinates, and speed, and such cells were termed border, head direction, and speed cells, respectively (Sargolini et al., 2006; Solstad et al., 2008; Kropff et al., 2015). Taken together as one circuit, hippocampal place cells and entorhinal grid cells may be considered as the substrate for a metric system of spatial navigation and memory (Moser et al., 2008; Buzsáki and Moser, 2013). Given their potentially central role in both navigation and episodic memory, the firing properties of these cells and mechanisms of their response formations called for further exploration.

Place cells, which represent particular positions in an environment, usually express stable place fields for many days in that same environment. However, changes in environmental cues may result in rescaling of place cell firing rate, called rate remapping, or even an abrupt change in the location of all place fields, called global remapping (Muller and Kubie, 1987; Bostock et al., 1991; Anderson and Jeffery, 2003; Leutgeb et al., 2005b, 2006). MEC grid cells show concomitant realignments only in instances when global remapping in ensemble of



hippocampal place cells occurs, and remain unchanged during manipulations that lead to rate remapping of place cells (Fyhn et al., 2007; Bush et al., 2014).

During exploration, the hippocampal local field potential (LFP), which reflects local neural ensemble activity, is dominated by a theta rhythm of 5-10 Hz (Vanderwolf, 1969). This prominent rhythm contributes to the fine temporal scale activity of place cells. While traversing its place field, a place cell fires at progressively earlier theta phases, a phenomenon known as theta phase precession (O'Keefe and Recce, 1993). Theta phase precession is stronger in CA1 than CA3 (Mizuseki et al., 2012). Furthermore, during theta oscillations, place cell activity at the ensemble level depicts temporal coordination in the form of forward sweeps through the animal's upcoming running trajectory, and which may be useful for navigational planning (Dragoi and Buzsáki, 2006; Foster and Wilson, 2007; Johnson and Redish, 2007; Foster and Knierim, 2012; Gupta et al., 2012). Although first suggested to be a consequence of phase precession in individual place cells, theta sequences show a dissociation with phase precession in a novel environment (Feng et al., 2015). They appear in rat hippocampus only after the first traversal of a novel track, while phase precession emerges from the first traversal, suggesting theta sequences may arise from a different mechanism than simple phase precession (Feng et al., 2015). The mechanisms of formation of

hippocampal theta rhythm, theta phase precession, and theta sequences require further explorations.

Higher-frequency rhythmic activity during run may also play crucial role in hippocampal information processing. Theta-dominated LFP contains slow gamma (25-55 Hz) and fast gamma (65-110 Hz) rhythms riding preferentially on different phases of theta cycles (Colgin et al., 2009; Carr et al., 2012; Bieri et al., 2014; Zheng et al., 2016). Correlational analysis shows that slow and fast gamma are synchronized with their counterpart oscillations in CA3 and MEC, respectively, indicating their possible origins (Colgin et al., 2009). Furthermore, place cells perform prospective coding mostly during slow gamma time spans and retrospective coding during fast gamma, which may be a possible interference prevention mechanism in CA1 that allows preferential weighting of signals coming from CA3 or EC in different circumstances (Bieri et al., 2014). However, the differential contributions of CA3 and EC to CA1 gamma oscillations are not yet causally shown.

Pharmacological and surgical lesions of CA3 have demonstrated that EC inputs to CA1 are sufficient to establish robust place fields and that spatial recognition tasks can be performed in the absence of CA3 input, though spatial

recall is impaired (Brun et al., 2002). These findings imply that EC has a capacity for directly transferring stable and precise positional information into CA1 place cells. This view is in accordance with DG and medial septum lesion studies that found disrupted normal activity in CA3 with unaffected CA1 place cell responses (McNaughton et al., 1989; Mizumori et al., 1989; Wang et al., 2014).

However, different studies have found contradictory effects of EC lesions on hippocampal activity (Bush et al., 2014). Following MEC lesioning, a reduction in the percentage of active place cells as well as the spatial information content and stability of their place fields was observed in a familiar environment, but nevertheless place cell responses did not get eliminated (Miller and Best, 1980). Another study demonstrated that CA1 place cell responses persist after pharmacological lesioning of MEC layer III cells, which directly project to CA1, though a subset of place fields become larger and stability of place fields during later exposure to the same environment is somewhat reduced (Brun et al., 2008). In contrast, though comprehensive lesion of the whole EC does not eliminate place cell responses, it does reduce CA1 place field size and firing and induces global remapping in place fields when animals are re-exposed to the same environment (Van Cauter et al., 2008). However, surgically removing the entire MEC does not perturb place cell responses, except their theta phase precessions

(Hales et al., 2014; Schlesiger et al., 2015). On the other hand, pharmacological silencing of MEC increases CA1 place field size and theta power, decreases in-field firing rate, and also induces substantial global remapping (Ormond and McNaughton, 2015). Moreover, LEC lesions result in slight rate remapping in hippocampal place cells (Lu et al., 2013). These contradictory findings from these studies seem to indicate that in a familiar environment, MEC, but not CA3, input is critical for completely normal expression of place fields in CA1, though none of these inputs are essential for the existence of location-specific activity in CA1 pyramidal cells.

As with CA3 lesions, genetically deleting NMDA receptors in CA3 pyramidal cells to impair hippocampal synaptic plasticity does not affect spatial reference memory or place cell responses (Nakazawa et al., 2002, 2003). However, exposing these transgenic mice to partial environmental cues to examine their pattern completion ability uncovered deficits in task performance as well as rate remapping in CA1 place cells (Nakazawa et al., 2002), suggesting plasticity is nevertheless critical for activity patterns more complex than the expression of place fields. Likewise, comprehensive genetic blockade of SCs does not change the field properties of CA1 pyramidal cells (Nakashiba et al., 2009). These mice had SCs which were not able to induce action potentials in CA1, and showed

normal spatial reference memory but deficits in contextual fear memory (Nakashiba et al., 2008, 2009). Interestingly, both CA3 NMDA deletion and SC silencing, while preserving place cell responses, reduced firing of fast-spiking interneurons by around 50% (Nakazawa et al., 2002, 2003). The proposed mechanism for preservation of CA1 place cell responses despite a loss of major CA3 input is that CA1 pyramidal cells receive less input, provide less excitation to fast-spiking interneurons within the local circuit, and produce a resulting disinhibition of pyramidal cells that compensates for the reduced CA3 to CA1 excitatory input. In a complementary study, genetic blockade of MEC layer III, the direct input to CA1, did not affect spatial reference memory, place field, or interneuron characteristics, but did impair spatial working memory (Suh et al., 2011). The genetic inactivation techniques used in these studies are chronic, requiring at least four weeks for effects to emerge. Therefore, a variety of compensatory mechanisms could potentially have developed to rescue hippocampal circuit function.

Overall, physical, pharmacological, and genetics methods depriving CA1 of input from CA3 or EC failed to abolish CA1 place cell activity. Each of these studies reports largely preserved and normal place field activity, except MEC layer III pharmacological lesions which caused somewhat larger place fields.

This is quite unexpected because CA3 and EC are the main carriers of positional information to CA1 circuitry. One possible explanation may be that all the methods used in these studies are chronic, where neural recordings are performed several weeks after inactivation. Therefore, compensatory and homeostatic mechanisms may play intricate roles in balancing CA1 circuit activity during this recovery period after intervention. Acute circuit modulation methods may rule out the effects of chronic compensatory mechanisms and reveal hippocampal ensemble dynamics in real-time.

Optogenetics is a millisecond-timescale, cell-type-specific *in vivo* method which uses light for activating or silencing neural ensembles (Boyden et al., 2005). Its temporal resolution, cell-type specificity, and ability to manipulate axonal projections makes it a leading technique for understanding neural basis of behavior in a wide range of animals (Tye and Deisseroth, 2012; Liu et al., 2015). It also has been influential in better understanding hippocampal function and circuitry (Liu et al., 2012; Ramirez et al., 2013; Song et al., 2013; Zhang et al., 2013; Stark et al., 2014, 2015; Miao et al., 2015; Rueckemann et al., 2016).

Optogenetic stimulation of retrogradely-labelled MEC pyramidal cells shows that diverse grid cells, head-direction cells, and border cells project to the

hippocampus, possibly affecting place cell responses (Zhang et al., 2013). Moreover, transient optogenetic silencing of MEC results in non-reversible global remapping in a subset of CA1 place cells, though the overall ensemble spatial information remains intact (Rueckemann et al., 2016). However, partial optogenetic inactivation of either MEC or MEC axons projecting to CA3 induces instantaneous global remapping in CA3 place cells (Miao et al., 2015). The difference in the reversibility of remapping observed in these two studies might be explained by the recording area in the hippocampus (Miao et al., 2015; Rueckemann et al., 2016). While CA1 place cells exhibit significant hysteresis in changing their firing patterns, CA3 place cells show fast remapping to changes in an environment (Leutgeb et al., 2005a). Moreover, both studies report that place cells do not change their field size when MEC input is suppressed (Miao et al., 2015; Rueckemann et al., 2016). This suggests that intrahippocampal circuitry may be responsible for refining place fields. Therefore, a complementary study to directly assess real-time influence of CA3 inputs on CA1 place cell response, by transient optogenetic silencing of SCs, may further uncover the mechanisms of hippocampal function.

## **Sharp-wave ripples**

In contrast to theta-dominated LFP during preparatory behavior, primarily explorative running, the hippocampus shows signature irregularly-occurring events during consummatory behavior, such as drinking, eating, grooming, immobility, and sleep. These high frequency (100- 250 Hz) events, which have durations around 100 milliseconds, are known as sharp-wave ripples (SWRs) and usually occur every one or two seconds when an animal is in such “off-line” brain states (Buzsáki et al., 1983; Buzsáki, 2015). SWRs are found in both CA1 and CA3 and are composed of a broad excitation response, known as sharp-wave, which leads to fast network oscillations known as a ripple.

SWRs are thought to be a vehicle for transferring hippocampus-based memory to neocortical and subcortical areas to enter long-term memory, a process known as memory consolidation (Buzsáki, 2015). They may also be crucial for route planning and decision making (Jadhav et al., 2012; Buzsáki, 2015). fMRI studies in monkeys show that during SWRs, most of neocortex and the limbic system are activated (Logothetis et al., 2012). Moreover, subcortical structures such as ventral striatum and ventral tegmental area show coordinated activity with hippocampal SWRs (Lansink et al., 2009; Gomperts et al., 2015). On the other hand, selective electrical disturbance of SWRs in awake or sleeping



rodents impairs spatial learning and memory (Girardeau et al., 2009; Ego-Stengel and Wilson, 2010; Jadhav et al., 2012). This raises interesting questions about the information content of neural ensemble spiking during SWRs, such as how exactly its disruption results in memory deficits.

Hippocampal ensemble recording from rodents running in a track showed that place cells that were sequentially active on the track are sequentially, but in a time-compressed format, reactivated during SWRs that occur while the rodent is paused on the track and also during later sleep, a phenomenon called hippocampal replay (Wilson and McNaughton, 1994; Nádasdy et al., 1999; Louie and Wilson, 2001; Lee and Wilson, 2002; Foster and Wilson, 2006; Diba and Buzsáki, 2007; Davidson et al., 2009; Karlsson and Frank, 2009; Carr et al., 2011). SWR-based replays may be the instantiation of fast mental time travel from the current time backward to a recent experience or from now to future possible actions, respectively known as reverse and forward replays (Foster and Wilson, 2006; Diba and Buzsáki, 2007). Reverse replays are sensitive to the magnitude of reward animal receives, showing their distinct role in memory consolidation, while forward replays are more crucial for goal-directed navigational planning (Pfeiffer and Foster, 2013; Ambrose et al., 2016).

The mechanisms that form novel SWR-based sequences, as well as theta sequences during run, are not well understood (Mehta et al., 2002; Lisman et al., 2005; Pfeiffer and Foster, 2015). Replays are heavily dependent on mechanisms of SWR generation and are thought to be reliant on CA3's autoassociative dynamics and slow gamma (Pfeiffer and Foster, 2015). Better understanding of the mechanism of generation of SWRs may shed further light on mechanisms for emergence of replays.

It is unclear from where CA1 SWRs are initiated. While some evidence supports CA3 as critical locus, others propose CA2 as the initiator. CA3 is the most intensive recurrent- associational system in the brain and may be the best candidate area for the formation of regenerative ensemble bursts (Traub and Wong, 1982; Wittner et al., 2007). Indeed, axons of each CA3 pyramidal cell project to one to two thirds of the septo-temporal axis of the rat hippocampus (Li et al., 1994; Wittner et al., 2007). The skewed distribution of inter-SWR intervals and lognormal distribution of SWR amplitudes suggest that generation of these ensemble bursts is a stochastic process (Sullivan et al., 2011; Mizuseki et al., 2012). SWRs may stochastically emerge from fluctuations in synchrony of coincidentally firing CA3 pyramidal cells, in the presence of neocortical inputs

such as slow oscillations and sleep spindles (Siapas and Wilson, 1998; Vladimirov et al., 2013; Schlingloff et al., 2014).

*In vitro* studies also support the role of CA3 in generation of SWRs. High frequency stimulation of SC-CA1 synapses in slices not only induces LTP, but also increases sharp wave incidence rate in CA1 (Buzsáki, 1984). Early lesion studies also support CA3 as the origin of sharp waves, since sharp waves survive and are even enhanced after neocortex removal (Jouvet et al., 1959; Buzsáki et al., 1983; Suzuki and Smith, 1988a), EC lesion (Bragin et al., 1995; Ylinen et al., 1995), and septal and fimbria-fornix lesions (Buzsáki et al., 1983). Moreover, isolated CA3 slices also generate sharp-wave-like events while isolated CA1 slices are not able to show these specific events (Colgin et al., 2004; Hofer et al., 2015). Overall, these studies propose that SWRs are a default emergent property of the CA3 collateral system in the hippocampus.

Correlational studies of *in vivo* electrophysiological activity in hippocampus suggest that synchronous CA3 pyramidal cell bursts induce depolarizing sharp waves in apical dendrites of CA3 and CA1 pyramidal cells which result in fast oscillation of locally interacting pyramidal cells and interneurons (Buzsáki et al., 1983; Buzsáki, 1986, 2015; Suzuki and Smith, 1988b; Sullivan et al., 2011; Stark et

al., 2014, 2015). However, simultaneous hippocampal ensemble recordings further clarified that most sharp wave events are generated earliest in CA2 and transferred to CA3a, CA3b, and CA3c, respectively, and from CA3c invade CA1 (Csicsvari et al., 2000; Oliva et al., 2016). This is in accordance with anatomical evidence that the extent of recurrent axons declines from distal CA3a (i.e. adjacent to CA2) to proximal CA3c (i.e. close to DG) (Ishizuka et al., 1990; Li et al., 1994; Wittner et al., 2007).

Generally, while the role of CA2 in SWR initiation is proposed to be stronger in the awake state, CA3 mostly takes the lead in triggering SWRs in sleep (Oliva et al., 2016). CA2 pyramidal cells also fire differentially to SWR, with one population of CA2 neurons ramping up before SWRs and then becoming suppressed during SWRs, while other CA2 neurons phasically increase their firing rate during SWRs (Kay et al., 2016; Oliva et al., 2016). A small subset of CA1 SWRs are directly induced by CA2 without apparent involvement of CA3 (Oliva et al., 2016). However, these findings were based on correlational analysis with delays highly dependent on sharp wave and ripple detection criteria (Oliva et al., 2016). For example, SWRs may still be initiated in CA3 but reach their peak power in CA2 sooner than CA3 itself, leading to statistical detection of the

SWR first in CA2. Taken together, these correlational studies support CA2-CA3a as initiators of SWRs.

The sharp wave propagation system in CA3 may be suppressed by changes in glutamate release, and cholinergic and cannabinoid receptors (Hasselmo, 2006; Robbe et al., 2006). For example, selective optogenetic activation of medial septum, the main source of cholinergic input to CA3, suppresses SWR incidence and increases theta power in anesthetized and freely moving mice (Vandecasteele et al., 2014). Other subcortical neuromodulators may have similar suppressive effects on SWR occurrence (Wang et al., 2015). Also, different subtypes of interneurons may play distinct roles in the initiation and persistence of SWRs (Csicsvari et al., 1999; Klausberger and Somogyi, 2008; Varga et al., 2012; Buzsáki, 2015).

However, in transgenic mice, selective genetic blockade of SCs, which serve as the synaptic output relay from CA3 to CA1, surprisingly does not change the rate of incidence of SWRs in CA1, but instead alters the quality of SWRs, reducing the peak frequency of the majority of SWRs (from ~150 Hz to ~110 Hz) as well as the pairwise reactivation of CA1 place cells during SWRs in post-experience sleep (Nakashiba et al., 2009). A follow-up study using the same

transgenic mice confirmed these findings, and further showed that the slow gamma rhythm in CA1, which was thought to be induced by CA3, remains unchanged as well (Middleton and McHugh, 2016). However, the temporal resolution of these genetic blockades was on the order of weeks and possible compensatory mechanisms may play crucial roles in the persistence of ripples. For example, some CA3 interneurons project to CA1 stratum lacunosum-moleculare (SLM) layer and inhibit excitatory MEC inputs (Buzsáki, 2015). Therefore, in addition to the intended blockade of SCs, these CA3 interneuron projections may also be suppressed in the mutant mice, resulting in a dominant effect of EC in CA1 ripple generation. Overall, these studies show that the formation of SWRs and SWR-associated replays may be more complex than the current CA3-based theory.

These genetic SC silencing studies leave open the possibility that non-hippocampal extrinsic inputs to CA1, such as MEC, in certain cases are able to induce ripples, though perhaps not necessarily sharp waves, in CA1. Indeed, although CA1 pyramidal cells are very poorly connected, CA1 ripples and sequential neural activity can be induced by direct optogenetic activation of a subset of CA1 pyramidal cells, possibly due to biophysical properties of neurons and intricate local interactions of pyramidal cells and different subtypes of

interneurons (Thomson and Radpour, 1991; Stark et al., 2014, 2015). In another study,  $\text{Ca}^{2+}$  imaging of hippocampal slices shows that, in subiculum, not only are many neurons activated after CA1 SWRs, but also a fraction of neurons fire before SWRs (Norimoto et al., 2013). This finding supports a direct role of EC layer III, or even other subiculum-projecting regions, such as prefrontal cortex, in triggering some ripples in both subiculum and CA1. However, other work has challenged this conclusion, by demonstrating SWR time-lag between CA1 and subiculum in which CA1 precedes subiculum, and failing to find EC layer III neurons firing before or during CA1 SWRs (Chrobak and Buzsáki, 1994, 1996; Mizuseki et al., 2009). Overall, it remains unknown how intrinsic CA3 input competes or cooperates with extrinsic EC input over CA1 ensemble activity.

### **Unanswered questions**

To summarize, these studies with their diverse approaches and techniques attempted to explain the contribution of extrinsic EC and intrinsic CA3 inputs in the expression of place cell responses and the generation of SWRs in CA1. Almost all place cell studies failed to find significant disruption in CA1 place fields when CA3 input is disrupted (Brun et al., 2002; Nakazawa et al., 2002, 2003, Nakashiba et al., 2008, 2009). Likewise, EC input disruption did not demolish CA1 place fields, although some cells showed larger fields, remapped

fields, or impaired theta phase precession (Brun et al., 2008; Hales et al., 2014; Miao et al., 2015; Schlesiger et al., 2015; Rueckemann et al., 2016). While these studies therefore show slightly more prominent control by entorhinal input, the fundamental question of how these CA1 place cells express robust responses in the absence of one of their major inputs remains unanswered.

The origin of SWRs remains similarly elusive. Although the majority of studies showed CA3 is essential for SWRs in CA1, others did not demonstrate a key influence from CA3. A major theory supported by correlation studies proposes that SWRs are triggered by CA2 and transferred to CA3a, CA3b, and CA3c, respectively, and from CA3c invade CA1 (Csicsvari et al., 2000; Oliva et al., 2016). In contrast, genetic silencing of SCs do not affect occurrence of SWRs (Nakashiba et al., 2009; Middleton and McHugh, 2016). However, the studies described above that have directly intervened in the hippocampal circuit have used methods which are chronic and cannot rule out compensatory and homeostatic effects. Therefore, a more temporally-specific, transient approach to manipulating hippocampal circuitry and inputs may shed light on the mechanisms of formation of SWRs.



Proceeding from this background, the work described in this dissertation addresses the following three main questions. First, what is the role of CA3 in the expression of CA1 place cell responses? Besides being highly recurrent, CA3 is the major projection to dorsal CA1, and likely carries rich positional information to CA1. While weeks of recovery post-lesion may allow place cell responses to reemerge in CA1 even while lacking CA3 input, transient optogenetic silencing will prevent such a compensatory mechanism. If CA3 is critical for relaying spatial information to generate CA1 place cell responses, transient optogenetic silencing of SCs is expected to result in substantial effects on CA1 place fields, such as loss of stability and spatial specificity. Also, hippocampal rhythms (such as theta, slow gamma, and fast gamma) during active exploration, as well as coordination of cellular activity with these rhythms, will be explored, to better understand how higher order firing properties of CA1 neurons, beyond basic spatial receptive fields, depend on CA3 input.

Second, what is the role of CA3 in the formation of CA1 SWRs? Despite contradictory findings from earlier work, I hypothesize that CA3 plays a causal role in the formation of CA1 SWRs during consummatory behaviors. I therefore expect optogenetic silencing of SCs to decimate the occurrence of SWRs, both

during sleep and awake restfulness. If SWR occurrence is not abolished, abnormalities in partially silenced SWRs will be examined.

Third, are place cell responses during run and SWRs during rest differently impaired in calcineurin mouse model of schizophrenia? Since these mice show deficits in spatial working memory and hippocampal synaptic plasticity, I hypothesize that CA1 place cells responses, SWRs, or both are disrupted. Moreover, hippocampal synapses in these mice show severely decreased LTD, while LTP is mildly enhanced (Zeng et al., 2001). Therefore, since excitatory synapses will be more effective I hypothesize that the hippocampus is more hyperactive, potentially with over-abundance of SWRs. Any impairment found in place fields or SWRs will shed light on state-dependent mechanisms for spatial learning and memory.

To address the first two questions, I devised a method for in vivo optogenetic silencing of SCs (Chapter 2). The animals were injected with a virus to bilaterally express the light-sensitive proton pump Archaelhodopsin (eArch3.0) opsin in their SCs. A novel bilateral “optetrode”, consisting of two optical fiber cannulas and up to forty tetrodes, was implanted over dorsal CA1. Either in the sleep box or during track traversals, I simultaneously recorded from CA1 neurons, CA1

LFP, and transiently and reversibly silenced SCs. In this experimental paradigm, the real-time effect of CA3 input on CA1 place cell responses and SWRs could thus be examined.

In answering the first question, I found that continuous CA3 input is necessary for the expression of place fields in CA1 pyramidal cells (Chapter 3). During silencing of SCs, the majority of place cell responses were demolished. Moreover, place cells that were partially silenced did not show global remapping. This may suggest that precise positional information on where a place cell fires comes from MEC, but the rate coding, i.e. the extent that a cell fires around that position, is dependent on CA3.

In answering the second question, I also found that SC input is essential for the formation of SWRs in CA1, both during sleep and during rest periods on the track (Chapter 3). Silencing SCs decimates SWR incidence and the associated neuronal spiking in a reversible way in both cases. This shows that CA3 has an indispensable role in the chain of causality for the formation of SWRs.

For addressing the third question, hippocampal place cell and SWR activity of calcineurin-KO mice traversing a track were examined (Chapter 4). In collaboration with the laboratory of Susumu Tonegawa at Massachusetts

Institute of Technology, which produced these transgenic mice and collected their electrophysiological data, I studied hippocampal neural circuit dysfunction. Surprisingly, while SWR incidence rate was dramatically increased, CA1 place field characteristics did not show any deficit (Suh et al., 2013). Although SWRs occurred more often, pair-wise reactivation of place cells during their time spans, which reflects the information content associated with replays, is sharply reduced. Since CA3, in contrast to CA1, is not genetically affected in these forebrain-specific calcineurin gene-deleted mice, the dissociations found in effects on CA1 place fields and SWRs may not be CA3-dependent (Suh et al., 2013). This brain state-dependent deficit may be explained by biophysical changes in CA1 cells or selective impairments in extrinsic inputs to CA1, such as EC input.

To conclude, this dissertation investigates formation mechanisms of hippocampal ensemble activity (Chapter 5). I found that the recurrent neural network of CA3 is necessary for the formation of place cell responses and SWRs in the rodent hippocampus. Moreover, disrupting hippocampal synaptic plasticity may selectively disrupt hippocampal ensemble activity in a particular brain states. These findings have significant implications in understanding the neural substrate of the cognitive map and episodic memory. Future work with

intricate techniques and experimental designs may shed further light on neural mechanisms of hippocampus-dependent cognition.

## Chapter 2 : General Methods

In this chapter, general methodologies as well as optogenetic technical developments for simultaneous SC silencing and multielectrode recording will be discussed. Detailed methods for studying neural ensembles in the calcineurin mouse model of Schizophrenia will be mentioned in Chapter 4.

### **Animal Training**

Male Long-Evans rats (2-3 months old, 250-400 g) were used for this study. All procedures were approved by Johns Hopkins University Animal Care and Use Committee and followed US National Institutes of Health animal use guidelines. Animals were housed on a standard, non-inverted, 12-h light cycle. Rats were food-restricted to achieve 85–90% of their normal weight and then trained to traverse a 165-cm linear track to receive a liquid chocolate-flavored reward (200  $\mu$ l, Carnation) at wells in either side of the track. Rats were trained for either 20 min or 30 complete laps (whichever was shorter) once per day for 3-5 consecutive days.

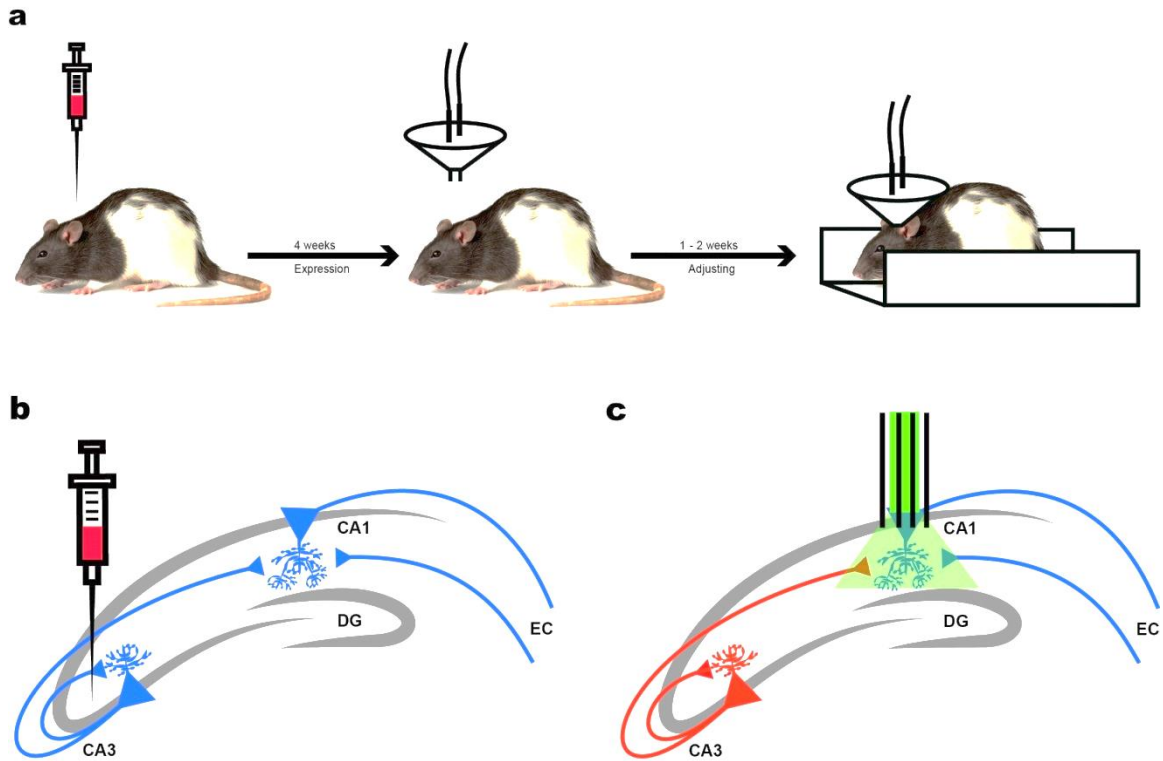


**Figure 2.1: Schematic of research design.**

a) Each rat undergoes two surgeries; one for virus injection and the other for drive implantation. b) CA3a-b is injected with eArch3.0-containing AAV and eArch3.0 gradually gets expressed in CA3 pyramidal cell bodies, recurrent collaterals, and SCs, all shown in orange. c) Optical fiber and tetrodes of the implanted optetrode gradually get adjusted until they reach stratum oriens and stratum pyramidale, respectively. CA1 LFP and cellular activity is recorded while silencing CA3 input to CA1.

### **Optogenetic setup**

Each trained rat underwent two surgeries (Figure 2.1a). The first surgery was for injecting adeno-associated virus (AAV) containing light-sensitive protein Archaelhodopsin (eArch3.0) to CA3 (Figure 2.1b). At least four weeks after

injection, when CA3 cells bodies and SCs strongly expressed eArch3.0 gene, the optetrode drive was implanted (Figure 2.1c). After a few days of adjusting tetropdes and optical fibers, hippocampal LFP and spiking activity in dorsal CA1 were able to be recorded while silencing SC input (Figure 2.1c). The details of each of these steps are as follows.

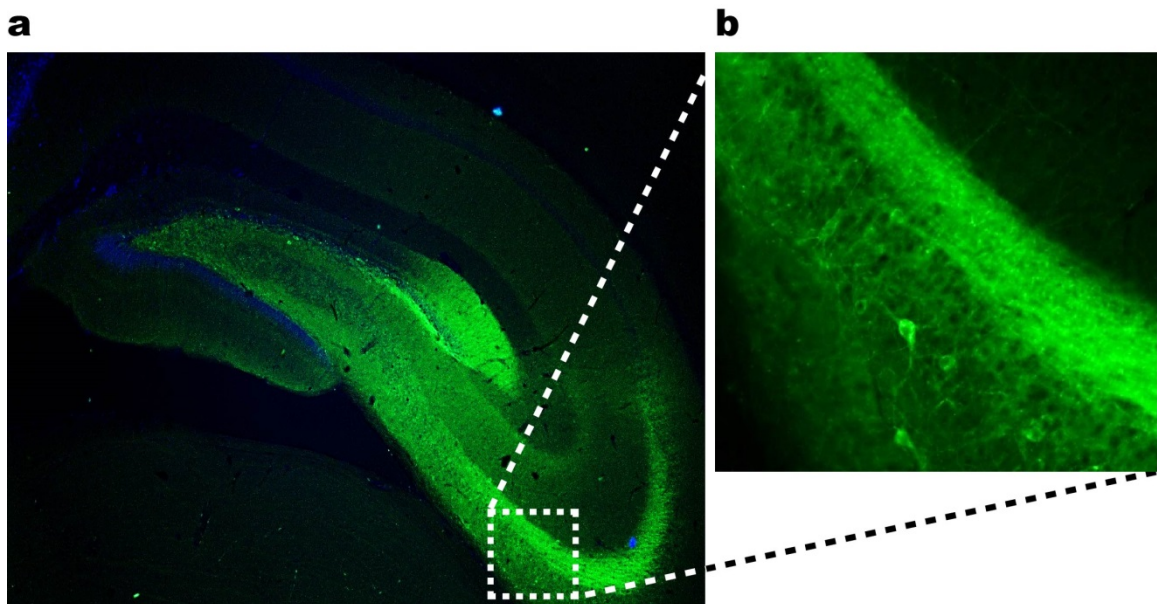


**Figure 2.2: eNpHR3.0 expression in CA3**

In a coronal slice of rat brain injected with AAV5\_CamKIIa\_eArch3.0\_EYFP construct, CA3 area expresses eYFP-tagged Halorhodopsin (eNpHR3.0). Note that, CA1 area receives poorly eYFP-expressing SCs in their stratum radiatum and stratum oriens.

### **Virus transduction (first surgery)**

AAVs provide diverse solutions to optogenetic experiments by offering low immunogenicity and diverse levels of neural tissue spread, genetic transduction,



cell body and neurite expression, and anterograde vs retrograde labeling (Yizhar et al., 2011). Recombinant AAV2 (rAAV2) vectors pseudotyped with various serotype packaging systems (e.g., rAAV2/1 to rAAV2/9, referred to simply as AAV1 to AAV9) are the most used viral vectors for optogenetic applications. Among these available AAVs, I chose AAV5 due to its transduction efficiency and high expression level (Yizhar et al., 2011).

Different opsins, such as genetically enhanced chloride ion pump Halorhodopsin (eNpHR3.0) and proton pump Archaeorhodopsin (eArch3.0) have been developed for optogenetic silencing of neural circuits (Gradinaru et al., 2010). In the beginning, I used eNpHR3.0 for expression verification in CA3 cell bodies and SCs (Figure 2.2). However, I found that eArch3.0 acquires much higher expression level, especially in SC axon terminals which are the region of interest in my silencing experimental design (Figure 2.4). Therefore, I used eArch3.0 in conjunction with CamKIIa promoter that specifically targets pyramidal cells and not interneurons (Gradinaru et al., 2010). All viral constructs were provided from University of North Carolina Vector Core under material transfer agreement with Karl Deisseroth laboratory.

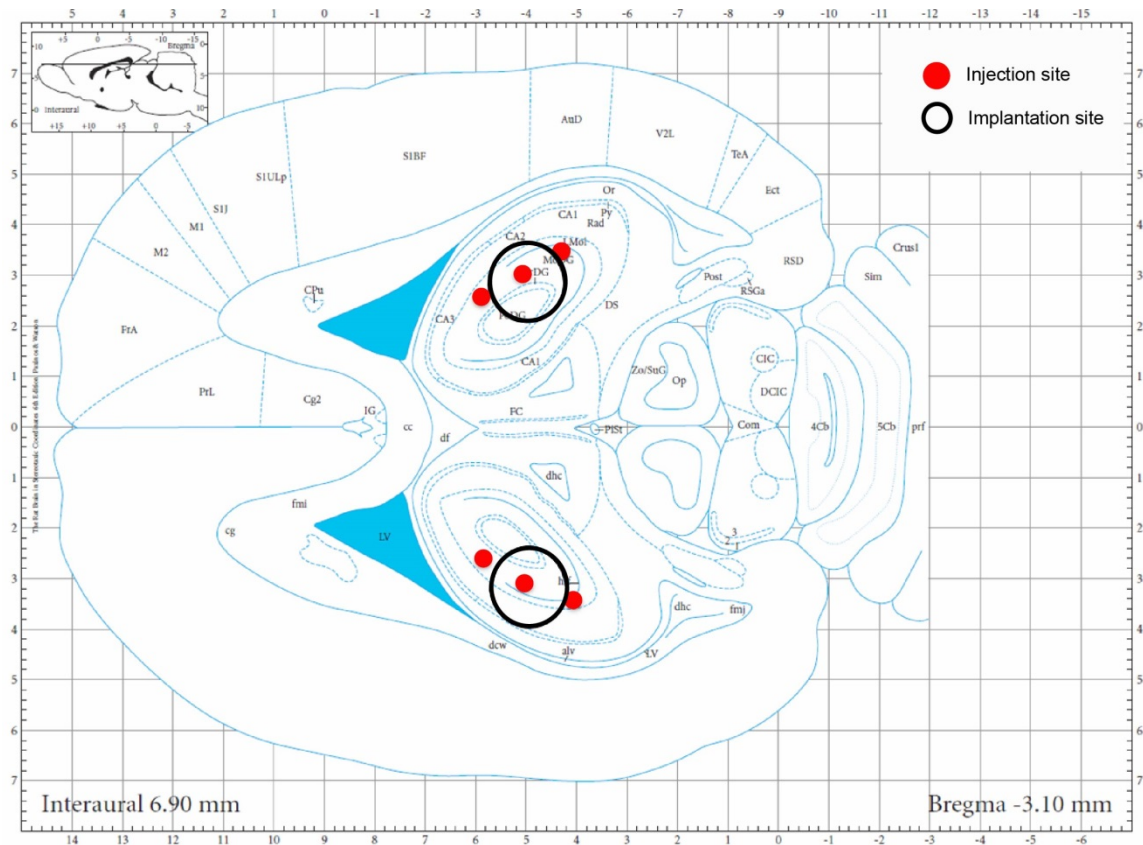


**Figure 2.3: Injection sites in dorsal and intermediate CA3.**

Six injection sites shown in red are overlaid on rat brain atlas (Paxinos and Watson, 2007). Black circles display the location of optetrode implanted in second surgery.

Four experimental (EXP) rats were injected with AAV5\_CamKIIa\_eArch3.0\_EYFP and two control (CON) rats were injected with AAV5\_CamKIIa\_EYFP in each of six sites in their dorsal and intermediate CA3a, and b. A total of 6  $\mu$ L of virus (1  $\mu$ L in each site) were stereotaxically injected in each rat (AP= -3.1 mm, ML =  $\pm$ 3.5, and DV= -3.5), (AP= -4.0 mm, ML =  $\pm$ 4.3, and DV= -4), and (AP= -4.7 mm, ML =  $\pm$ 4.8, and DV= -4.8) where AP, ML, and DV

stand for anterior-posterior in relation to bregma, medio-lateral, and dorso-ventral axes in relation to surface of skull, respectively. Figure 2.3 depicts these six injection sites in dorsal and intermediate CA3 as well as implantations sites of fibers and tetrodes.

Four to six weeks after AAV injections, eArch3.0 became expressed in CA3a-b cell bodies and axons including SCs (Figure 2.4). As expected, while SCs reaching CA1 stratum radiatum and stratum oriens express eArch3.0, CA1 cell bodies do not express this opsin (Figure 2.4). Also, CA2 pyramidal neurons were to some extent affected by viral transduction (Figure 2.4). However, since CA2 axons mainly project to CA1 striatum oriens where the optic fibers are to be placed below them, they will not be under laser light cone (van Strien et al., 2009; Dudek et al., 2016).

### **Optetrode design (second surgery)**

A bilateral optetrode with two optical fibers (200  $\mu\text{m}$  diameter) and up to 40 tetrodes (20 tetrodes in each hemisphere) was designed (Figure 2.5). For monitoring the position of each optical fiber in the brain, one tetrode was glued to each fiber, too. Both fibers and all of tetrodes were independently adjustable. Each tetrode consists of a twisted bundle of four 17.8  $\mu\text{m}$  platinum/10% iridium

wires (Neuralynx), and by gold-plating the tip of each tetrode an impedance of  $<150\text{ k}\Omega$  was achieved before implantation.

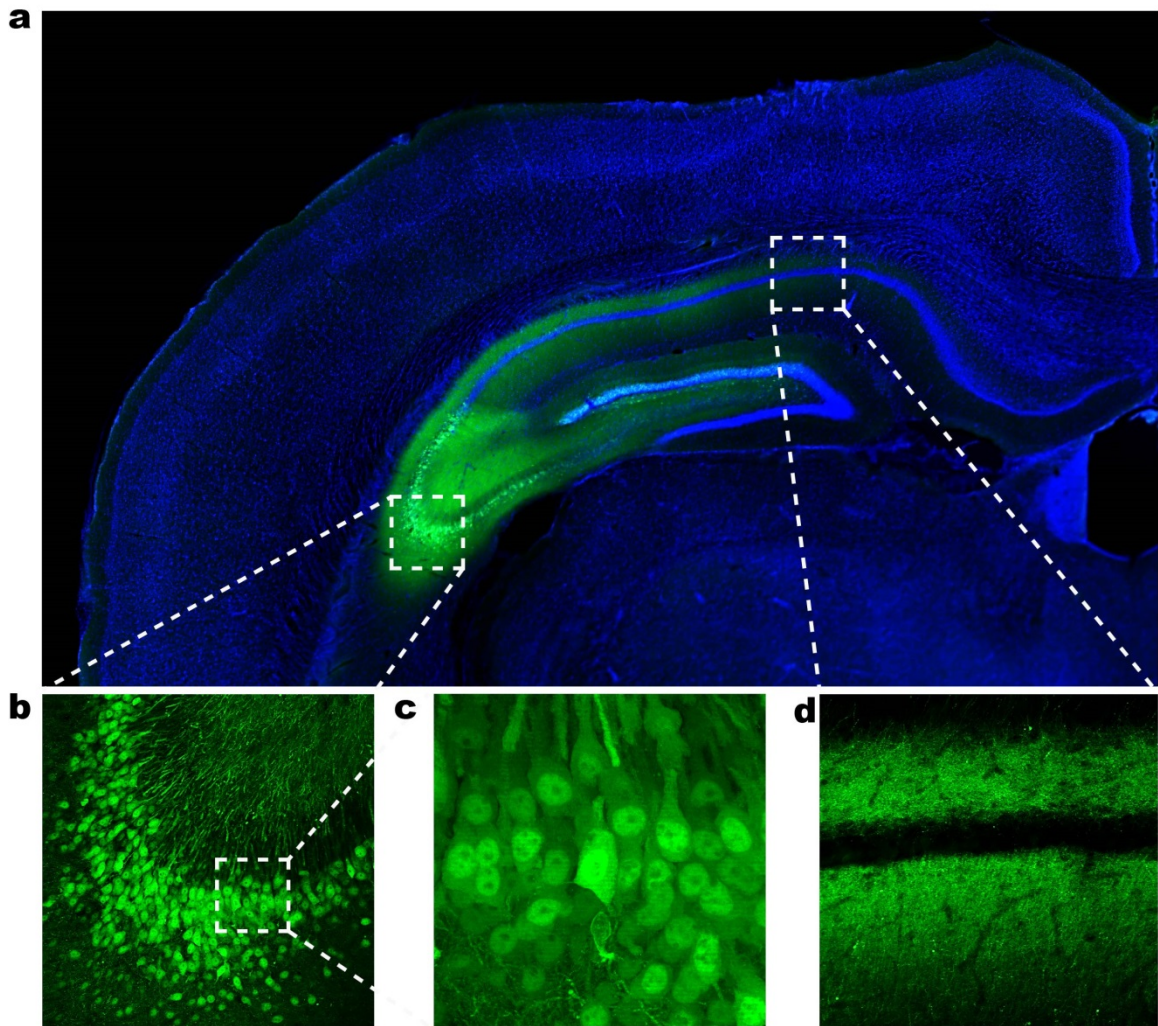


**Figure 2.4: eArch3.0 is expressed in CA3 but not CA1 pyramidal cells.**

In a coronal slice of rat brain, CA3 and partially CA2 cell bodies and axons express GFP-tagged eArch3.0. Zooming in CA3a region shows that the majority of pyramidal cells is affected by virus and strongly express eArch3.0. In contrast, CA1 pyramidal cells do not express this opsin but still receive eArch3.0-expressing SCs in their stratum radiatum and stratum oriens.

This design outperforms the existing optetrodes in difference ways. First, while the existing optetrodes are mostly unilateral and with only few (up to 16) tetrodes, this design is bilateral with 40 tetrodes (Halassa et al., 2011; Siegle et al., 2011; Anikeeva et al., 2012; Voigts et al., 2013, Figure 2.5). Second, in most of these optetrodes, tetrodes are either fixed to the optical fiber or either tetrodes or fiber are not individually adjustable. In contrast, in our design both fibers and tetrodes are individually and independently adjustable.

### **Optetrode implantation (second surgery)**

At least four weeks after viral injection, optetrodes were implanted on rats. A bone screw firmly connected to the rat's skull worked as electrical ground. Following surgical implantation, optical fibers and tetrodes were slowly lowered into the dorsal CA1 pyramidal layer over a few days using characteristic LFP patterns (mostly SWRs) and neural firing patterning as a guide. Placement of tetrodes and recordings were performed as previously described (Foster and Wilson, 2006; Pfeiffer and Foster, 2013). Optical fibers were adjusted to stay in stratum oriens, i.e. 100-200  $\mu\text{m}$  above the pyramidal layer, to be able to silence a broad region in dorsal CA1.

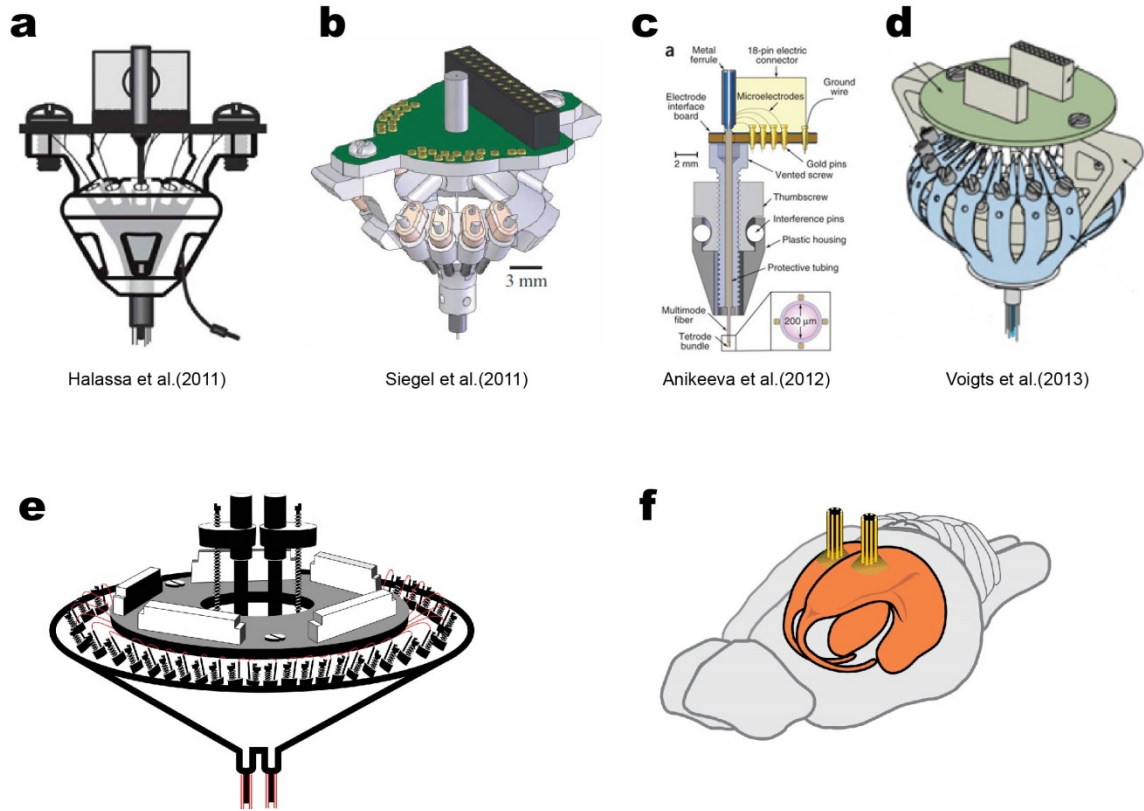


**Figure 2.5: The designed optetrode outperforms existing designs.**

a-d) Existing optetrodes are unilateral and have many fewer (4-16) tetrodes (Halassa et al., 2011; Siegle et al., 2011; Anikeeva et al., 2012; Voigts et al., 2013). In most of these optetrodes, the tetrodes are fixed to the optical fiber or either tetrodes or fiber is not individually adjustable. e) Our designed optetrode with 40 tetrodes. Both fibers and tetrodes are individually and independently adjustable.

## **LFP and cellular unit recording**

All data were collected using Digital Lynx data acquisition system (Neuralynx, Boseman, MT). The rat's position was tracked in darkness via blue and red LEDs mounted on the optetrode, and continuously recorded at 30 frames/s by an overhead camera. Analog neural signals were digitized at 32,000

Hz. The threshold for spike (extracellular action potential) detection was set to 60  $\mu$ V. LFP data was digitally filtered between 0.1 and 500 Hz and recorded at 3,200 Hz after ten times downsampling. Individual units were also identified by manual clustering based on spike waveform peak amplitudes using a custom software (xclust2, Matt A. Wilson, MIT). Only well-isolated cluster with high complex spike index (CSI) were considered as putative pyramidal cells and included in later analysis. CSI is defined as the percentage of spikes with first lag interspike intervals that fall between 2 and 15 ms and whose second spike amplitude is smaller than the first (McHugh et al., 1996b). A minority (< %10) of clustered units identified as putative fast-spiking inhibitory neurons on the basis of their spike width, low CSI (close to zero), and high firing rate.

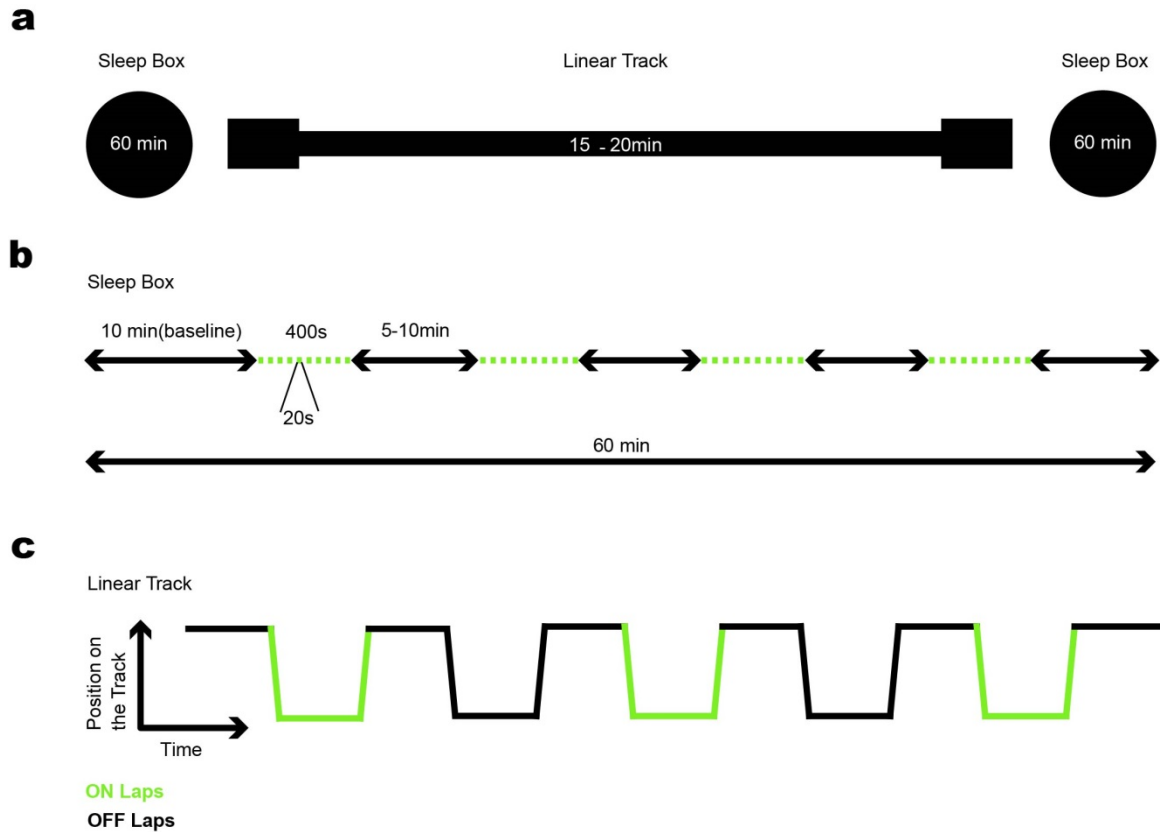


**Figure 2.6: Experimental design and stimulation paradigm.**

a) Schematic of an experimental session containing recordings from a rat in a sleep box, followed by linear track traversals, and then returning to the same sleep box. . b) In the sleep box, optical silencing is performed by four pulse trains each lasting 400 seconds. Each train consists of ten 20-s-long stimulations separated by ten 20-s-long light off time spans. c) For the track traversal session, light is manually and consecutively turned on and off for ON and OFF laps. For each ON lap, the light is continuously on while the rat was traversing the track, staying at one end of the track and returning to the first position.



## Task Design

A recording day consisted of a one-hour recording session in a sleep box (“Pre” rest session), followed by either 30 traversing laps or 20 min (whichever was shorter) on a familiar 165 cm linear track (“Run” session), and one hour of recording in the sleep box (“Post” rest session). Figure 2.6 depicts the task design and recording/stimulation paradigm. In each rest session, light was delivered in four pulse trains each lasting 400 seconds. Each pulse train consisted of alternating 20-s light on stimulation periods (“ON” periods) followed by 20-s light off periods (“OFF” periods), with this on/off cycle repeating 10 times (Figure 2.6b). Light was delivered from a 532 nm (green) laser and the estimated light power at the tips of optical fibers in each hemisphere was around 100 mW/mm<sup>2</sup> (3.25 mW). Laser commands were generated by a custom-written MATLAB (Mathworks) graphic user interface and were delivered to laser by multifunction data acquisition device NI USB-6341(National Instruments).

Next, rats were put on a familiar linear track. For the Run session, light was manually and consecutively turned on and off for ON and OFF laps (Figure 2.6c). For each ON lap light was continuously on while the rat was traversing the track, staying at one end of the track and returning to the first position. The stimulation paradigm for “Post” rest sessions where similar to “Pre” rest sessions.

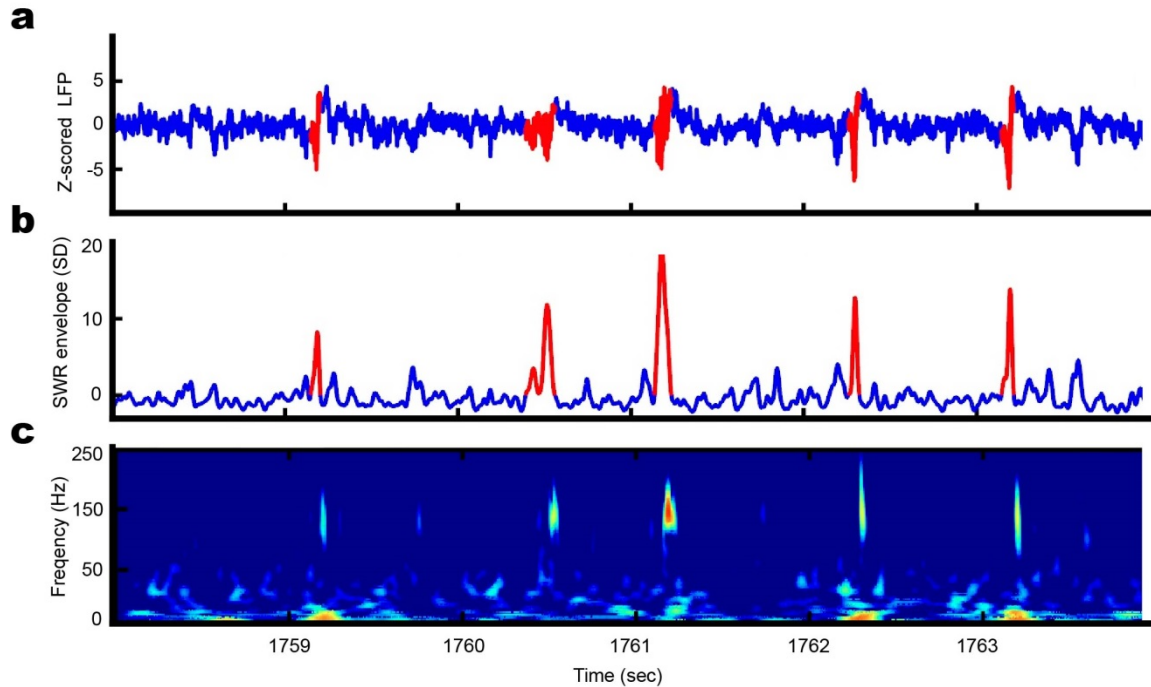


**Figure 2.7: SWR detection algorithm.**

A 6-s sample of z-scored raw LFP recorded from dorsal CA1 (top). Whenever, the envelope of smoothed, ripple-band filtered LFP, passes 5 SD, it was detected as a SWR (middle). In the wavelet spectrogram of raw LFP (bottom), five detected SWR events show a clear isolated activity in the ripple frequency band (100-250 Hz) of the LFP spectrogram. Red time spans show detected ripple activity.

## **Analysis**

### **LFP analysis**

Tetrodes that were able to detect any SWRs were included in the LFP analysis, regardless of whether they showed any modulation by light or not. For SWR detection in the sleep box study, only Pre rest sessions were analyzed and, using a speed threshold of 7 cm/s, moments that rat intensely moved where

excluded from the analysis. One electrode from each acceptable tetrode was considered for LFP analysis (Figure 2.7 top). The LFP signal of each electrode was denoised for 60 Hz electric noise and its 180 Hz harmonic using a second-order IIR notch filter. Then, denoised LFP was filtered at SWR frequency range (100–250 Hz) with a fifth-order Butterworth band-pass filter. The envelopes of each band-passed LFP were obtained using the absolute value of its Hilbert transform. After applying a Gaussian smoothing filter with 5 ms standard deviation, the envelope was z-scored (Figure 2.7 middle).

Events that passed 5 standard deviations (i.e., mean + 5 SD of averaged non-z-scored envelope) for more than 3 ms were considered as SWR events, and SWRs that were less than 20 ms apart were merged and considered as one extended ripple. The beginning and end of each SWR were defined as where the smoothed envelope crossed its mean value (i.e., zero for the z-scored signal) (Figure 2.7 middle). Tetrodes with SWR incidence rate of more than 0.05 ripples/s (e.g. at least one ripple on average in every 20 s either during OFF or ON periods) during sleep box recording were considered for further analysis. This tetrode selection criterion was decreased to 0.02 ripples/s in rest periods for linear track recording sessions.

Morlet wavelet scalogram with bandwidth of 10 was used for spectrogram visualization of raw LFP (Figure 2.7 bottom). SWR power was obtained by applying Welch's method on each individual non-z-scored non-enveloped SWR and then averaging over calculated powers. Furthermore, using Welch's method, the power of raw LFP signals during Run was calculated and, in particular, theta (5–10 Hz), slow gamma (25-55 Hz), and fast gamma (65-110 Hz) powers for ON and OFF laps were compared.

### **Place field calculation and features**

All the place cell analyses, except spatial coherence, were done on 1-D place fields. 1-D Place fields were obtained by binning the linear track using 2 cm bins, and these raw place fields were smoothed by applying a Gaussian filter with a 2.4 cm SD. Only cells that showed a peak field firing rate of more than 3 Hz either in OFF or ON conditions were considered as place cells. Also, all analyses were done independently on directional fields and OFF and ON conditions. Therefore, for the same direction, two place fields were calculated, one by only considering OFF laps and the other only by considering ON laps.

The size of place fields was calculated as the number of 2-cm-wide bins above 1 Hz threshold. Major place field size was calculated by only considering the longest portion of place field which was continuously above 1 Hz.

Directionality index of each place field was defined as the percentage of its dominant direction (the direction that a specific cell has higher peak firing) divided by the summation of both leftward trajectory and rightward trajectory firing rates. The sparsity index ranges from 0 to 1, where a lower value means a less diffuse and more spatially specific place field (Skaggs et al., 1996). Having 2 cm bins ( $n = 90$ ) each having firing rate of  $f_i$  and occupancy time of  $t_i$ , sparsity is defined as:

$$\text{Sparsity} = \frac{(\sum_{i=1}^n p_i \cdot f_i)^2}{\sum_{i=1}^n p_i \cdot f_i^2}$$

where  $p_i$  is the occupancy probability:  $p_i = t_i / \sum_{i=1}^n t_i$ .

Spatial information, which is the amount of information about an animal's position by each spike of a place cell, is calculated as follows (Skaggs et al., 1996):

$$\text{Spatial Information} = \sum_{i=1}^n p_i \frac{f_i}{f} \log_2 \frac{f_i}{f}$$

Where  $f$  is the mean firing rate,  $f = \sum_{i=1}^n p_i f_i$ .

The center of mass (COM) of a place field was calculated using the following equation:

$$\text{COM} = \frac{\sum_{i=1}^n x_i \cdot f_i}{\sum_{i=1}^n f_i}$$

where  $x_i$  is the  $i$ th position bin on the track.

The skewness of each place field was defined as:

$$\text{Skewness} = \frac{\sum_{i=1}^n f_i \cdot (x_i - \text{mean}(x))^3}{\sigma_x^{3/2} \cdot \sum_{i=1}^n f_i}$$

with  $\sigma_x$  defined as:

$$\sigma_x = \frac{\sum_{i=1}^n f_i \cdot (x_i - \text{mean}(x))^2}{\sum_{i=1}^n f_i}$$

Spatial coherence, which quantifies smoothness and local orderliness of a place field, is the autocorrelation of each place field with its nearest neighbor average (Muller et al., 1989). To do this, the  $6 \times 165$  cm linear track was binned into  $2 \times 2$  cm bins and the new firing map for each pixel was calculated as the average firing rate of the eight unsmoothed neighbor pixels. Then, the 2-D correlation coefficient between the original unsmoothed firing map and the new one was calculated and to be statistically comparable we applied a Fisher transform (or z-transform,  $z = \text{arctanh}(r)$ ) on correlation coefficients before calculating Z-values. Spatial correlation, which was defined as the normalized

Pearson correlation coefficient of place fields in light OFF and light ON conditions, was also Fisher-transformed for statistical comparison.

### **Theta phase preference and phase precession**

For each tetrode, instantaneous theta phase was calculated using Hilbert transform of theta-band filtered LFP. Then, for each place cell, spikes and LFP timestamps were used to linearly interpolate theta phase for each spike. The degree of modulation of each place cell by theta phase was obtained by calculating its circular mean resultant vector (MRV). MRV may vary from 0 (no phase preference) to 1 (every spike occurred at the same theta phase).

To calculate theta phase precession, circular-linear regression was used (Kempster et al., 2012). A linear model  $\varphi(x) = 2\pi ax + \varphi_0$  was fit into phase-position circular-linear pairs  $\{x_i, \varphi_i\}_{i=1}^n$  for each place cell independently for ON and OFF place fields. Precession slope  $a$  was varied between range  $\mathcal{C} = (-5, 0)$  to find optimal  $\hat{a} = \operatorname{argmax}_{a \in \mathcal{C}} R(a)$  that maximizes  $R(a)$ , the MRV of the circular errors between the measured phase  $\varphi_i$  and the model predictions  $\varphi(x)$ :

$$R(a) = \sqrt{\left(\frac{1}{n} \sum_{i=1}^n \cos(\varphi_i - 2\pi ax_j)\right)^2 + \left(\frac{1}{n} \sum_{i=1}^n \sin(\varphi_i - 2\pi ax_j)\right)^2}$$

If  $a^*$  found to exactly match border sides of C it will not be considered a precession. Next, phase offset  $\hat{\varphi}_0$  is calculated as follows:

$$\hat{\varphi}_0 = \arctan 2 \frac{\sum_{i=1}^n \sin(\varphi_i - 2\pi\hat{a}x_i)}{\sum_{i=1}^n \cos(\varphi_i - 2\pi\hat{a}x_i)}$$

Now, to examine the statistical significance of the circular-linear correlation, the circular-linear correlation coefficient is first calculated:

$$\rho = \frac{\sum_{i=1}^n \sin(\varphi_i - \bar{\varphi}) \sin(\theta_i - \bar{\theta})}{\sqrt{\sum_{i=1}^n \sin(\varphi_i - \bar{\varphi})^2 \sum_{i=1}^n \sin(\theta_i - \bar{\theta})^2}}$$

where  $\bar{\varphi} = \frac{\sum_{i=1}^n \sin(\varphi_i)}{\sum_{i=1}^n \cos(\varphi_i)}$  and  $\bar{\theta} = \frac{\sum_{i=1}^n \sin(\theta_i)}{\sum_{i=1}^n \cos(\theta_i)}$ , and  $\theta_i = 2\pi|\hat{a}|x_i \pmod{2\pi}$  is the linearly fitted phase. To determine statistical significance, the scaled correlation was calculated. For large  $n$  and under the null hypothesis that phases are from an uncorrelated Gaussian random distribution, the scaled correlation is given by

$$z = \rho \sqrt{n \frac{\lambda_{02} \lambda_{20}}{\lambda_{22}}}$$

where

$$\lambda_{ij} = \frac{1}{n} \sum_{k=1}^n \sin^i(\varphi_k - \bar{\varphi}) \sin^j(\theta_k - \bar{\theta})$$



Given  $z$ , the significance value can be derived from the cumulative normal distribution:

$$p = 1 - \operatorname{erf}\left(\frac{|z|}{\sqrt{2}}\right).$$

### **Statistical analysis**

For most analyses, if data points had a Gaussian distribution (checked by Lilliefors test), depending on the type of comparison a paired-sample or two-sample t-test was applied. For non-Gaussian distributions, depending on the type of comparison the non-parametric paired-sample Wilcoxon signed rank test or two-sample Wilcoxon rank sum test (aka Mann–Whitney U (MWU) test) was used. The effect of optogenetic silencing of CA3 SCs on several properties of CA1 SWR and place cell activity (e.g. SWR incidence rate and peak in-field firing rate) was tested using five statistical comparisons. The first two comparisons were between OFF vs ON conditions in EXP and CON. The next two statistical analyses consisted of comparing EXP vs CON separately in OFF and ON conditions. For the fifth analysis, the modulation index for each feature defined as  $(\text{ON} - \text{OFF})/(\text{ON} + \text{OFF})$  was calculated and EXP and CON sets were compared. For COM, this index was simply defined as  $(\text{ON} - \text{OFF})/180$ .

# Chapter 3 : The role of CA3 in neural ensemble activity in CA1

Hippocampal area CA1 local field potential (LFP) exhibits high frequency (100- 250 Hz) events known as sharp-wave ripples (SWRs). These events occur during both slow-wave sleep and awake restfulness and have been shown to be important for the consolidation of spatial memory. During exploration, CA1 pyramidal neurons show location-specific modulation of firing rates, with the location of maximum activity known as a place field. However, the mechanisms of formation of SWRs and place fields are not well understood. Here we report that, using multi-tetrode recording and reversible optogenetic manipulation, the silencing of Schaffer collateral (SC) projections from CA3 to CA1 greatly diminishes the incidence rate of SWRs. Furthermore, SC silencing substantially suppresses hippocampal place cell activity and enhances theta rhythm in LFP during exploration. These findings shed light on the functional interconnections between hippocampal subregions that support episodic memory.

## **Introduction**

Hippocampus has been shown to be crucial for the formation of a spatial cognitive map and episodic memory (O'Keefe and Nadel, 1978). Hippocampal

pyramidal cells respond selectively to particular locations in an environment, and are therefore called, “place cells” (O’Keefe and Nadel, 1978). These place cells are sequentially reactivated during SWR events, a phenomenon known as hippocampal replay (Wilson and McNaughton, 1994; Nádasdy et al., 1999; Lee and Wilson, 2002; Foster and Wilson, 2006; Diba and Buzsáki, 2007; Davidson et al., 2009; Karlsson and Frank, 2009; Carr et al., 2011). However, the mechanisms for the formation of place fields and SWRs are still unclear. In particular, the contribution of hippocampal area CA3 and entorhinal cortex (EC), the main cortical projection to hippocampus, in the expression of these neural responses in CA1 is not well understood.

Simultaneous hippocampal ensemble recordings have provided evidence that synchronous pyramidal neuron bursts in the highly recurrent network of CA3 induce depolarizing sharp waves in apical dendrites of CA3 and CA1 pyramidal neurons, which result in ripple-frequency oscillation of locally interacting pyramidal cells and interneurons (Buzsáki et al., 1983; Buzsáki, 1986, 2015; Suzuki and Smith, 1988b; Sullivan et al., 2011; Stark et al., 2014, 2015).

Further work has suggested that most of sharp wave events are generated in CA2 and CA3a (near CA2), then transferred to CA3b, and CA3c (near dentate

gyrus), and from CA3b-c invade CA1 (Csicsvari et al., 2000; Oliva et al., 2016). However, these findings were based on correlational analysis with delays highly dependent on sharp wave and ripple detection criteria (Oliva et al., 2016). For example, SWRs may still be initiated first in neural ensembles in CA1 but reach their peak power in CA2 earlier than CA3 itself and, consequently, be detected sooner.

When SC projections from CA3 to CA1 were genetically silenced over the time course of a few weeks, surprisingly the number of SWRs did not change, while the average peak frequency of SWRs decreased (Nakashiba et al., 2009; Middleton and McHugh, 2016). However, these studies are based on chronic causal manipulations that are prone to compensatory homeostatic plasticity mechanisms such as inhibition adjustment and synaptic scaling which may be on the timescale of hours to days (Turrigiano et al., 1998; Vogels et al., 2011; Keck et al., 2017; Turrigiano, 2017). Therefore, a causal but transient approach using optogenetics may shed light on the formation mechanisms of SWRs.

Many studies with diverse approaches and techniques have attempted to explain the contribution of internally-generated CA3 input and extrinsic EC, especially position-tuned medial EC (MEC), inputs in the expression of place

cell responses in CA1. Previous work has found either no or only slight disruption in CA1 place fields when CA3 input is impaired in rodents exploring a familiar environment (Brun et al., 2002; Nakazawa et al., 2002, 2003, Nakashiba et al., 2008, 2009). Pharmacological and surgical lesions of CA3 have demonstrated that other inputs to CA1, probably predominantly EC inputs, are sufficient to establish robust place fields (Brun et al., 2002). This is in accordance with dentate gyrus and medial septum lesion studies that found disrupted activity in CA3 with unaffected CA1 place cell responses (McNaughton et al., 1989; Mizumori et al., 1989; Wang et al., 2014). Likewise, either genetically deleting NMDA receptors in CA3 pyramidal cells or comprehensive genetic blockade of SCs does not change the field properties of CA1 pyramidal cells in mice traversing familiar tracks (Nakashiba et al., 2009). These findings imply that other input to CA1, such as from EC, is crucial for the expression of already-established place fields in CA1.

In contrast to the relatively consistent lack of major effects on CA1 place fields following CA3 manipulations, EC input disruption using a variety of methods has often found inconsistent effects (Bush et al., 2014). EC input disruption using physical, pharmacological, genetic, and optogenetic techniques has not been shown to demolish the persistence of CA1 place fields as well, but has been

found to cause some cells showed larger place fields, remapped fields, or impaired theta phase precession (Brun et al., 2008; Hales et al., 2014; Miao et al., 2015; Schlesiger et al., 2015; Rueckemann et al., 2016).

Following MEC lesioning, a reduction in the percentage of active place cells as well as the spatial information content and stability of their place fields was observed in a familiar environment, but nevertheless, place cell responses did not get eliminated (Miller and Best, 1980). CA1 place fields have been shown to expand following lesion of the medial EC (MEC) layer III cells that directly project to CA1 (Brun et al., 2008) or pharmacological silencing of all of MEC (Ormond and McNaughton, 2015). However, other groups have found surgical removal of MEC to cause no change in place field sizes in CA1 (Hales et al., 2014; Schlesiger et al., 2015), while lesion to the entirety of EC can cause place field sizes to decrease (Van Cauter et al., 2008). Moreover, lateral EC (LEC) lesions result in decreases firing rate in hippocampal place cells (Lu et al., 2013).

Similarly, different groups have found inconsistent effects of MEC manipulation in the degree to which place cells remap upon re-exposure to the same environment. While LEC lesions only resulted in a slight rate remapping (Lu et al., 2013), lesions to whole EC or whole MEC, as well as MEC optogenetic

silencing result in global remapping in a subset of CA1 place fields (Brun et al., 2008; Van Cauter et al., 2008; Miao et al., 2015; Ormond and McNaughton, 2015; Rueckemann et al., 2016). Moreover, physical and pharmacological lesions of MEC suppress CA1 theta power (Ormond and McNaughton, 2015) and phase precession (Hales et al., 2014; Schlesiger et al., 2015), respectively.

These contradictory findings from these studies indicate that in a familiar environment, EC input is critical for completely normal expression of place fields in CA1, though not essential for the existence of location-specific activity in CA1 pyramidal cells. On the other hand, while CA3 lesion and genetic silencing studies have failed to find a major effect on CA1 place fields, they were also chronic manipulations and prone to compensatory mechanisms. Therefore, whether a real-time manipulation of CA3 inputs would affect CA1 place cell responses remains unknown.

In this study, we used transient optogenetic silencing of SCs to address the following two main questions. First, what is the role of CA3 in the expression of CA1 place cell responses? Besides being highly recurrent, CA3 is the major projection to dorsal CA1, and likely carries rich positional information to CA1. While weeks of recovery post-lesion may allow place cell responses to reemerge

in CA1 even while lacking CA3 input, transient optogenetic silencing will prevent such a compensatory mechanism. If CA3 is critical for relaying spatial information to CA1 in order to generate place cell responses, transient optogenetic silencing of SCs is expected to result in substantial effects on CA1 place fields, such as loss of stability and spatial specificity. Second, what is the role of CA3 in the formation of CA1 SWRs? Despite contradictory findings from earlier work, we hypothesize that CA3 plays a causal role in the formation of CA1 SWRs during consummatory behaviors. We therefore expect optogenetic silencing of SCs to greatly diminish the occurrence of SWRs, both during sleep and awake rest.

We found that continuous CA3 input is necessary for the expression of place fields in CA1 pyramidal cells. During optogenetic silencing of SCs, the majority of place cells had the firing rates in their place field almost completely silenced. However, place cells that were partially silenced did not show global remapping, and instead simply had lower peak firing rates in their same characteristic place field. This suggests that precise positional information on where a place cell fires comes from EC or other inputs, but the extent that a cell fires around that position is dependent on CA3. We also found that SC input is essential for the formation of SWRs in CA1, both during sleep and during rest periods on the



track. Silencing SCs drastically reduced SWR incidence and the associated neuronal spiking in a reversible way in both behavioral states. This shows that CA3 has an indispensable role in the chain of causality for the formation of SWRs.

### **CA3 input is necessary for SWRs in CA1 during sleep**

We designed and implanted a bilateral optetrode consisting of two optical fibers and up to 40 tetrodes in rats expressing the light-sensitive proton pump Archaelhodopsin (eArchT3.0) in their dorsal CA3 pyramidal cells and SCs (Figure 3.1). Tetrodes were gradually lowered into the pyramidal layer of dorsal CA1. Using a tetrode attached to each optical fiber, the fibers were similarly gradually lowered and positioned slightly above the pyramidal layer (Figure 3.1a-b). Although viral injections were targeted for distal CA3a-b regions, some CA2 pyramidal cells were potentially affected (Figure 3.1c). However, as expected, in contrast to CA3 cell bodies and SCs, CA1 pyramidal cells were not affected (Figure 3.1c-f).

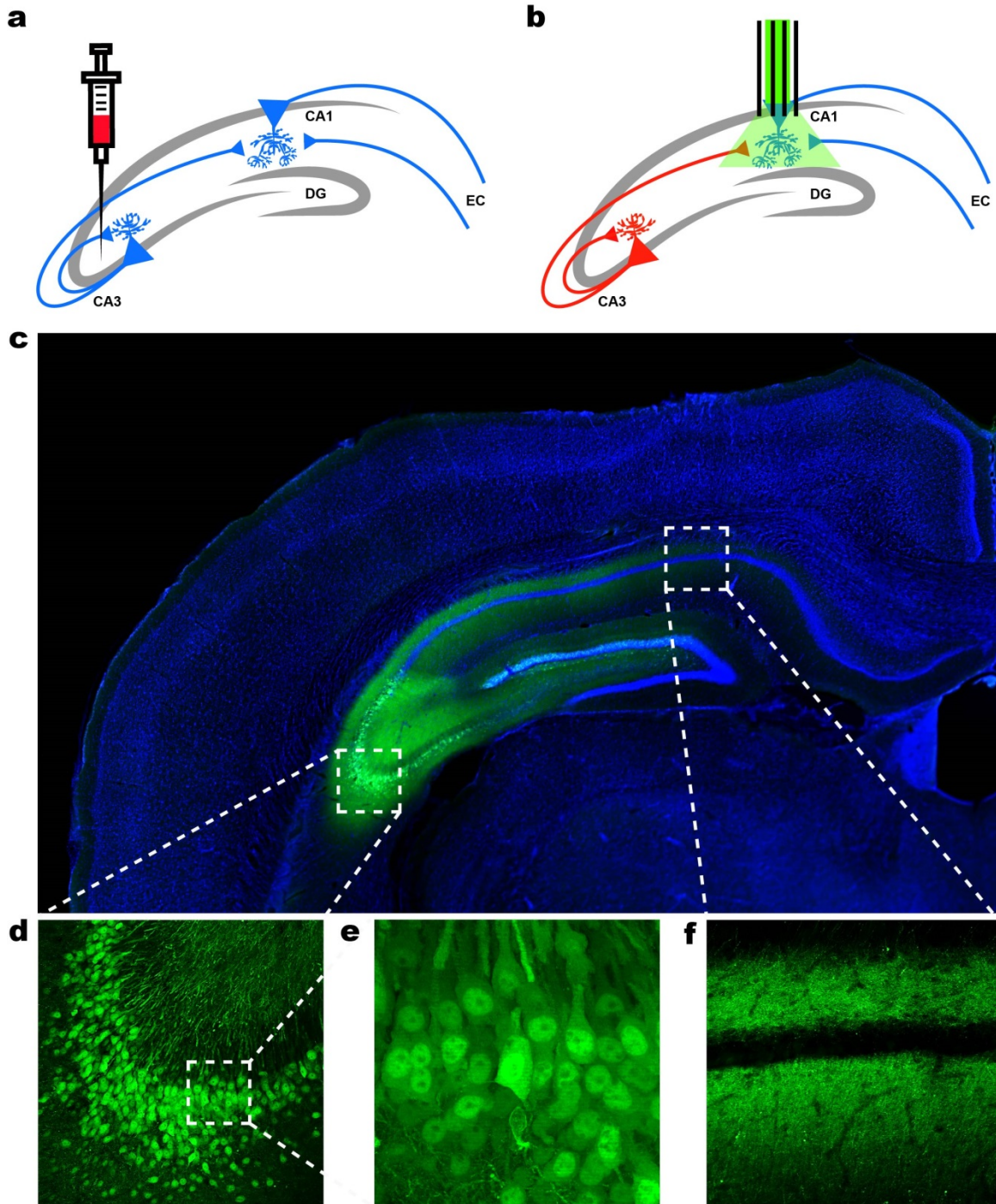


Figure 3.1: Strategy for control of CA3 input to CA1 during recording of CA1 activity.

a-b) Each rat undergoes two surgeries. The first for virus injection (a) and the second for optetrode implantation (b). CA3a-b is injected with eArch3.0-containing adeno-associated virus (AAV) and eArch3.0 gradually gets expressed in CA3 pyramidal cell bodies, recurrent collaterals, and SCs (shown in red). The optical fiber and tetrodes of the implanted optetrode are gradually adjusted until they are able to shine light on and record from the CA1 pyramidal layer, respectively. CA1 LFP and cellular activity is recorded while silencing CA3 input to CA1. c-f) eArch3.0 is expressed in CA3 but not CA1 pyramidal cells. In a coronal slice of rat brain, CA3 (and possibly CA2) cell bodies and axons express GFP-tagged eArch3.0 (c). In a magnified view, the CA3a region shows pyramidal cells strongly express the GFP-tagged eArch3.0 (d and e). In contrast, CA1 pyramidal cells do not express this opsin but still receive eArch3.0-expressing SCs in their stratum radiatum and stratum oriens, above and below the pyramidal layer, respectively (f).

Four eArch3.0-expressing experimental (EXP) and two GFP-only expressing control (CON) rats were implanted (See Chapter 2). SWRs were detected on a total of 233 and 106 tetrodes in EXP and CON rats, respectively, and these tetrodes were chosen for further analysis. When rats were at rest in a sleep box, CA1 SWR incidence rates were significantly suppressed in the majority of EXP tetrodes during light ON periods (OFF:  $0.32 \pm 0.01$  SWR/s (mean  $\pm$  standard error); ON:  $0.23 \pm 0.01$  SWR/s, paired-sample t-test,  $F(1, 224) = 128.08$ ,  $p < 10^{-23}$ , Figure 3.2a-b), while CON tetrodes slightly increased their SWR incidence rate under illumination (OFF:  $0.28 \pm 0.01$ ; ON:  $0.31 \pm 0.01$ , paired-sample t-test,  $F(1, 105) = 33.13$ ,  $p < 10^{-7}$ , Figure 3.2b). These significant yet opposing effects of light

were observed in all individual rats (Figure 3.3a). Moreover, the degree of modulation of SWR incidence (SWR modulation index =  $[\text{ON} - \text{OFF}]/[\text{ON} + \text{OFF}]$ , see Chapter 2) was significantly different in CON and EXP rats (CON:  $0.03 \pm 0.01$ ; EXP:  $-0.19 \pm 0.02$ , two-sample Wilcoxon rank sum test,  $z(1, 329) = 10.28$ ,  $p < 10^{-24}$ , cumulative density plot is shown in Figure 3.2c). The increased SWR incidence in CON tetrodes might be due to the depolarization effect of heat induced by continuous laser light (3.5 mW, 100 mW/mm<sup>3</sup>, 20 s ON periods) on dorsal CA1 (Stujenske et al., 2015). EXP tetrodes also show a significant decrease in power spectral density in the ripple frequency band of their raw LFPs (OFF:  $4.6 \times 10^4 \pm 4.8 \times 10^3$ ; ON:  $3.3 \times 10^4 \pm 3.2 \times 10^3$ , paired-sample t-test after logarithmic transformation,  $F(1, 224) = 99.50$ ,  $p < 10^{-18}$ , Figure 3.2f), reaffirming the suppression of SWR activity during rest state, while CON tetrodes slightly increase their ripple frequency band activity (OFF:  $8.1 \times 10^4 \pm 6.6 \times 10^3$ ; ON:  $8.2 \times 10^4 \pm 6.5 \times 10^3$ , paired-sample t-test after logarithmic transformation,  $F(1, 105) = 10.03$ ,  $p < 0.01$ , Figure 3.2f). Multi-unit spikes were also significantly suppressed in EXP tetrodes during ON condition (CON: OFF:  $21.96 \pm 2.85$  spikes/s and ON:  $22.04 \pm 2.86$  spikes/s, paired-sample t-test after logarithmic transformation,  $F(1, 99) = 2.55$ , N.S.; EXP: OFF:  $22.70 \pm 1.87$  spikes/s; ON:  $17.02 \pm 1.53$  spikes/s, paired-sample t-test after logarithmic transformation,  $F(1, 213) = 95.95$ ,  $p < 10^{-18}$ ,

Figure 3.2d). This effect was significant in all individual EXP rats except rat EXP3 (Figure 3.5b). Moreover, the degree of modulation ( $[\text{ON-OFF}]/[\text{ON+OFF}]$ ) of rest-state spiking activity was significantly different in CON and EXP rats (CON:  $-0.01 \pm 0.01$ ; EXP:  $-0.19 \pm 0.02$ , two-sample Wilcoxon rank sum test,  $z(1, 312) = 6.42$ ,  $p < 10^{-9}$ , cumulative density plot is shown in Figure 3.2e). These findings pinpoint CA3 as critical for the generation of SWRs and rest-state baseline spiking activity in CA1.

In spite of the difficulty of estimation of tetrode position in the brain in relation to the optic fiber due to potential deviation of each tetrode and the nonlinearity of modulation effect due to silencing traversing axons, we found a significant correlation between horizontal distance from fiber optic and the degree of modulation of SWR incidence rate by light only among EXP rats (CON:  $r = 0.16$ ;  $F(1,329) = 2.8$ , N.S.; EXP:  $r = 0.26$ ,  $F(1,329) = 15.9$ ,  $p < 10^{-4}$ , Figure 3.4). This suggests a key contributor to the heterogeneity between modulations at different sites (Figure 3.2) was simply light intensity there, rather than necessarily true functional diversity.

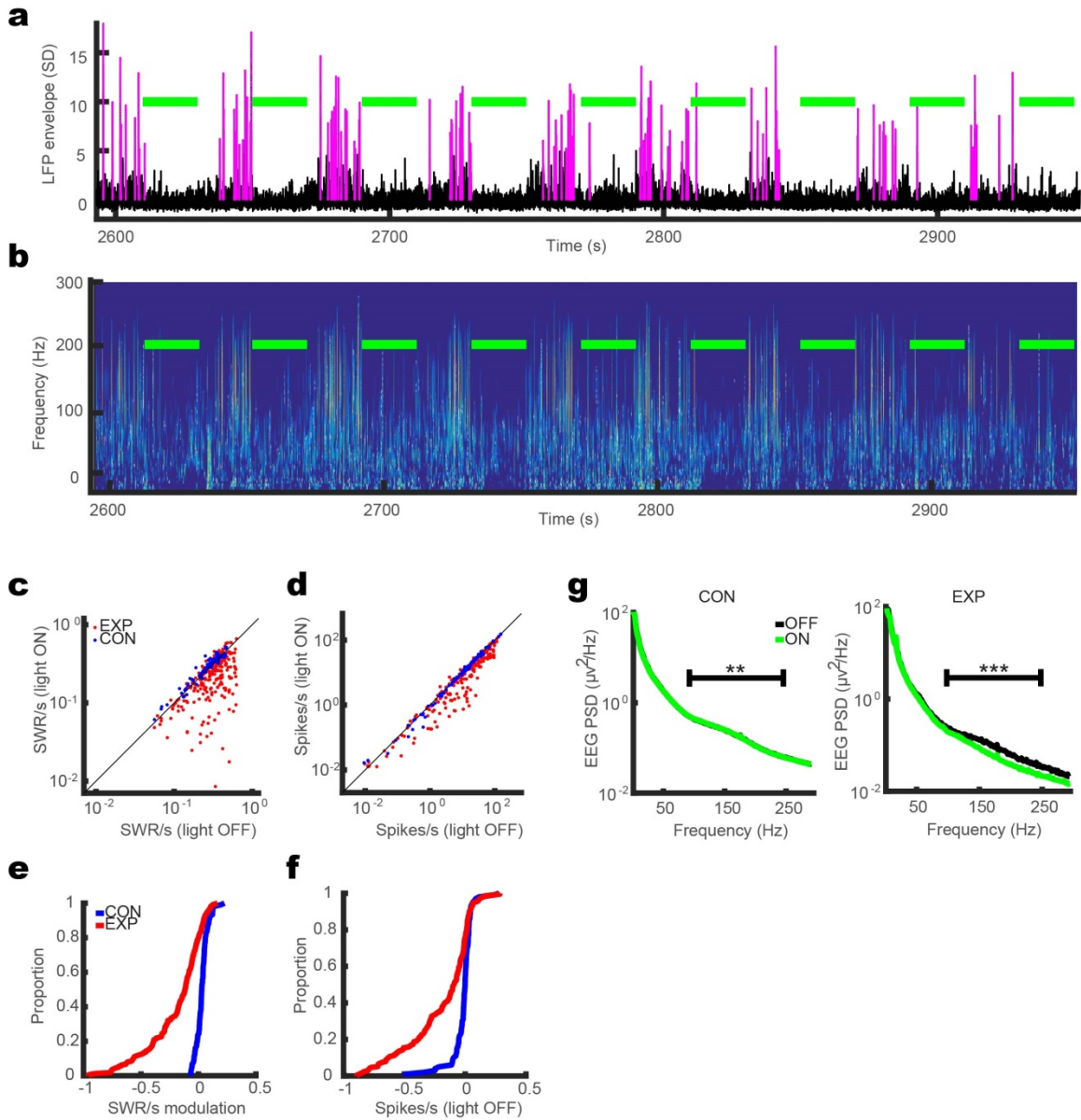


**Figure 3.2: CA3 input is necessary for SWRs in CA1.**

a) An example tetraode in CA1 region which the detected SWRs in its filtered LFP envelope show strong modulation by SC silencing. Red traces are periods in the LFP that meet criteria for SWR detection. b) Wavelet scalogram of raw LFP from the same tetraode in (a). Green horizontal bars denote 20-s long light ON periods intermingled by 20-s light OFF periods. c) SWR incidence rate for each tetraode in light ON vs. light OFF

conditions. Each dot represents a tetrode and red and blue represent EXP and CON rats, respectively. d) Multi-unit activity for each tetrode in light ON vs. light OFF conditions. Each dot represents a tetrode and red and blue represent EXP and CON rats, respectively. e) Cumulative density plot of the amount of modulation of SWR incidence rate calculated from all CON (blue) and EXP (red) tetrodes. f) Cumulative density plot of the amount of modulation of spiking activity by light in CON (blue) and EXP (red) tetrodes. g) Power spectral density (PSD) of raw LFP during light OFF (black) and light ON (green) conditions. The LFP power in the ripple frequency range (100- 250 Hz) is marked by horizontal black bars. \*\* and \*\*\* denote  $p < 0.01$  and  $p < 0.001$ , respectively.

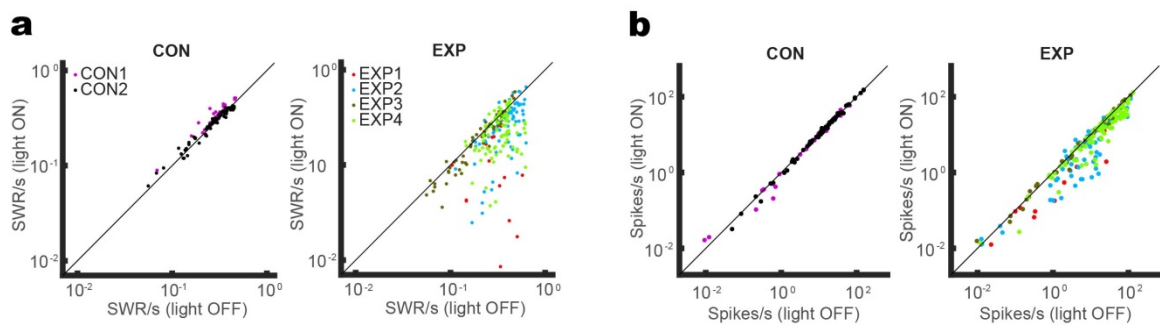


**Figure 3.3 Effect of light on rest-state CA1 activity in individual rats**

a) SWR incidence rate for each tetrode in light ON vs. light OFF conditions colored for individual CON (left) and EXP (right) rats. b) Multi-unit activity for each tetrode in light ON vs. light OFF conditions colored for individual CON (left) and EXP (right) rats. In all of these scatter plots, each dot represents a tetrode.

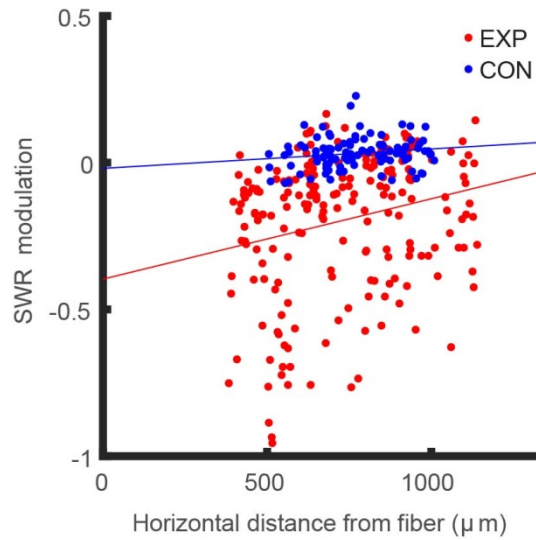


**Figure 3.4: SWR modulation correlates with the tetrodes distance to optical fiber**

The relationship between the horizontal distances of each tetrode from optical fiber and the modulation of the incidence of SWRs by light. A SWR modulation of -1 means complete silencing of SWR incidence, negative values correspond to decreases in SWR incidence, 0 means no effect of light on SWR rate, and positive values correspond to increases in SWR incidence with light. Each dot represents a tetrode and red and blue represent EXP and CON rats, respectively.

We found subtle abnormalities in the expression of SWRs (Figure 3.5). SWR power peak frequency was slightly decreased in EXP rats during ON periods (OFF:  $144.60 \pm 0.71$  Hz; ON:  $140.57 \pm 0.69$  Hz, paired-sample t-test,  $F(1, 224) = 79.10$ ,  $p < 10^{-15}$ , Figure 3.5b), though a slight decrease was also observed in CON tetrodes (OFF:  $146.95 \pm 1.20$  Hz; ON:  $146.33 \pm 1.12$ , paired-sample t-test,  $F(1, 105) = 6.86$ ,  $p < 0.05$ , Figure 3.5b). The decline in SWR power peak frequency in EXP



tetrodes is consistent with previous genetic SC silencing studies (Nakashiba et al., 2009). SWR amplitude was also significantly increased in OFF vs ON states in EXP rats (CON: OFF:  $7.61 \pm 0.07$  sd and ON:  $7.55 \pm 0.08$  sd, paired-sample t-test,  $F(1, 105) = 2.33$ , N.S.; EXP: OFF:  $8.22 \pm 0.11$  sd and ON:  $7.67 \pm 0.09$  sd, paired-sample t-test,  $F(1, 224) = 49.81$ ,  $p < 10^{-10}$ , Figure 3.5c). This may be due to rebound excitation effects caused by seconds-long SC silencing which results in stronger population bursts (Cobb et al., 1995; Harris et al., 2001; Girardeau et al., 2009; Ellender et al., 2010; Papatheodoropoulos, 2010; Stark et al., 2013; Wang et al., 2015). Moreover, SWR duration was shorter in EXP compared to CON tetrodes either in OFF (CON:  $121.06 \pm 1.04$  ms; EXP:  $104.48 \pm 0.80$  ms, two-sample t-test,  $F(1, 330) = 146.25$ ,  $p < 10^{-27}$ ) or ON (CON:  $121.37 \pm 0.93$ ; EXP:  $104.65 \pm 1.23$ , two-sample t-test,  $F(1, 330) = 77.26$ ,  $p < 10^{-16}$ , Figure 3.5d) states which was due to shorter SWRs in Rat EXP4 (OFF:  $96.51 \pm 0.98$  ms; ON:  $90.19 \pm 1.04$  ms,  $F(1,84) = 13.64$ , paired-sample t-test,  $p < 10^{-5}$ ). However, there was no significant effect on modulation of SWR duration in CON (paired-sample t-test,  $F(1, 105) = 0.23$ , N.S.) and EXP (paired-sample t-test,  $F(1, 224) = 0.04$ , N.S.) tetrodes, independently (Figure 3.5d). These findings, most notably the decline in power peak frequency of SWRs, show that SWRs that occur in the SC silencing condition have subtle abnormalities in their properties.

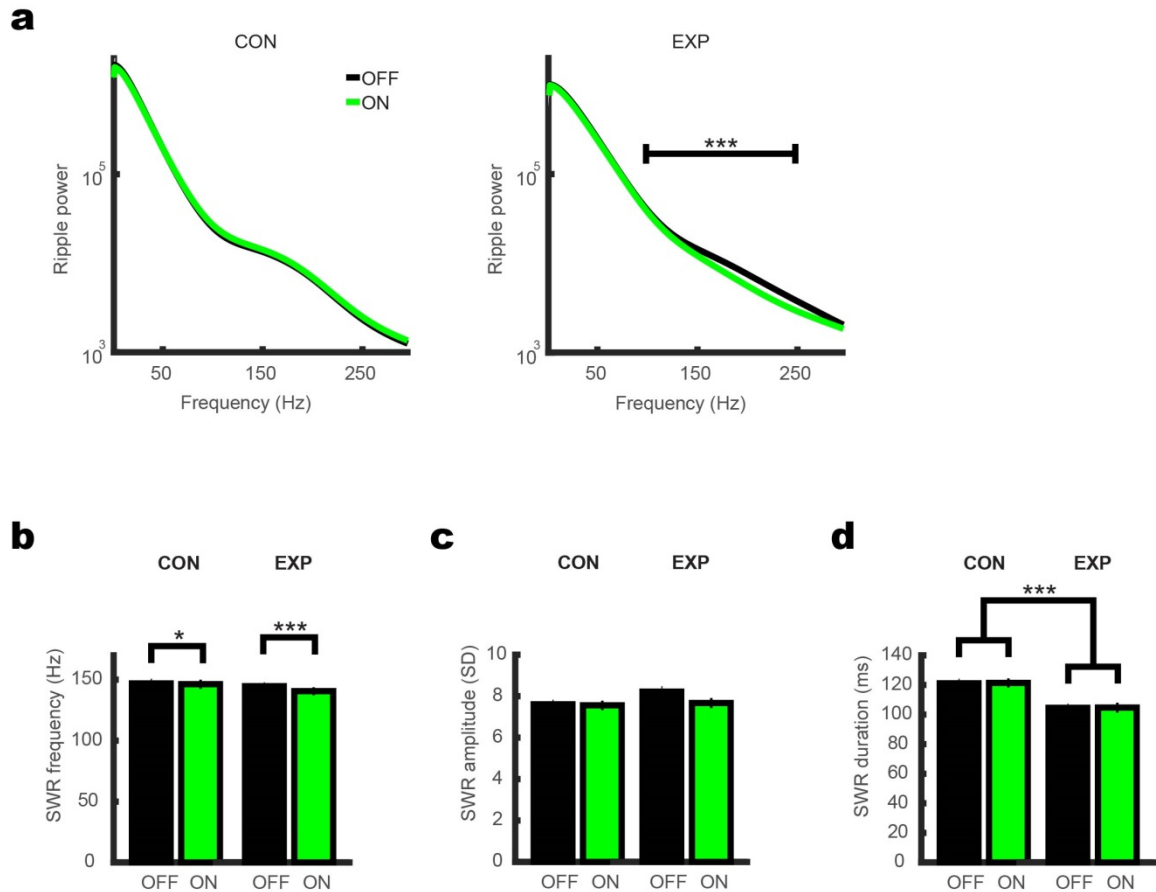


**Figure 3.5: Effect of light on SWR characteristics.**

a) PSD of raw LFP only during SWR time windows and separately calculated for light OFF (black) and light ON (green) conditions in CON (left) and EXP (right) tetrodes. The horizontal black bar denotes the ripple frequency ban. b-d) Ripple peak power frequency (b), z-scored SWR amplitude (c), and SWR duration (d) calculated from SWRs occurring in OFF and ON conditions. \*, \*\*, \*\*\* denote  $p < 0.05$ ,  $p < 0.01$ , and  $p < 0.001$ , respectively.

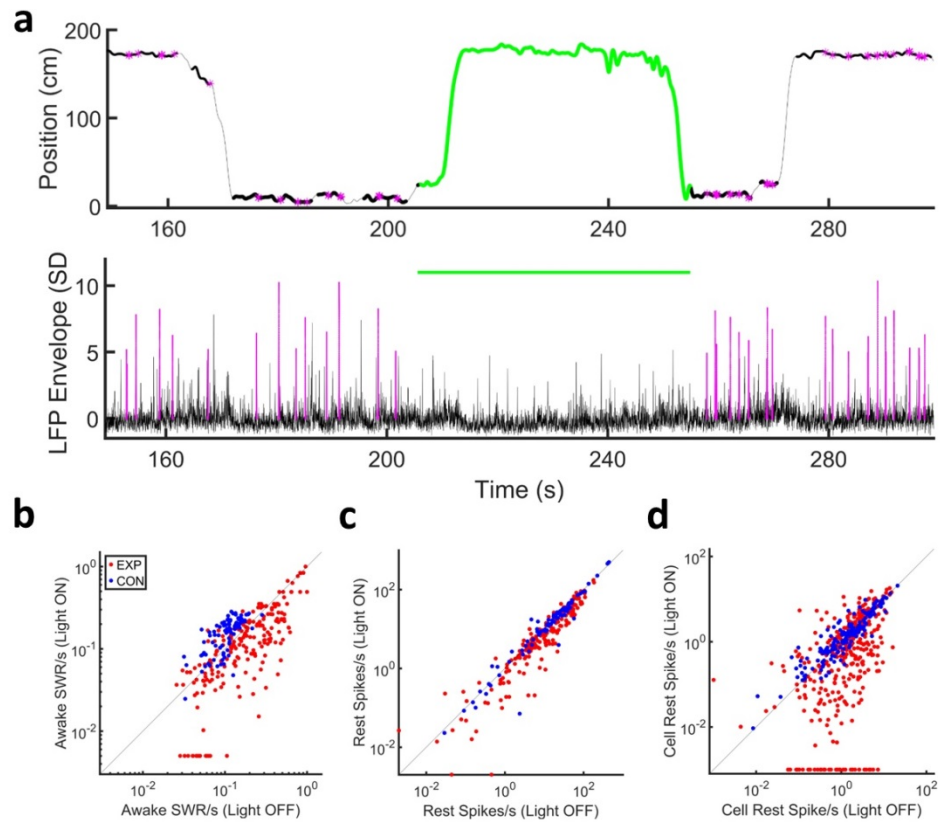
## **CA3 input is necessary for awake SWRs in CA1 during explorative behavior**

It is not clear whether awake SWRs during rest periods of an explorative behavior are generated by a mechanism different than those occurring during rest periods in sleep (Buzsáki, 2015; Oliva et al., 2016). Therefore, we investigated the effect on SWRs recorded in CA1 while silencing SCs. Rats experienced alternating ON and OFF laps while running on a linear track (Figure 3.6a). ON laps consisted of forward run, a pause at one end of the track to consume fluid reward, and then a run to the other end of the track. LFP and spiking activity during consummatory and rest periods, time windows that rats had low speed movements, were investigated (Figure 3.6a). SC silencing strongly suppressed the incidence rate of SWRs in EXP tetrodes, while slightly increasing the incidence rate in CON tetrodes (CON: OFF:  $0.11 \pm 0.01$  SWR/s and ON:  $0.16 \pm 0.01$  SWR/s, paired-sample t-test after logarithmic transformation,  $F(1, 86) = 78.14$ ,  $p < 10^{-12}$ ; EXP: OFF:  $0.23 \pm 0.01$  SWR/s and ON:  $0.17 \pm 0.01$  SWR/s paired-sample t-test after logarithmic transformation,  $F(1,201) = 81.12$ ,  $p < 10^{-15}$ ; Figure 3.6b). These results were observed among all individual rats, except rat CON1 which SWR incidence rate did not change by light (Figure 3.8a). Multi-unit spikes were also significantly suppressed in EXP tetrodes during rest periods on the linear track (CON: OFF:  $39.01 \pm 8.81$  spikes/s and ON:  $39.71 \pm 9.79$  spikes/s, paired-sample

Wilcoxon signed rank test,  $z(1, 84) = 0.29$ , N.S.; EXP: OFF:  $22.87 \pm 2.10$ , ON:  $17.61 \pm 1.76$ , paired-sample Wilcoxon signed rank test,  $z(1, 199) = 7.33$ ,  $p < 10^{-13}$ , Figure 3.6c) and individual EXP rats while did not significantly change in CON rats (Figure 3.7). Similarly, rest-state spiking activity in reward zones of the linear track in EXP putative pyramidal cells are suppressed during ON periods (CON: OFF:  $2.50 \pm 0.25$  Hz and ON:  $2.56 \pm 0.25$  Hz, paired-sample t-test after logarithmic transformation,  $F(1, 153) = 0.36$ , N.S., EXP: OFF:  $2.37 \pm 0.14$  Hz and ON:  $1.78 \pm 0.16$  Hz, paired-sample Wilcoxon signed rank test,  $z(1, 339) = 6.30$ ,  $p < 10^{-9}$ , Figure 3.7). This effect was significant in all individual EXP rats while CON rats did not individually show any significant change (Figure 3.7c). These findings further support the critical role of CA3 in the generation of awake SWRs and rest-state spiking activity in CA1.

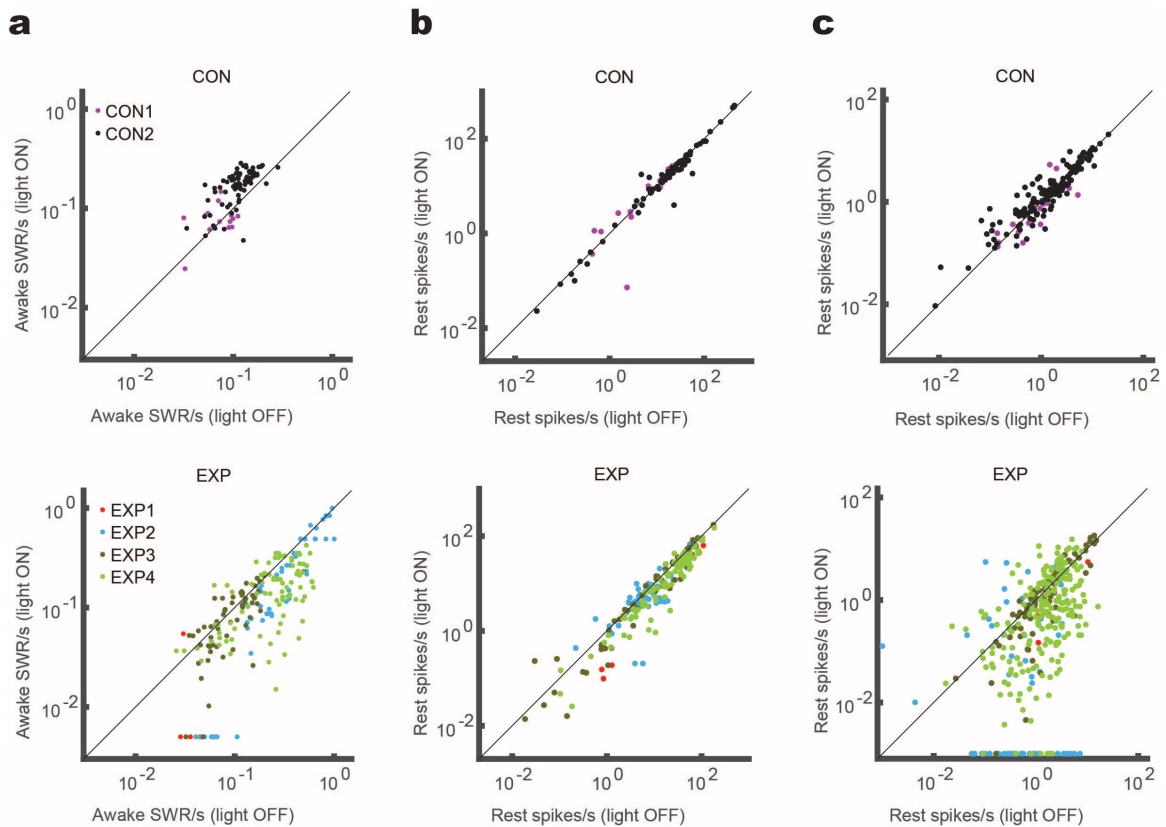
We found subtle abnormalities in the expression of awake SWRs on linear track comparable to the effects in sleep box (Figure 3.8). SWR peak power frequency showed significant yet opposing modulations with SC silencing, by being increased in CON tetrodes and decreased in EXP tetrodes (CON: OFF:  $160.74 \pm 1.94$  Hz and ON:  $163.52 \pm 2.05$  Hz, paired-sample Wilcoxon signed rank test,  $z(1, 77) = -3.46$ ,  $p < 0.001$ ; EXP: OFF:  $149.75 \pm 1.14$  Hz and ON:  $143.90 \pm 1.92$  Hz; paired-sample Wilcoxon signed rank test,  $z(1, 165) = 3.54$ ,  $p < 0.001$ ;

Figure 3.8). Moreover, SWR peak power frequency was lower in EXP SWRs occurring during light OFF period compared to CON (Wilcoxon rank sum test,  $z(1, 245) = -5.11$ ,  $p < 10^{-6}$ , Figure 3.8). Moreover, awake SWR amplitude in EXP tetrodes was slightly lower than CON tetrodes (CON:  $7.74 \pm 0.21$  s.d. and  $7.39 \pm 0.22$  s.d., paired-sample t-test,  $F(1, 86) = 1.95$ , N.S.; EXP: OFF:  $7.50 \pm 0.22$  s.d. and  $6.82 \pm 0.16$  s.d., paired-sample Wilcoxon signed rank test,  $z(1, 201) = 2.55$ ,  $p = 0.01$ , Figure 3.8). Similar to the sleep box, while SWR duration was significantly shorter in EXP compared to CON tetrodes both in ON and OFF states, neither EXP nor CON showed a modulation by light (CON: OFF:  $124.20 \pm 2.55$  ms and ON:  $125.87 \pm 1.86$  ms, paired-sample Wilcoxon signed rank test,  $z(1, 86) = -1.03$ , N.S.; EXP: OFF:  $96.65 \pm 1.26$  ms and ON:  $95.33 \pm 1.64$  ms, paired-sample t-test,  $F(1, 184) = 0.02$ , Figure 3.8). Overall, these findings may indicate that the mechanisms for awake SWR generation in CA1 during the rest period of an explorative task are similar to the ones during slow-wave sleep and quite wakefulness in sleep box.



**Figure 3.6: CA3 input is necessary for awake SWRs in CA1 in exploratory behavior.**

a) An example tetrode in CA1 region shows strong SWR modulation by SC silencing (above) when a rat stays at one end of track. Each magenta star marker (above) and signal (below) depicts a detected SWR event. The thick black line shows the moments that the rat's speed was less than 7 cm/sec ("rest" time spans). b) Incidence of SWR events for each tetrode in light ON vs. light OFF conditions only considering rest moments. c) multi-unit spiking activity in each tetrode in light ON vs. light OFF conditions. d) Single unit spiking activity for each putative pyramidal cell recorded from CA1 in light ON vs. light OFF conditions. In b and c, each dot represents a tetrode. In d, each dot it represents a CA1 pyramidal cell. Blue and red colors represent EXP and CON rats, respectively. Tetrodes or cells that were completely silenced were assigned with a fixed low value only for visualization purpose in these logarithmic plots.



**Figure 3.7: SC silencing effect on CA1 activities of individual explorative rats**

a) Awake SWR incidence rate for each tetraode in light ON vs. light OFF conditions colored for individual CON (left) and EXP (right) rats. b) Multi-unit spiking activity for each tetraode in light ON vs. light OFF conditions colored for individual CON (left) and EXP (right) rats. c) Single unit spiking activity for each putative pyramidal cell recorded from CA1 in light ON vs. light OFF conditions colored for different rats. In a and b, each dot represents a tetraode. In c, each dot represents a CA1 pyramidal cell. Tetraodes or cells that were completely silenced were assigned with a fixed low value only for visualization purpose in these logarithmic plots.

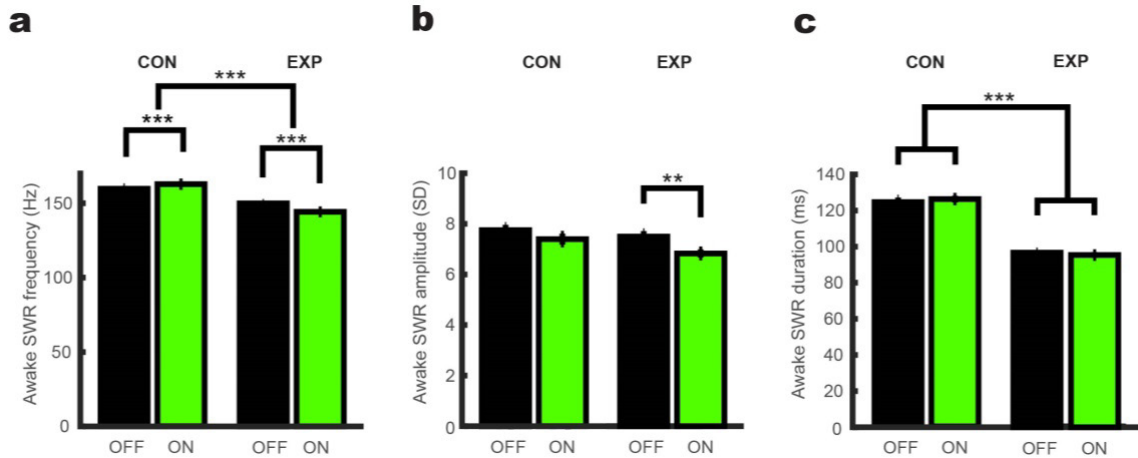


**Figure 3.8: Subtle abnormalities in awake SWRs**

a-c) Ripple peak power frequency (a), z-scored SWR amplitude (b), and SWR duration (c) calculated from SWRs occurring in OFF and ON conditions in CON (left) and EXP (right) rats. \*\* and \*\*\* denote  $p < 0.01$  and  $p < 0.001$ , respectively.

### **CA3 input is necessary for normal place cell responses**

Although chronic lesioning and genetic silencing studies do not show a major contribution from CA3 in expression of CA1 place fields in a familiar environment, transient optogenetic silencing of CA3 could demonstrate a real-time effect. 219 and 488 cell clusters were manually defined in neural spike recordings from CON and EXP rats in run sessions, respectively, and among them 140 and 325 clusters showed qualified place fields in at least one direction on the familiar linear track (see Chapter 2). Also, 9 and 49 putative fast-spiking interneurons were defined in CON and EXP rats, respectively. Overall, CON and EXP place cells respectively expressed 233 and 534 qualified directional place



fields in either ON or OFF periods which were calculated independently (Figure 3.9). Laser illumination did not impair expression of place fields in CON place cells (Figure 3.9a-b and Figure 3.11). In contrast, the majority of EXP place fields substantially, or in many cases completely, were suppressed (Figure 3.9c-d and Figure 3.12). In addition, a few silent cells became active by expressing place fields and some place cells also enhanced their in-field activity (Figure 3.13). Figure 3.10 also shows the effect of SC silencing on CA1 place fields separated by rats. Rat EXP1 is not shown in this figure due to its low number of qualified place fields, although three out of its four fields were strongly modulated and suppressed by light. Altogether, CA1 cell populations in EXP rats show a general decrease in their place field firing which requires further analysis (Figure 3.9 and Figure 3.10).

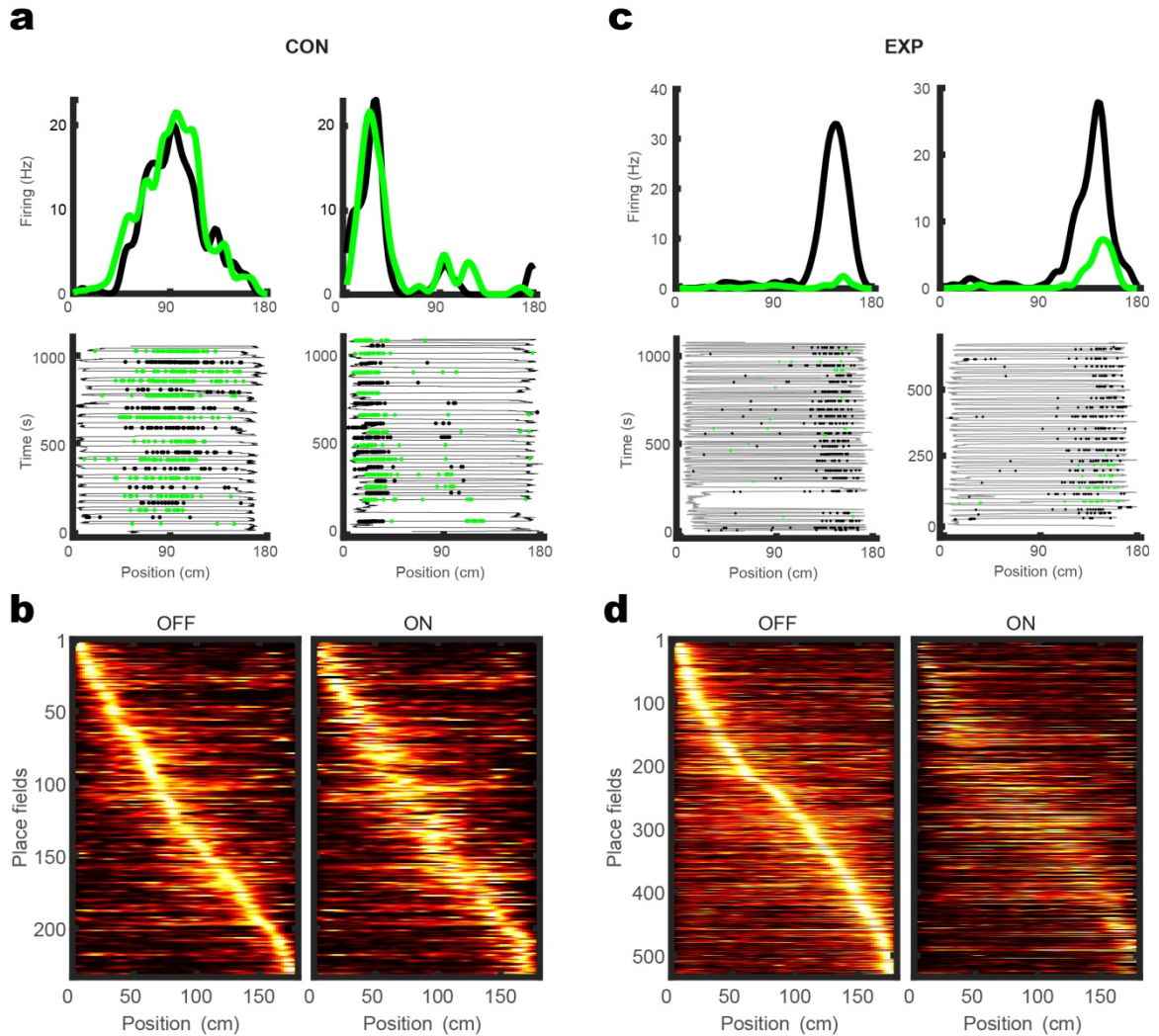


**Figure 3.9: SC silencing suppresses place fields in CA1.**

a) Top: two example CA1 place fields for light OFF (black) and ON (green) conditions in a CON rat. Bottom: Rat position as a function of time during linear track traversals (thin line), overlaid with spiking activity of the above place cell (dots). Spikes in OFF and ON conditions are shown as black and green dots, respectively. b) All 236 CON place fields sorted by their OFF peak firing position on the linear track. Each row depicts color map of a place field in light OFF (left) and light ON (right) conditions. Both OFF and ON fields are normalized by maximum peak firing rate in either conditions. c-d) Two

example CA1 place field (c) and all 534 sorted fields from EXP rats (d). Details are as described for a-b.

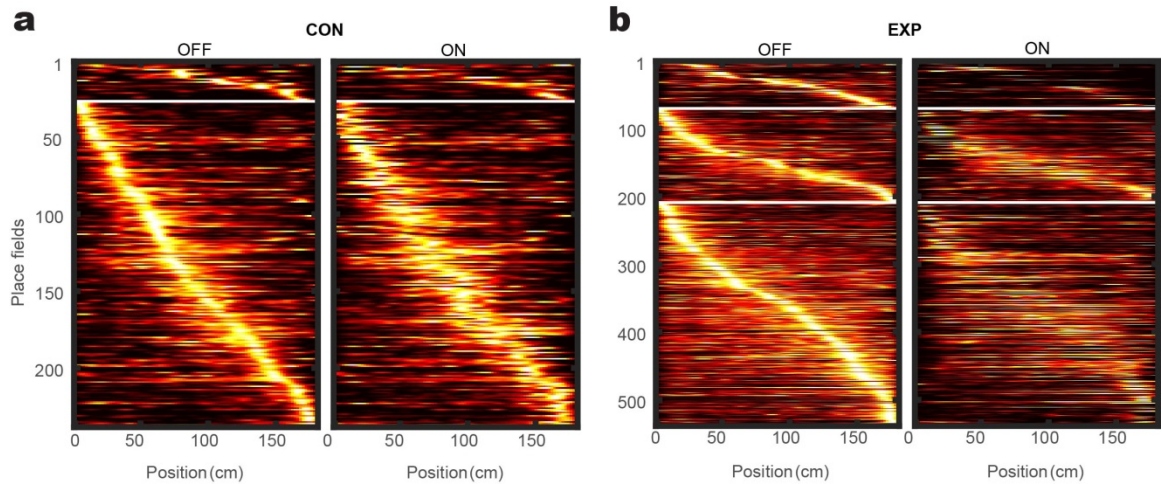


**Figure 3.10: Place cell firing in CON and EXP rats.**

a-b) All place fields for two CON (a) and three EXP rats (b) are sorted by their peak firing position on linear track during light OFF condition. Each row depicts color map of a place field in light OFF (left) and ON (right) conditions. Both OFF and ON fields are normalized by maximum peak firing rate in either conditions. Because only four place fields were recorded in Rat EXP1, it is excluded from b for visualization purposes.

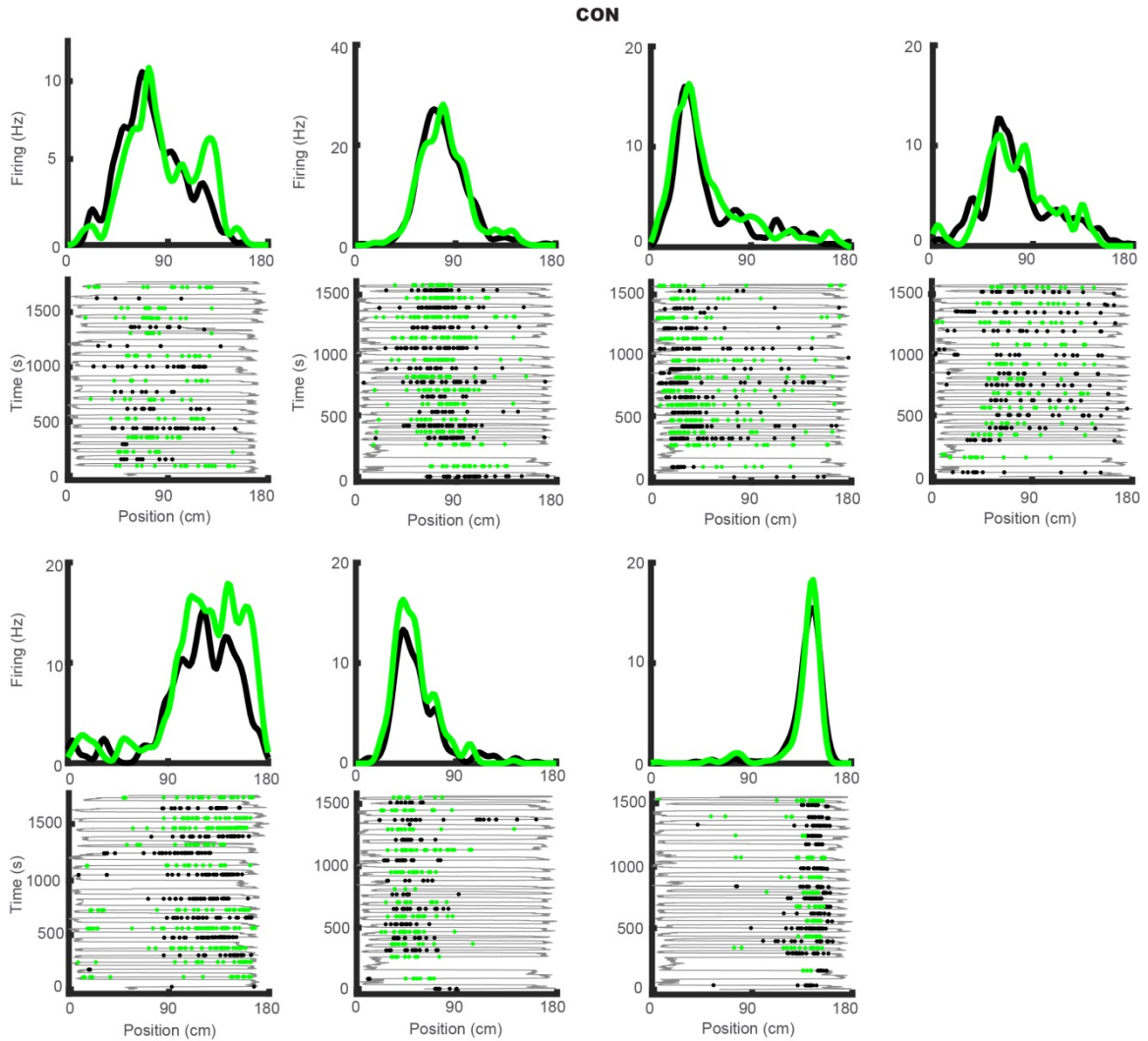


**Figure 3.11: Examples of CON place fields**

Seven examples of CA1 place fields for light OFF (black) and ON (green) conditions in CON rats. In bottom of each place field panel, rat position is shown as a function of time during linear track traversals (thin line), overlaid with spiking activity of the above place cell (dots). Spikes in OFF and ON conditions are shown as black and green dots, respectively.

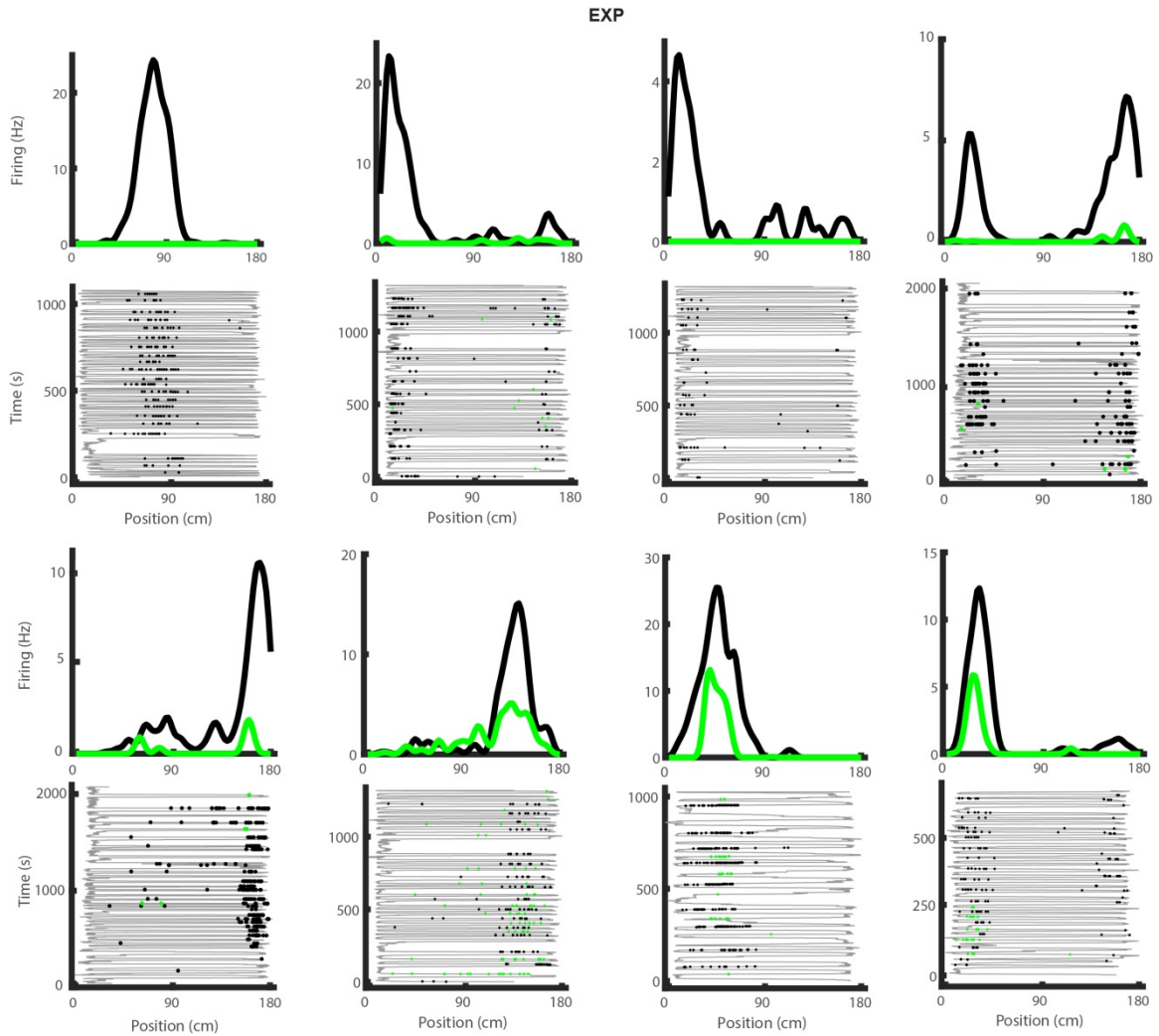


**Figure 3.12: Examples of suppressed EXP place fields**

Eight examples of CA1 place fields for light OFF (black) and ON (green) conditions in EXP rats. In bottom of each place field panel, rat position is shown as a function of time during linear track traversals (thin line), overlaid with spiking activity of the above place cell (dots). Spikes in OFF and ON conditions are shown as black and green dots, respectively.

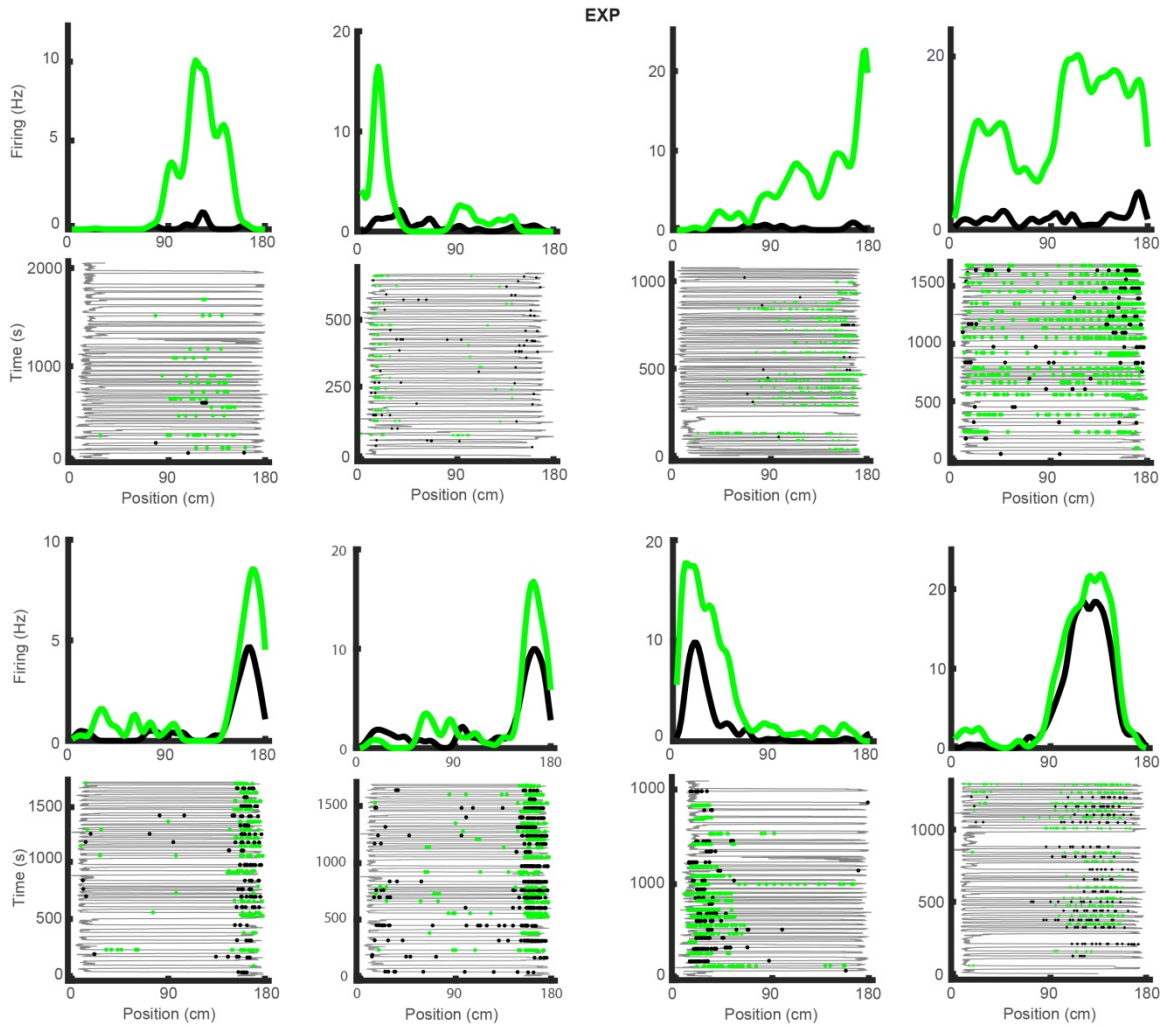


**Figure 3.13: Examples of emerged and enhanced EXP place fields**

Eight examples of CA1 place fields for light OFF (black) and ON (green) conditions in EXP rats. In bottom of each place field panel, rat position is shown as a function of time during linear track traversals (thin line), overlaid with spiking activity of the above place cell (dots). Spikes in OFF and ON conditions are shown as black and green dots, respectively.

We quantified the effect of SC silencing on place cell properties and we found that the majority of place fields are heavily suppressed during light ON periods (Figure 3.14a). Place field peak firing (CON: OFF:  $12.79 \pm 0.64$  Hz and ON:  $13.20 \pm 0.64$  Hz, paired-sample t-test after logarithmic transformation,  $F(1, 235) = 0.65$ , N.S.; EXP: OFF:  $8.98 \pm 0.29$  Hz and ON:  $7.03 \pm 0.33$  Hz, paired-sample Wilcoxon signed rank test,  $z(1, 533) = 8.81$ ,  $p < 10^{-17}$ , Figure 3.14a) and place field size (CON: OFF:  $100.74 \pm 3.26$  cm and ON:  $99.96 \pm 3.18$  cm, paired-sample Wilcoxon signed rank test,  $z(1, 235) = 0.87$ , N.S.; EXP: OFF:  $109.30 \pm 2.42$  cm and  $74.52 \pm 2.74$  cm; paired-sample Wilcoxon signed rank test,  $z(1, 533) = 14.47$ ,  $p < 10^{-4}$ , Figure 3.14b) were significantly suppressed in EXP place cells during run. In addition to place cells, the firing rate of putative interneurons also slightly decreased in EXP animals (CON: OFF:  $22.56 \pm 3.79$  Hz and ON:  $21.49 \pm 3.56$  Hz, paired-sample t-test after logarithmic transformation,  $F(1, 16) = 1.65$ , N.S.; EXP: OFF:  $23.40 \pm 1.97$  Hz and ON:  $21.00 \pm 1.78$ , paired-sample t-test after logarithmic transformation,  $F(1, 88) = 8.99$ ,  $p < 0.005$ ). On the other hand, spatial information, which measures how much information a spike gives about animal's position, while is significantly decreased in EXP place fields in light OFF condition compared to CON, which may be due to their slightly larger place fields, significantly increase in light ON condition (CON: OFF:  $0.90 \pm 0.04$  bits/spike and ON:  $0.84 \pm 0.04$

bits/spike, paired-sample t-test after logarithmic transformation,  $F(1, 235) = 5.52$ ,  $p < 0.02$ ; EXP: OFF:  $0.57 \pm 0.02$  bits/spike and ON:  $0.89 \pm 0.04$  bits/spike, paired-sample t-test after logarithmic transformation,  $F(1, 494) = 93.29$ ,  $p < 10^{-19}$ ; also to compare light OFF conditions in CON and EXP rats: two-sample t-test after logarithmic transformation,  $F(1, 729) = 78.06$ ,  $p < 10^{-17}$ , Figure 3.14c). The increase in spatial information is consistent with the decreased peak firing rate and field size in light ON condition in EXP place cells. Overall, these results show that the extent of CA1 place cell firing pattern is heavily dependent on CA3 input.

To find whether SC silencing results in changes in the peak position of place field we calculated the center of mass (COM) and spatial correlation, two field properties that are independent of the magnitude of place cell firing. These, these measures showed converging results (Figure 3.14d and Figure 3.15). During light ON condition, COM slightly shifted rightward in both CON and EXP rats (CON: OFF:  $95.62 \pm 2.13$  cm and  $97.56 \pm 2.19$ , paired-sample t-test,  $F(1, 225) = 7.81$ ,  $p < 0.01$ ; EXP: OFF:  $88.69 \pm 1.58$  cm and ON:  $90.91 \pm 1.75$  cm, paired-sample t-test,  $F(1, 338) = 5.17$ ,  $p < 0.05$ , Figure 3.14d). Place fields with low spatial coherence ( $< 0.2$ ) are excluded from COM and spatial correlation analyses. This slight shift is because of the delay caused by the manual switching of laser light when rats start to run which results in place fields with suppressed tails at the beginning of



the track in some recording sessions (Figure 3.16d). In other words, this is simply a sampling error, where specific parts of the track where light was turned on were poorly or not at all sampled, leading to measured field positions during ON laps that were shifted artifactually.

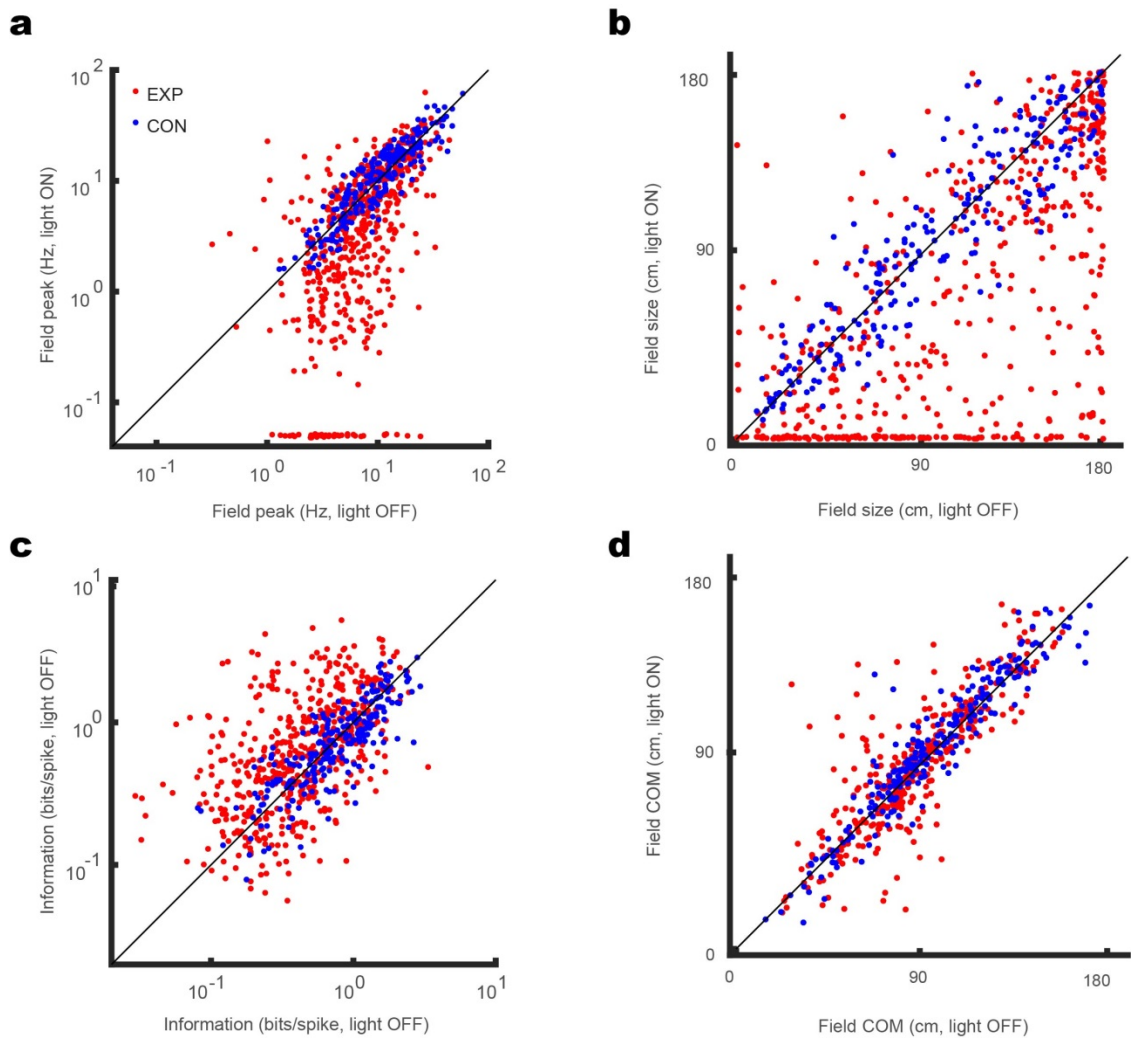


**Figure 3.14: SC silencing suppresses CA1 place cell activity.**

a-d) Four place field characteristics including peak firing rate (a), field size (b), spatial information (c), and center of mass (COM, d) are plotted in light ON vs. light OFF

conditions. In all plots, each dot represents a place field and red and blue colors represent EXP and CON rats, respectively.

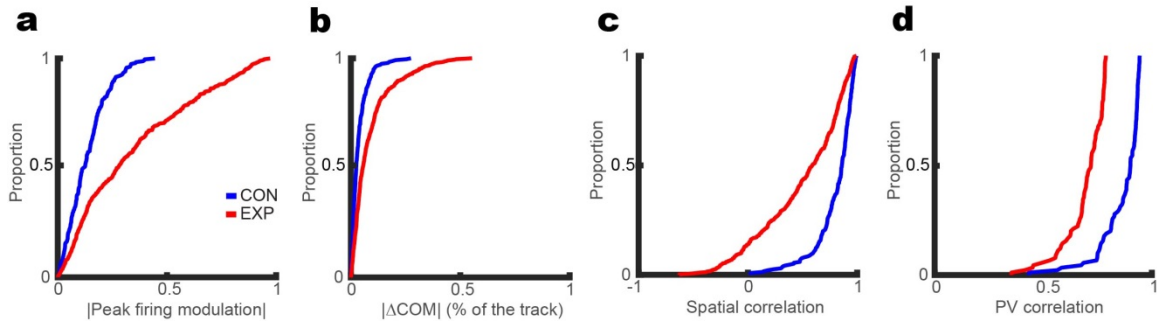


**Figure 3.15: Cumulative density analysis depicts remapping-like effects in CA1 place fields**

a-b) Cumulative density plot of the absolute value of the modulation index of peak firing rate (a) and absolute shift in COM (b) of place fields during light ON vs. light OFF conditions in CON (blue) and EXP (red) rats. c-d) Spatial (c) and PV (d) correlation of place fields in light ON vs. light OFF conditions.

However, the extent of the shift in COM was significantly greater in EXP compared to CON place fields ( $|\Delta\text{COM}|$ : CON:  $6.59 \pm 0.48$  cm and EXP:  $11.70 \pm 0.66$  cm, two-sample Wilcoxon rank sum test,  $z(1, 563) = -6.16$ ,  $p < 10^{-9}$ , cumulative density plot is shown in Figure 3.15b). On the other hand, spatial correlation and population vector (PV) correlation, which compares cell population responses for each track position bin, significantly decreased in EXP place fields (spatial correlation: CON:  $0.81 \pm 0.01$  and EXP:  $0.64 \pm 0.02$ , two-sample t-test after Fisher Z transform,  $F(1, 563) = 71.26$ ,  $p < 10^{-15}$ , cumulative

density plot is shown in Figure 3.15c; PV correlation: CON:  $0.87 \pm 0.01$  and EXP:  $0.69 \pm 0.01$ , paired-sample Wilcoxon signed rank test after Fisher Z transform,  $z(1, 729) = 8.24$ ,  $p < 10^{-16}$ , cumulative density plot is shown in Figure 3.15d).

Overall, no shift in COM but a decline in spatial correlation may be explained by a “subtractive” rather than a “scalar” (e.g. multiplicative) suppression model (Figure 3.16). While different extents of subtractive suppression do not change COM, spatial correlation which is sensitive to the firing pattern gradually declines due to the cut tails of a place field during light ON condition (Figure 3.16). Therefore, removing CA3 inputs to CA1 results in substantial decrease in place cell firing rate, resembling the phenomenon of “rate remapping”, where place cells change their place field peak firing in response to changes in environmental cues, but do not undergo a major shift in place field positions.

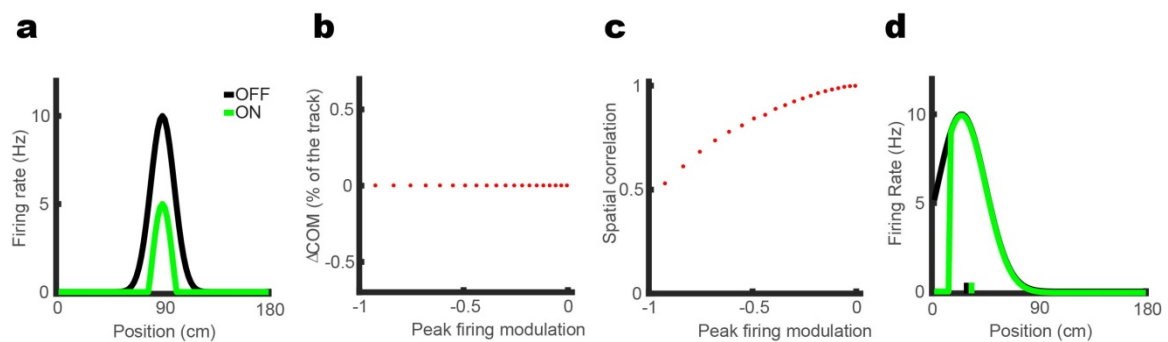


**Figure 3.16: Place fields undergo subtractive suppression and resemble rate remapping**

a-c) A simple subtractive suppression model (a) may explain both the lack of change in COM (b) and decrease in spatial correlation (c). In this schematic place cell varying the amount of place field suppression from 0.1 to 9.9 Hz results in nonlinear changes in spatial correlation while COM remains unchanged. (d) a hypothetical place field shows a rightward shift in its COM if animal is not exposed to a fraction of the linear track during light ON (green) condition. Two small vertical lines show calculated COMs. Black and green, denote light OFF and light ON conditions, respectively.

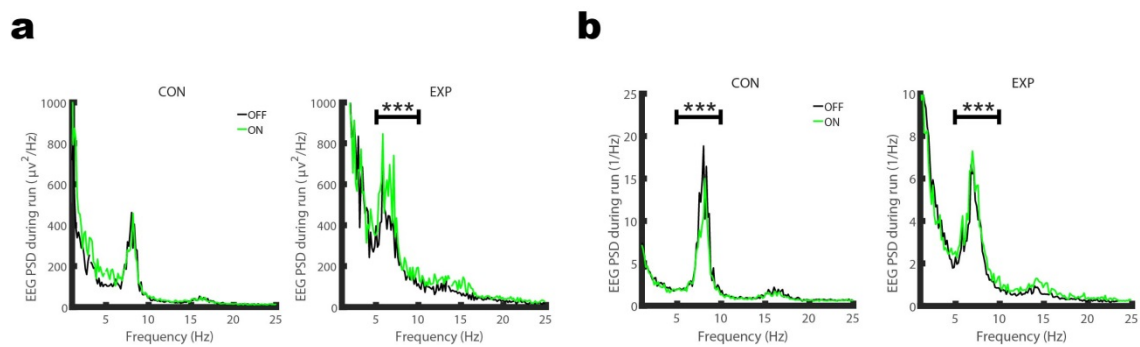


**Figure 3.17: SC silencing increases theta power during explorative behavior**

a) PSD of raw CA1 EEG during track traversals in light OFF (black) and light ON (green) conditions. The theta frequency band (5-10 Hz) is marked by the black bar. b) PSD of Z-scored CA1 LFP. Same format as a. \*\*\* denotes  $p < 0.001$ .

### **SC silencing increases theta power and place cell theta locking**

During exploration, the hippocampal LFP is dominated by a theta rhythm of 5-10 Hz that is essential for the fine temporal scale activity of place cells. While traversing its place field, a place cell fires at progressively earlier theta phases, a phenomenon known as theta phase precession (O'Keefe and Recce, 1993; Skaggs et al., 1996). However, the mechanisms of formation of hippocampal theta

rhythm, and associated neural activity resulting in theta phase precession are not well understood (Hales et al., 2014; Vandecasteele et al., 2014; Schlesiger et al., 2015; Middleton and McHugh, 2016).

Therefore, we next examined the contribution of CA3 input to CA1 synchronous activity during exploratory behavior. CA1 theta power during run increased in EXP tetrodes during ON laps (CON: OFF:  $996.82 \pm 105.82 \mu\text{V}^2$  and ON:  $1042.20 \pm 145.05 \mu\text{V}^2$ , paired-sample t-test after logarithmic transformation,  $F(1, 89) = 2.14$ , N.S.; EXP: OFF:  $1757.77 \pm 461.25 \mu\text{V}^2$  and ON:  $2261.69 \pm 521.78$ , paired-sample t-test after logarithmic transformation,  $F(1, 211) = 12.82$ ,  $p < 5 \times 10^{-4}$ , Figure 3.17a). Z-scored EEG shows similar increase in theta power in EXP tetrodes, though CON tetrodes show slightly decreased theta power in ON periods (CON: OFF:  $32.37 \pm 2.49$  and ON:  $25.96 \pm 2.31$ , paired-sample Wilcoxon signed rank test,  $z(1, 89) = 3.80$ ,  $p < 5 \times 10^{-4}$ ; EXP: OFF:  $16.27 \pm 1.04$  and ON:  $20.66 \pm 1.35$ , paired-sample Wilcoxon signed rank test,  $z(1, 211) = -4.72$ ,  $p < 10^{-5}$ , Figure 3.17b). The lower z-scored theta power values in EXP compared to CON is due to lower frequency background activity in EXP tetrodes which scaled the normalization. These results show that suppressing CA3 input to CA1 increases theta-dominated activity in CA1 circuit, which might happen by disinhibition of cortical and medial septal inputs to CA1 (Vandecasteele et al., 2014).

Moreover, we found increased rhythmicity in spiking activity when CA3 input to CA1 was inhibited during run (Figure 3.18). In EXP animals and during light ON condition, not only the preferred phases of place cells to theta rhythms, at an ensemble level, became uniformly distributed (CON: OFF:  $2.16 \pm 0.09$  rad, Rayleigh test for circular non-uniformity,  $z(1, 165) = 20.88$ ,  $p < 10^{-9}$  and ON:  $2.21 \pm 0.09$  rad, Rayleigh test for circular non-uniformity,  $z(1, 179) = 13.26$ ,  $p < 10^{-5}$ , two-sample Watson-Williams test,  $F(1, 344) = 0.07$ , N.S.; EXP: OFF:  $-0.14 \pm 0.07$  rad, Rayleigh test for circular non-uniformity,  $z(1, 325) = 3.21$ ,  $p < 0.05$ ; ON:  $-1.11 \pm 0.09$  rad, Rayleigh test for circular non-uniformity,  $z(1, 240) = 0.20$ , N.S.; only place fields with significant tuning to theta were considered for these analyses, Figure 3.18 and Figure 3.19c), but also their locking strength measured by circular mean resultant vector (MRV) did significantly increase (CON: OFF:  $0.28 \pm 0.01$  and ON:  $0.27 \pm 0.01$ , two-sample t-test after logarithmic transformation,  $F(1, 344) = 1.46$ , N.S.; EXP: OFF  $0.24 \pm 0.01$  and ON:  $0.30 \pm 0.01$ , two-sample t-test after logarithmic transformation,  $F(1, 564) = 19.56$ ,  $p < 10^{-4}$ , Figure 3.18 and Figure 3.19a).

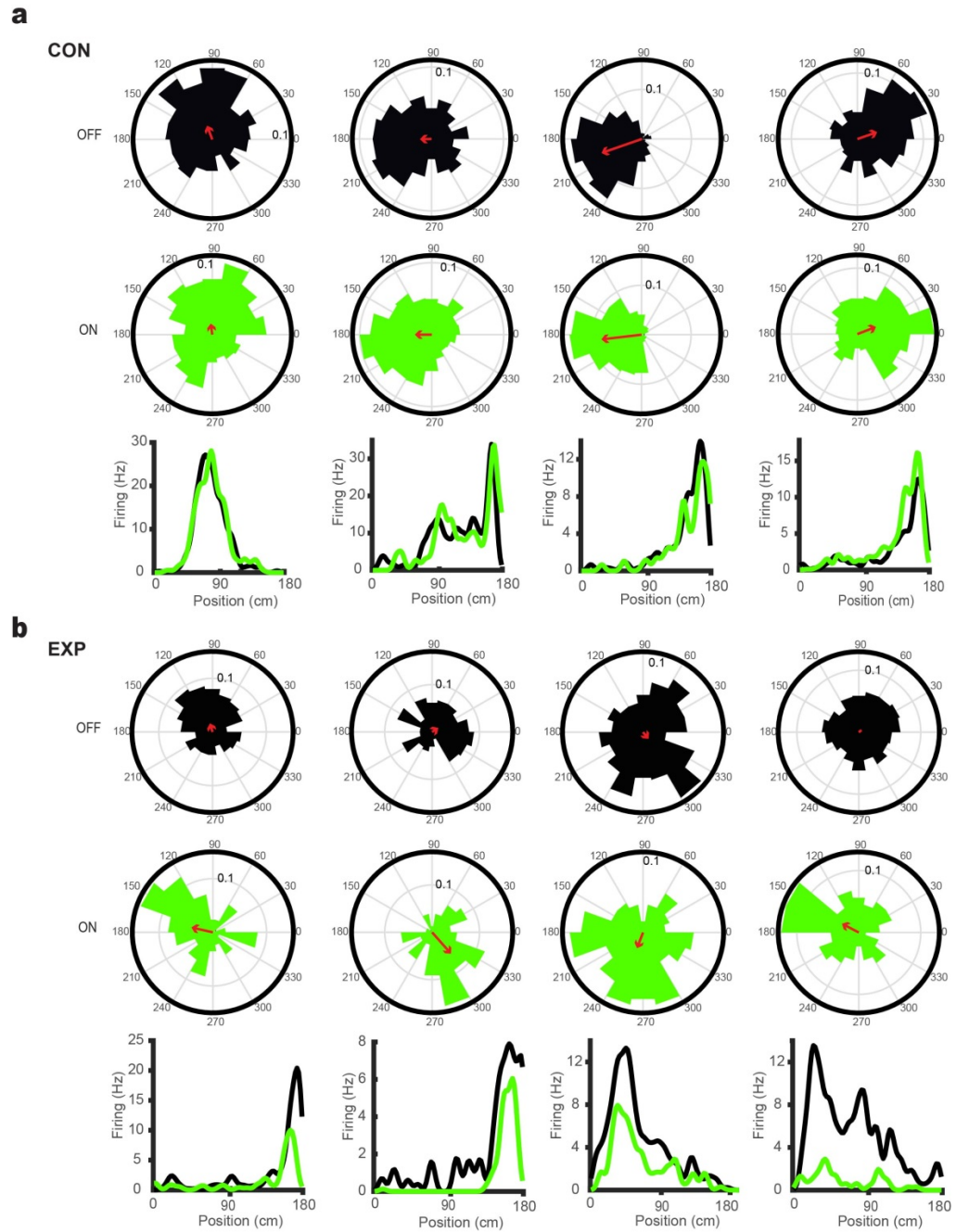


**Figure 3.18: Examples of place cell theta locking**

a) Four examples of place cell theta locking in CON rats. Theta phase preference of individual place fields is shown during light OFF (top polar plot) and light ON (bottom polar plot) conditions. The red bar in each polar plot indicates the MRV for each

condition. The bottom panel shows each associated place field in OFF (black) and ON (green) conditions. b) Four examples of place cell theta locking in EXP rats. Same format as (a).

To remove the possible effect of place field peak firing on MRV values, CON and EXP data were corrected by a linear regression model driven from CON data. EXP fields with significantly tuned spiking to theta showed an increase in their MRVs in light ON compared to the CON light ON condition (CON:  $0.08 \pm 0.01$ ; EXP:  $0.11 \pm 0.01$ , two-sample Wilcoxon rank sum test,  $z(1, 316) = -2.59$ ,  $p < 0.01$ , Figure 3.19b). MRVs were corrected by a linear regression model driven from CON data and only place fields with significant tuning to theta in both light OFF and light ON conditions were considered for these analyses. Moreover, while CON phases show a statistically significant preference at a population level, EXP phases lose their population preference during light ON condition (CON: OFF:  $2.17 \pm 0.09$  rad, Rayleigh test for circular non-uniformity,  $z(1, 166) = 20.88$ ,  $p < 10^{-9}$  and ON:  $2.21 \pm 0.09$ , Rayleigh test for circular non-uniformity,  $z(1, 180) = 13.26$ ,  $p < 10^{-5}$ ; two-sample Watson-Williams test for circular comparison of OFF vs ON mean phases in CON place fields:  $F(1, 344) = 0.07$ , N.S.; EXP: OFF:  $-0.14 \pm 0.07$ , Rayleigh test for circular non-uniformity,  $z(1, 326) = 3.21$ ,  $p < 0.05$  and ON:  $-1.1 \pm 0.09$  rad, Rayleigh test for circular non-uniformity,  $z(1, 240) = 0.20$ ,



N.S.; only place fields with significant phase preference were considered for this analysis). These results imply that while CA3 input is essential for the tuning of theta phase preference of CA1 place cells, it inhibits the extent of locking of place cell spikes to theta rhythm.

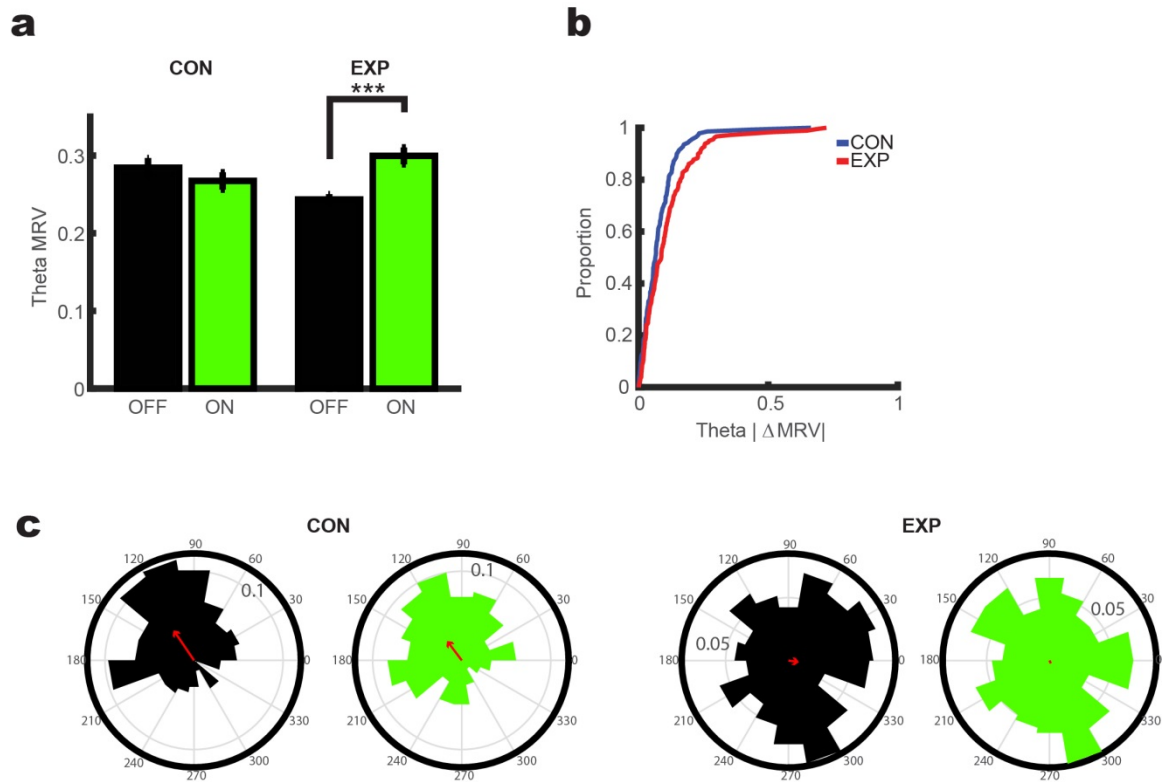


**Figure 3.19: SC silencing increases place cell theta locking and diminishes population phase preference.**

a) Place cell theta locking strength measured by MRV in CON (left) and EXP (right) place fields during light OFF (black) and light ON (green) conditions. Only place fields with significant tuning to theta were considered for these analyses. b) Cumulative distribution of the corrected absolute difference of MRV in light OFF and light ON conditions shows a rightward shift in EXP (red) versus CON (blue) rats. \*\*\* denotes  $p <$

0.001. c) Distribution of the preferred phases of place fields in light OFF (black) and light ON (green) conditions in CON (left) and EXP (right) rats. Red arrow denotes the population MRV.

In spite of increased theta locking in EXP place cells during light ON condition, theta phase precession is not impaired in these cells. While phase precession slopes of all place fields become slightly steeper (CON: OFF:  $-1.64 \pm 0.1$  and ON:  $-1.60 \pm 0.10$ , paired-sample Wilcoxon signed rank test,  $z(1, 235) = -0.37$ , N.S.; EXP: OFF:  $-1.5 \pm 0.07$  and ON:  $-1.77 \pm 0.09$ , paired-sample Wilcoxon signed rank test,  $z(1, 399) = 2.47$ ,  $p < 0.05$ ), place fields with statistically significant slopes did not change during light ON condition (CON: OFF:  $-1.65 \pm 0.14$  and  $-1.72 \pm 0.13$ , two-sample Wilcoxon rank sum test,  $z(1, 201) = 0.33$ , N.S.; EXP: OFF:  $-1.44 \pm 0.11$  and ON:  $-1.62 \pm 0.13$ , two sample Wilcoxon rank sum test,  $z(1, 288) = 1.36$ , N.S., Figure 3.20 and Figure 3.21). On the other hand, the distribution of phase offsets of phase precession regression lines were not significantly different from uniform distribution and therefore were not statistically comparable in light OFF and light ON conditions in either CON or EXP place cell populations (CON: OFF:  $3.00 \pm 0.01$  rad, Rayleigh test for circular non-uniformity,  $z(1, 99) = 1.16$ , N.S. and ON:  $-2.65 \pm 0.01$  rad, Rayleigh test for circular non-uniformity,  $z(1, 106) = 3.89$ ,  $p < 0.05$ ; EXP: OFF:  $1.28 \pm 0.01$  rad,

Rayleigh test for circular non-uniformity,  $z(1, 196) = 0.15$ , N.S.; ON:  $2.92 \pm 0.01$  rad, Rayleigh test for circular non-uniformity,  $z(1, 131) = 1.10$ , N.S.; only place fields with significant phase precession were considered for this analysis).

Overall, these findings show that even with the lack of CA3 input, CA1 place cells could significantly entrain to the theta rhythm, without theta phase precession being affected. Moreover, they imply that CA3 might inhibit theta activity in CA1, and that phase precession in CA1 place cells either is generated locally or comes from outside the hippocampus, possibly from MEC.

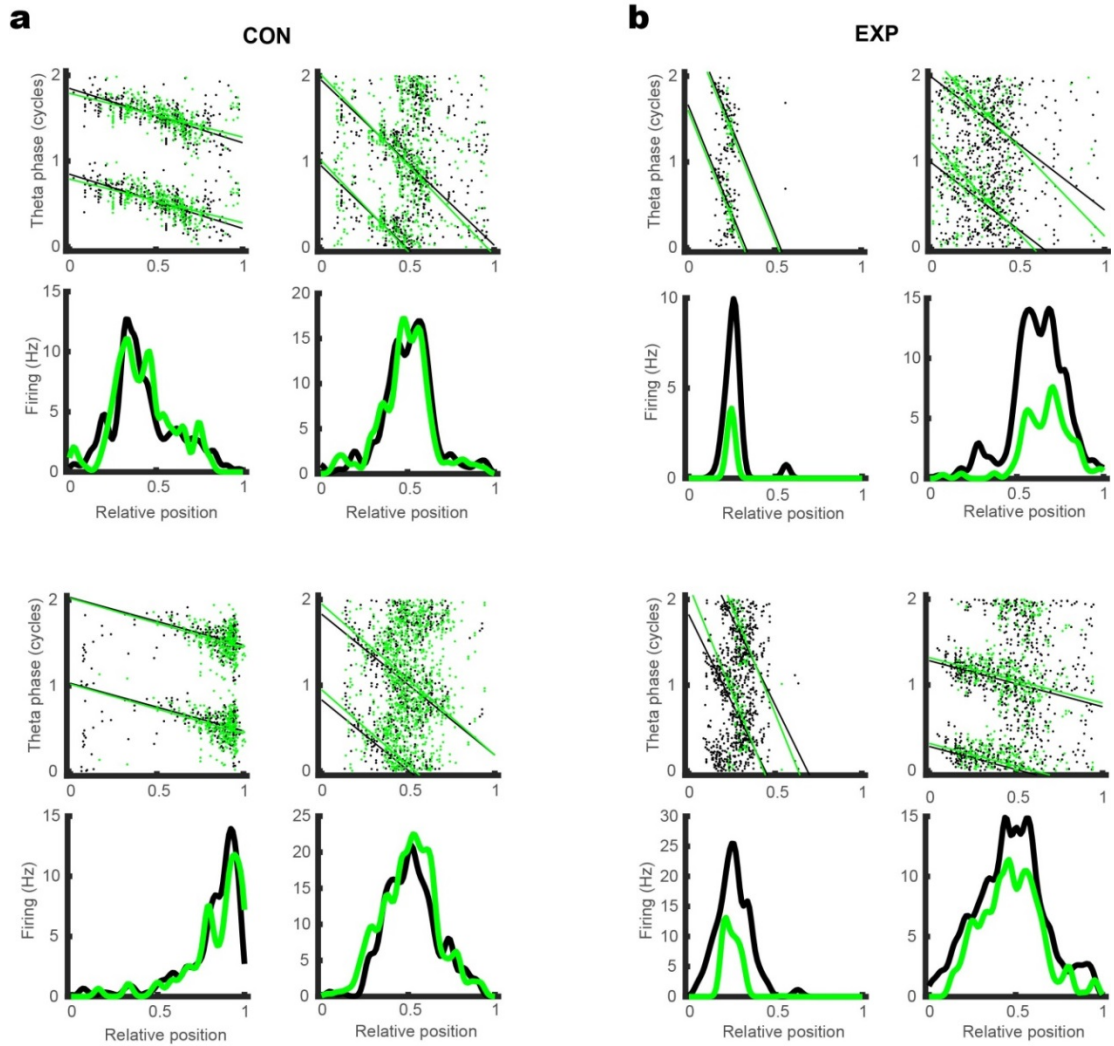


**Figure 3.20: Examples of place cell theta phase precession**

a) Four examples of place cell theta phase precession in CON rats. Top: each dot represents the theta phase of individual spikes occurring either during light OFF (black) or light ON (green) conditions in relation to its relative position on the linear track. Bottom: associated place fields in light OFF (black) and light ON (green) conditions. b) Four examples of place cell theta phase precession in EXP rats. Same format as in (a)

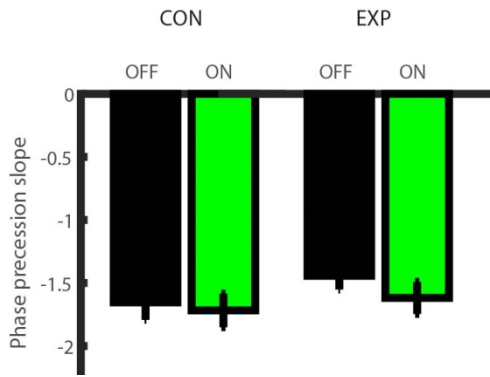


**Figure 3.21: SC silencing does not affect phase precession slope**

Phase precession slope does not significantly change in light ON (green) versus light OFF (black) conditions in place fields with significant phase precession in CON (left) and EXP (right) rats.

## Discussion

We have shown that CA3 input to CA1 is necessary for the formation of SWRs in hippocampal output circuitry during consummatory behavior.

Transient optogenetic silencing of SCs dramatically decreases the incidence rate of CA1 SWRs and partially degrades the normal properties of the ones that still occur under the silencing. Furthermore, during preparatory behavior, CA1 place fields are heavily suppressed in absence of CA3 input. Although the extent of place cell firing is significantly reduced, CA1 cells do not show major global remapping. Moreover, while SC silencing enhances the entrainment of CA1 place cells to theta rhythm and abolishes the population preference among phases, but does not affect theta phase precession in these cells (Figure 3.19 and Figure 3.21).

Altogether, CA3 is essential in the formation of SWRs, the normal expression of place field firing in CA1, and plays an inhibitory role to theta-dominated activity in CA1.

There are two pathways, direct and indirect, for cortical information to reach the hippocampus that are crucial for spatial memory (van Strien et al., 2009). The direct input is the monosynaptic temporoammonic branch of the perforant path (TA) from EC layer III to CA1. Indirect inputs consist of the trisynaptic pathways from EC layer II to DG to CA3 to CA1 as well as the disynaptic pathway from EC layer III to CA2 to CA1 (van Strien et al., 2009). Both direct and indirect inputs have been shown to be important for spatial learning and memory (Brun et al., 2002, 2008; Nakazawa et al., 2003; Remondes and Schuman, 2004; Nakashiba et al., 2008; Suh et al., 2011; Van Cauter et al., 2013).

However, at the electrophysiological level, neither manipulations of CA3 nor EC have shown major causal effects on formation of CA1 SWRs and expression of place fields. This might be explained by the chronic manipulation approaches used in these studies. For example, in the chronic absence of CA3 or CA3 inputs, EC direct input may be able to homeostatically compensate, e.g. by stronger inputs from EC to CA1 pyramidal cells and interneurons or by suppression of

inhibitory input from CA3 interneurons to CA1 SLM layer (Buzsáki, 2015).

Therefore, we investigated whether the transient optogenetic approach may reveal the real-time contribution of CA3 in the formation of SWRs and expression of place fields in CA1.

We have demonstrated that CA3 is necessary for the formation of SWRs and expression of place fields in CA1. Although viral injections were aimed for the CA3a-b regions, a fraction of CA2 pyramidal cells were affected by virus and expressed eArchT3.0. However, CA2 axons mostly project to the stratum oriens layer of CA1, while the optical fiber terminated below the CA1 stratum oriens and almost in the pyramidal layer (van Strien et al., 2009; Dudek et al., 2016). This placement at pyramidal layer was achieved by attaching a tetrode to each optical fiber as a position readout to reach the specific LFP and cellular activity of pyramidal layer. Therefore, the volume of stratum oriens under the light cone was negligible in respect to the large volume of stratum radiatum where most of CA3 projections end up (van Strien et al., 2009; Dudek et al., 2016). In light of this, our experimental design almost exclusively investigates the effect of CA3 input on CA1 neural activity. On the other hand, CA3 and CA2 are both elements of the indirect pathway for EC to communicate with CA1, and thus even if CA2 projections are also silenced, this does not substantially influence

our interpretation of how the direct and indirect pathways contribute to CA1 place cell activity.

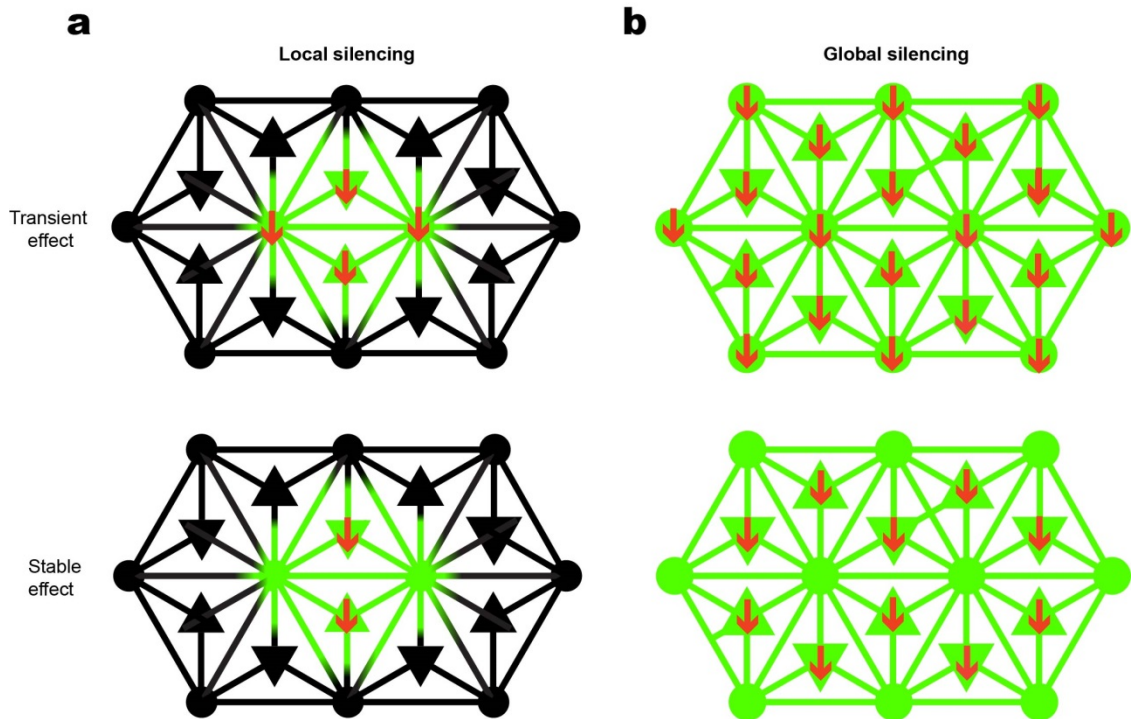


**Figure 3.22: A possible model explaining E/I imbalance.**

**a)** In our study, local SC silencing suppresses excitatory drive to both CA1 pyramidal cells (triangles) and interneurons (circles) and decreases their firing rate (top). However, while CA1 pyramidal cells have poor interconnections, fast-spiking interneurons compose an intensely-connected network possibly enabling interneurons affected by light to be rescued by unaffected interneurons (below). **b)** In contrast, genetic SC silencing globally suppresses CA3's excitatory drive to almost all CA1 pyramidal cells and interneurons, resulting in circuit-level decrease in interneuron firing rate (top). This results in disinhibition of CA1 pyramidal cells which cancels out the decrease in excitatory drive (below).



We showed that while CA1 place cells are dramatically suppressed, light only slightly decreases the firing rates of fast-spiking interneurons. This overall decrease in excitation/inhibition (E/I) balance is in contrast to previous genetic studies that showed preserved E/I balance in CA1 place cells, but around 50% decrease in CA1 interneuron firing (Nakazawa et al., 2002; Nakashiba et al., 2009; Middleton and McHugh, 2016). Explaining these different results may be difficult mainly due to the different techniques used in these studies. While our transient optogenetic silencing is local in space and acute in time, the genetic silencing studies are global in space, silencing almost all SCs, and chronic in time.

It is challenging to dissect the influence of these two differences, simultaneously. Only considering the local versus global silencing, this different E/I balance in inputs that CA1 pyramidal cells receive may generally be explained (Figure 3.22). In our study, SC silencing suppresses excitatory drive to both CA1 pyramidal cells and interneurons. However, while CA1 pyramidal cells have poor interconnections, fast-spiking interneurons compose a densely-connected network possibly enabling interneurons affected by light to be rescued by unaffected interneurons (e.g. through gap junctions) (Figure 3.22a). Therefore, normal interneuron firing rate results in overinhibition of CA1

pyramidal cells. In contrast, genetic SC silencing globally suppresses CA3's excitatory drive to almost all CA1 pyramidal cells and interneurons, resulting in a circuit-level decrease in interneuron firing rate (Nakazawa et al., 2003; Nakashiba et al., 2009; Figure 3.22b). This results in disinhibition of CA1 pyramidal cells which cancels out the decrease in excitatory drive. Therefore, in global SC silencing CA1 place cells preserve their normal activity.

However, E/I imbalance cannot explain the increase in run theta power under SC silencing. We found that SC silencing, although not affecting animal behavior, modulates CA1 LFP by suppressing SWRs during rest state and increasing theta power during run. This is consistent with selective optogenetic activation of medial septum, the main source of cholinergic input to CA3, which suppresses SWR incidence and increases theta oscillations in anesthetized and freely moving mice (Vandecasteele et al., 2014). Therefore, CA3 input is crucial for shifting CA1 circuitry from theta-dominated state associated with preparatory behavior to SWR-dominated off-line state associated with consummatory behavior.

Our findings show that despite being suppressed, place cells do not globally remap. This suggests precise positional information comes from outside hippocampus, possibly from an integration of MEC grid, border, and head-

direction cell responses (Bush et al., 2014). This is consistent with previous MEC manipulation studies reporting global remapping and disrupted theta precession in CA1 place cells (Brun et al., 2008; Hales et al., 2014; Miao et al., 2015; Schlesiger et al., 2015; Rueckemann et al., 2016). MEC grid cells show concomitant realignments only in instances when global remapping in ensemble of hippocampal place cells occurs, and remain unchanged during manipulations that lead to rate remapping of place cells (Fyhn et al., 2007; Bush et al., 2014).

These results further suggest that the extent of spatial firing in CA1 place fields is controlled by input from CA3. In contrast to previous studies, which suggested the sufficiency of EC for expression of CA1 place fields (Brun et al., 2002; Nakazawa et al., 2002, 2003, Nakashiba et al., 2008, 2009), we showed that the existence of place cell responses is highly dependent on continuous CA3 input. Indeed, neonatal studies have shown that place cells appear before grid cells (Langston et al., 2010; Wills et al., 2010), and disrupting grid cell responses in adult rats does not affect normal hippocampal place cell activity (Koenig et al., 2011). This evidence further supports the role of CA3 in the formation and expression of place cell responses in CA1.

Impaired preferred phase distribution and intact phase precession may suggest they are dissociable phenomena. We showed that at a population level while place cells increase their entrainment to theta, they lose their population phase preference. This uniform distribution of phases in lack of CA3 input resembles the uniformity of phase offsets in phase precession occurring in the first lap of traversing a novel linear track where recurrent network of CA3 is not presumably yet trained enough to maturely influence the population activity in CA1 (Feng et al., 2015). On the other hand, intact phase precession during SC silencing is consistent with previous MEC manipulation studies showing disrupted theta precession in CA1 place cells (Brun et al., 2008; Hales et al., 2014; Miao et al., 2015; Schlesiger et al., 2015; Rueckemann et al., 2016). Altogether, these findings imply that while sensory-driven cortical input controls timing of spiking activity in individual place cells, CA3 input induces synchrony among CA1 place cells at an ensemble level (Middleton and McHugh, 2016).

Overall, we showed that CA3 input to CA1 is necessary for the formation of SWRs, the expression of place fields, and the control of ensemble-level timing in CA1 place cells. These findings shed light on the function of hippocampal circuitry in spatial memory. Future studies may investigate the effect of transient

silencing of this pathway on hippocampal output in novel environments and navigational planning.

## Chapter 4 : Hippocampal ensemble activity in a mouse model of schizophrenia

In the previous chapter, I examined the contribution of CA3 input to CA1 place cell and SWR activity during rats' preparatory and consummatory behaviors, respectively. The contributions of cortical and CA3 inputs to CA1 in these behavioral states can also be studied from a synaptic plasticity viewpoint. Transgenic mice with selective abruptions in proteins essential for synaptic plasticity are plausible candidates for this aim. Therefore, I investigated the calcineurin knock-out mice which not only show impairments in learning and memory but also exhibit cognitive symptoms of schizophrenia. The findings of project which was a collaboration with Susumu Tonegawa laboratory at MIT, is published in journal *Neuron* (Suh et al., 2013) . Tonegawa laboratory generated this mouse model and did the electrophysiological recordings. Dr. David Foster and I did all the data analysis for this work. The rest of this chapter is from the material of that paper, with some minor modifications and updated literature review in specific sections.

We recorded neural activity in the hippocampus of freely behaving mice with a forebrain-specific knockout of the synaptic plasticity-mediating phosphatase

calcineurin, that were previously shown to exhibit behavioral and cognitive abnormalities, recapitulating the symptoms of schizophrenia. Calcineurin knockout (KO) exhibited a 2.5-fold increase in the abundance of sharp-wave ripple (SWR) events during awake resting periods and single units in KO were overactive during SWR events. Pairwise measures of unit activity, however, revealed that the sequential reactivation of place cells during SWR events was completely abolished in KO. Since this relationship during the post-experience awake rest periods has been implicated in learning, working memory and subsequent memory consolidation, our findings provide a novel mechanism underlying impaired information processing, potentially resulting in the cognitive impairments in schizophrenia.

## **Introduction**

Cognitive disorders such as schizophrenia are associated with multiple genetic and environmental factors, but presumably involve systematic impairments of information processing in specific neural circuits. Animal models can provide insight into such disorders by associating impairments at a behavioral level with disruption of distinct mechanisms at a neural circuit level (Arguello and Gogos, 2006). Furthermore, the ability to monitor the activity of individual neurons is a key advantage of using the animal models. However,

very little previous work has examined neural information processing in such models. In this study, we applied high-density electrophysiological recording techniques to investigate information processing at a circuit level in a mouse model of schizophrenia.

We [i.e. Tonegawa laboratory] previously generated a mouse model that offered three features: first, an altered synaptic plasticity; second, a profile of behavioral impairments recapitulating those seen in schizophrenia patients; and third, an preliminary association of the mutated gene with schizophrenia (Zeng et al., 2001; Gerber et al., 2003; Miyakawa et al., 2003; Gerber and Tonegawa, 2004). Specifically, mice with a forebrain-specific knockout (KO) of the only regulatory subunit of calcineurin, a major phosphatase expressed in the brain, are severely deficient in long-term depression (LTD) at hippocampal synapses, while long-term potentiation (LTP) is mildly enhanced (Zeng et al., 2001), leading to a left-ward shift in the BCM curve (Dudek and Bear, 1992). The KO mice exhibit a comprehensive array of behavioral impairments characteristic of schizophrenia patients (Goldman-Rakic, 1994; Elvevåg and Goldberg, 2000), including impairments in latent inhibition, pre-pulse inhibition and social interaction (Miyakawa et al., 2003), as well as a severe deficit in working memory (Zeng et al., 2001). Furthermore, the mutated calcineurin gene (*PPP3CC*) was



shown to map to chromosomal loci previously implicated in schizophrenia by genetic linkage studies (Gerber et al., 2003; Eastwood et al., 2005; Liu et al., 2007; Yamada et al., 2007; Murata et al., 2008; Wada et al., 2012, 2017). However, the linkage to schizophrenia was not found in some other human population studies (Kinoshita et al., 2005; XI et al., 2007; Sanders et al., 2008; Kyogoku et al., 2011). Taken together, these features suggest that the calcineurin KO may provide a worthy opportunity to investigate the neural basis of dysfunction in a schizophrenia model.

The hippocampus is a brain structure critical for episodic memory (Scoville and Milner, 1957; Olton and Samuelson, 1976; Gaffan, 1994; Steele and Morris, 1999) and spatial learning (Morris et al., 1982). In freely moving rodents, the hippocampus exhibits distinct activity profiles dependent on behavioral state (Buzsáki, 1989), suggesting distinct modes of information processing within the structure. During running, hippocampal electroencephalogram (EEG) exhibits a 4-12 Hz theta rhythm (Vanderwolf, 1969; Skaggs et al., 1996), and hippocampal principal neurons exhibit location-specific responses, known as place fields, as reported in rats (O'Keefe and Dostrovsky, 1971), mice (McHugh et al., 1996a), monkeys (Matsumura et al., 1999) and humans (Ekstrom et al., 2003). By contrast, during awake rest periods, hippocampal EEG is distinguished by sharp-

wave-ripple (SWR) events (Buzsáki, 1989) and hippocampal principal neurons take part in extended sequences of coactivity, which replay previous behavioral episodes (Foster and Wilson, 2006; Diba and Buzsáki, 2007; Davidson et al., 2009; Gupta et al., 2010) as well as preplay subsequent behavioral episodes (Dragoi and Tonegawa, 2012, 2013).

There is substantial evidence linking schizophrenia with damage to the hippocampus (Weinberger, 1999). Dysfunction of the hippocampus and related medial temporal lobe structures has also been reported in schizophrenia patients (Small et al., 2011), together with selective impairments in learning and memory. In addition, abnormal brain activity in schizophrenia patients was detected in various brain structures, including the hippocampus, during rest periods (Buckner et al., 2008) and during passive task epochs (Harrison et al., 2007). Since the pattern of impairments of calcineurin KO mice – synaptic plasticity changes in the hippocampus and hippocampal-dependent behavioral phenotypes such as working memory – suggested that hippocampal function might be affected in this mouse model of schizophrenia, we targeted the hippocampus for electrophysiological recordings in freely behaving KO and littermate controls (CT) and investigated changes in information processing during exploratory behavior and resting periods.

## **Experimental Procedures**

### **Mouse Breeding**

To obtain the conditional knockout (KO) mice, we followed the breeding paradigm published previously (Zeng et al., 2001). Briefly, female homozygous for the floxed CNB (fCN) allele and carrying the CaMKII-Cre transgene was crossed to male homozygous fCN to produce KO and littermate fCN control (CT). All mice were maintained in a pure C57BL/6 background and housed in a room with a 12-hr light/dark cycle (light on at 7 am) with access to food and water *ad libitum*. Tail DNA was collected to identify the genotypes of animals using PCR. All procedure relating to animal care and treatment conformed to the Institutional and NIH guidelines.

### **In vivo recording**

Male mice (KO and CT) between 12-16 weeks of age were anesthetized i.p. with avertin (300 mg/kg, 1.25% solution) and implanted with a microdrive hosting six independently adjustable tetrodes. The tetrode tips were gold-plated before surgery in order to reduce impedances to 200-250 kOhms. The tetrodes were positioned above the right hippocampus (AP -1.8 mm, ML 1.6 mm) to aim for dorsal CA1. The microdrive was secured to the skull using watch screws and dental cement and a screw fixed to the skull served as a ground electrode. The

tetrodes were lowered over 10-14 days in steps of 40  $\mu\text{m}$  until ripple and the hippocampal units could be identified. One designated electrode was targeted to the white matter above hippocampus to record a reference signal. Recorded unit signals were amplified 8 k to 20 k times and high-pass filtered above 6 kHz, whereas EEG signals from the same tetrodes were amplified 5 k times and band-pass filtered between 1 and 475 Hz. The animal's position was tracked with a 30 frames/sec camera using a pair of infrared diodes attached to the animal's head. Hippocampal activity was recorded using a 16-channel Neuralynx recording system, (Neuralynx, Bozeman, MT) while mice were in either a square enclosure (17 x 17 x 17 cm; "sleep box"), or a linear track (76 x 10 cm). The recording session consisted of one "RUN" epoch on the track (40-60 min) bracketed by two "SLEEP" epochs (30-60 min) in which the animal rested quietly in the sleep box in the same room. Following the recording session, manual clustering of spikes was done with XCLUST2 software (developed by M.A. Wilson, MIT). At the end of the experiment, mice were given a lethal dose of avertin and an electric current (50 mA) was delivered to create a small lesion at the tip of each tetrode. Animals were then transcardially perfused with 4% paraformaldehyde in 1 x phosphate-buffered saline and brains were removed, sliced in 50  $\mu\text{m}$  with a Vibratome, and mounted on slides to verify the recording positions. All experiments were

conducted and analyzed by [Tonegawa laboratory] researchers blind to the genotype of the individual animals.

### **Neural data analysis**

**Ripple analysis:** One electrode from each tetrode that had at least one cluster was considered for EEG analysis. EEG signal of each electrode was denoised for 60 Hz electric noise and its 180 Hz harmonic using a second-order IIR notch filter. Denoised EEG was filtered at ripple frequency range (100-240 Hz) with a fifth-order Butterworth band-pass filter. The envelopes of each band-passed EEG were obtained using the absolute value of its Hilbert transform and these envelopes were averaged over all electrodes. After applying a Gaussian smoother with 5 ms standard deviation, the averaged envelope was z-scored. Events that passed 5 standard deviations (i.e. mean + 5 sd of averaged non-z-scored envelope) for more than 3 ms were considered as ripples, and ripples that were less than 20 ms apart were merged and were considered as one extended ripple. The beginning and end of each ripple were considered as where the smoothed envelope crossed its mean value (i.e. zero for z-scored signal). Ripples events that happened when mice were not immobilized were excluded. Mice were considered as immobilized when their head speed was below 0.5 cm/s. Ripple power was obtained by applying Welch's method on each individual

non-z-scored non-enveloped ripples and then averaging over calculated powers. Morlet wavelet scalogram with bandwidth of 10 was used for spectrogram visualization of raw EEG. The same ripple-finding algorithm was also applied for gamma frequency range (25-80 Hz), to investigate if the impairment in EEG power is only selective for ripple events or can be found in gamma activity when animal is in immobilized state. Also, using Welch's method, the power of raw EEG signals during run was calculated and, in particular, theta (4-12 Hz) powers for CT and KO mice were compared. For a robustness analysis, EEGs were filtered with 50-Hz-wide frequency filters ranging from 50 Hz to 600 Hz with 40 Hz overlap between two consecutive filters.

**Cluster analysis:** Manual clustering of spikes was done based on spike waveform peak amplitude using XCLUST2 software (M.A. Wilson, MIT). Putative interneurons were also excluded from analysis on the basis of their spike width. To compare the quality of clusters in mice genotypes a modified  $L_{ratio}$  value for each cluster of a tetrode was calculated (Schmitzer-Torbert et al., 2005; Pfeiffer and Foster, 2013):

$$L_{ratio} = \left( \sum_{i \notin C} \left( 1 - CDF_{\chi^2_{df}}(D_{i,C}^2) \right) \right) / n_s$$

where  $i \notin C$  is the set of spikes that do not belong to target cluster C and  $D_{i,c}$  is the Mahalanobis distance of these spikes from this cluster.  $CDF_{\chi^2_{df}}$  is the cumulative distribution function of  $\chi^2$  distribution with  $df = 4$  (feature space for clusters is four dimensional).  $n_s$  is the total number of spikes from all the clusters (including target cluster C) of the tetrode.

**Place cell analysis:** All the place cell analyses, except spatial coherence, were done on 1-D place fields. These 1-D place fields were obtained by using 2 cm bins on linear track, and these raw place fields were smoothed by applying a Gaussian smoother with a 2.4 cm standard deviation. Place field size was calculated as the number of 2-cm-wide bins above 1 Hz threshold. Sparsity and spatial information are defined as described in Chapter 2.

Spatial coherence which quantifies smoothness and local orderliness of a place field is the autocorrelation of each 2-D place field with its nearest neighbor average (Muller and Kubie, 1989). To do this, 10×70 cm linear track was binned to 2 cm × 2 cm bins and the new firing map for each pixel was calculated as the average firing rate of 8 unsmoothed neighbor pixels. Then, 2-D correlation coefficient between original unsmoothed firing map and the new one was

calculated and to be statistically more meaningful this coefficient became Fisher-transformed (z-transformed).

For visualization purpose, 2-D place fields were calculated using 1×1 cm bins smoothed with a 1-cm standard deviation Gaussian smoother.

**Burst analysis:** For each place cell spikes that happened in less than 10 ms apart during run were considered as in-burst spikes. For each burst, amplitude difference was defined as the average of the change in peak of new spike waveform in relation to previous spike waveform. These calculated values were averaged over all bursts and using ISI of in-burst spikes, each cell was able to be shown as one point in a 2-D (amplitude difference versus ISI) feature space.

**Reactivation analysis:** For each ripple, spikes happening from 300 ms before it to 300 ms after it were considered as ripple-associated spikes, and cells with at least one spike in one ripple were called “active cells”. Only these ripple-associated spikes were considered for calculation of pair-wise cross-correlogram. For each pair of cells the histograms of these spikes were calculated in 5 ms bins. Each histogram was smoothed with a 5-sample moving-average smoother. Then, cross-correlation of this pair of smoothed histograms was calculated. Calculation was performed for all the cell-pairs for each mouse and averaged over the cell-



pairs that their place field peaks fall within same 3-cm-binned distance. These cross-correlograms were averaged and normalized for all mice in different genotypes and shown only for visualization purpose. However, for statistical analysis of reactivation, the average of spike timing of each pair was calculated. Knowing the place field distance of all pairs, each pair becomes a point in a 2-D (spike separation versus place field distance) coordinate space. Regression was used to fit these points, and the amount of correlation and its statistical significance measured the extent to which pairs of cells with spatially separated fields fired at longer temporal separations during ripples, compared with pairs of cells with spatially proximal fields. To further confirm this, pair cells with less than 10 cm distance between their place fields were considered as “close” cells while cells with more than 40 cm distance were considered as “far” cells. The average relative spike timing of these “close” and “far” cells was calculated for each genotype.

Furthermore, to directly compare pairs between CT and KO, a 3-way nested analysis of variance (ANOVA) was used which considered distance between pairs (“far” versus “close” categories) and genotypes (CT versus KO categories) as fixed-effect factors, and mice as a random-effect factor “nested” in genotypes. Only the F-values and p-values for the interactions between genotype and close-

far distance are reported here. Moreover, to investigate if the mean of correlation coefficients is significantly different in CT versus KO we use z-test. To be statistically comparable we applied a Fisher transform (or z-transform,  $z = \text{arctanh}(r)$ ) on correlation coefficients before calculating Z-values.

## **Results**

To characterize hippocampal activity in our mouse model, we employed microdrives with multiple independently adjustable tetrodes to record single-unit spikes and EEG from the CA1 subregion of the dorsal hippocampus of freely behaving KO mice ( $N = 7$ ) and floxed littermate CT ( $N = 5$ ).

### **Overabundance of SWR in calcineurin KO mice**

We hypothesized that the bias toward enhanced synaptic strength in KO would lead to an increase in excitability in hippocampal circuits. We therefore analyzed hippocampal EEG in KO and CT during both running and awake non-exploratory periods. During immobility, both groups exhibited SWRs, defined as increases in amplitude in the ripple frequency band (100-240 Hz), and typically lasting up to hundreds of milliseconds (Figure 4.1A). However, the non-Z-scored EEG in KO exhibited a significant increase in ripple power compared to CT (Mann-Whitney,  $p < 0.05$ ; Figure 4.1B). By contrast, there was no increase in power in either the gamma band (25-80 Hz; Mann-Whitney, NS; Figure 4.1C)

during non-exploratory period or theta band (4-12 Hz; Mann-Whitney, NS; Figure 4.1D) frequency during run.

To investigate further the specific increase in ripple-related activity, we quantified the characteristics of SWR events. No change was found in the duration (CT:  $88.35 \pm 3.6$  ms; KO:  $88.36 \pm 2.42$  ms;  $F(1, 10)=1.17e^{-5}$ , NS) or Z-scored amplitude (CT:  $7.06 \pm 0.32$  sd; KO:  $7.72 \pm 0.12$  sd;  $F(1, 10)=4.8$ , NS) of SWRs. The abundance of SWRs, however, was 2.5 times greater (CT:  $0.089 \pm 0.02$  s<sup>-1</sup>; KO:  $0.224 \pm 0.014$  s<sup>-1</sup>;  $F(1,10)=31.7$ ,  $p < 0.001$ ; Figure 4.1E). We then varied our analysis parameters in order to test how robust the results were. Varying the SWR detection threshold, in standard deviations from the mean, we found a consistent effect as the amplitude threshold was increased (Figure 4.1F). Indeed, at 8 standard deviations, the number of SWRs was a full order of magnitude greater in KO than CT.

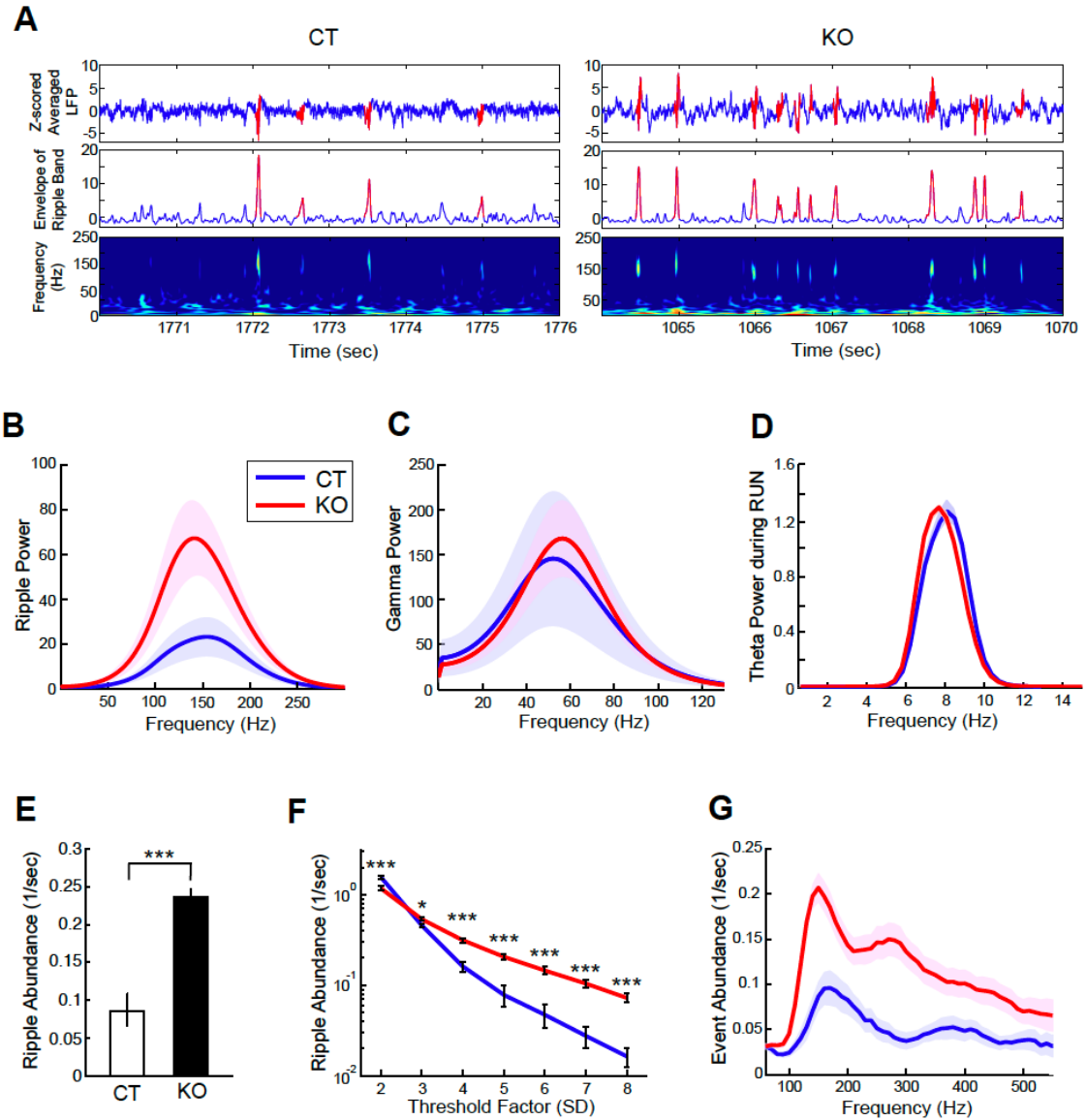


**Figure 4.1: Increased hippocampal ripple activity in calcineurin KO mice during awake resting periods.**

(A) Examples of EEG recording from CT (left) and KO (right) mice. Each EEG trace is shown as z-scored raw EEG (top), envelope of smoothed ripple-band-filtered EEG (middle) and wavelet power spectrogram of raw EEG (bottom). Note that sharp waves and their associated ripples are clearly isolated events in this spectrogram. (B-C) Comparison of spectral power of EEG filtered at ripple (b, 100-240 Hz) and gamma (c,

25-80 Hz) frequency bands, in both cases for EEG. (d) Comparison of spectral power of z-scored raw EEG filtered at theta (4-12 Hz) band during run. (e) Comparison of ripple abundance during awake resting period. (f) Quantitative measurement of ripple abundance at different threshold factors (standard deviations of z-scored, smoothed, filtered EEG). (g) The abundance of EEG events measured by a 50 Hz frequency window that filtered raw EEG at different frequency bands.

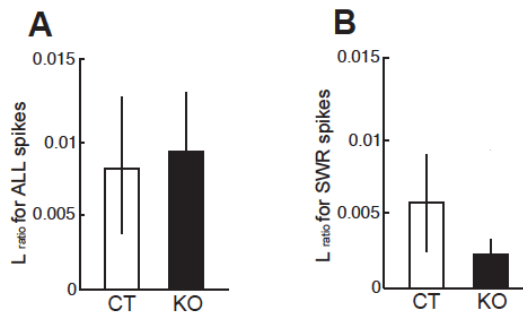


**Figure 4.2: Cluster robustness in preserved in KO.**

$L_{ratio}$  which is a measure of cluster robustness is not significantly different in KO and CT, either by (a) including all spikes of each place cell or (b) by including only spikes happening during SWRs.

We further conducted a robustness analysis varying the frequency range for which events were defined, for a 50 ms window, varied from 50 Hz to 600 Hz in 10 Hz steps (Figure 4.1G). There were significantly more events over a wide range of frequencies, between 100 Hz and 480 Hz (all windows in the range were significant at  $p < 0.05$ , two-sample t-test), however, the most significant zone was between 120 Hz and 150 Hz (all windows in this range were significant at  $p < 0.001$ , two-sample t-test). This range matched the frequency of peak at ripple

power (CT:  $149.8 \pm 5.3$  Hz; KO:  $143.4 \pm 4.4$  Hz;  $F(1,10)=0.83$ , NS; Figure 4.1B).

Taken together, these results indicate that calcineurin KO exhibit higher excitability in the EEG during immobility, whereas EEG activity associated with active exploration does not appear to be affected.

### **Normal place fields in calcineurin KO during exploratory behavior**

Across multiple species, hippocampal pyramidal neurons are active in spatially restricted regions of an environment during exploration, a pattern of activity referred to as place fields (O'Keefe and Dostrovsky, 1971; Wilson and McNaughton, 1993; McHugh et al., 1996a; Matsumura et al., 1999; Ekstrom et al., 2003). Given the great increase in ripple activity in the EEG during rest periods and the overall shift in synaptic plasticity toward potentiation (Zeng et al., 2001), we next hypothesized that higher excitability in KO may be manifested in the activity of individual neurons. We therefore isolated single unit activity in pyramidal neurons simultaneously recorded from CA1 during running (Total cells: CT:  $N = 59$ , KO:  $N = 122$ ; simultaneously: CT:  $11.8 \pm 1.0$  cells per mouse; KO:  $17.4 \pm 2.1$  cells per mouse; Figure 4.3A) and analyzed units (CT:  $N = 48$ ; KO:  $N = 92$ ) that formed good place fields on the track. Fine quantification revealed no differences in these responses across multiple measures (Figure 4.3 and Figure 4.2).

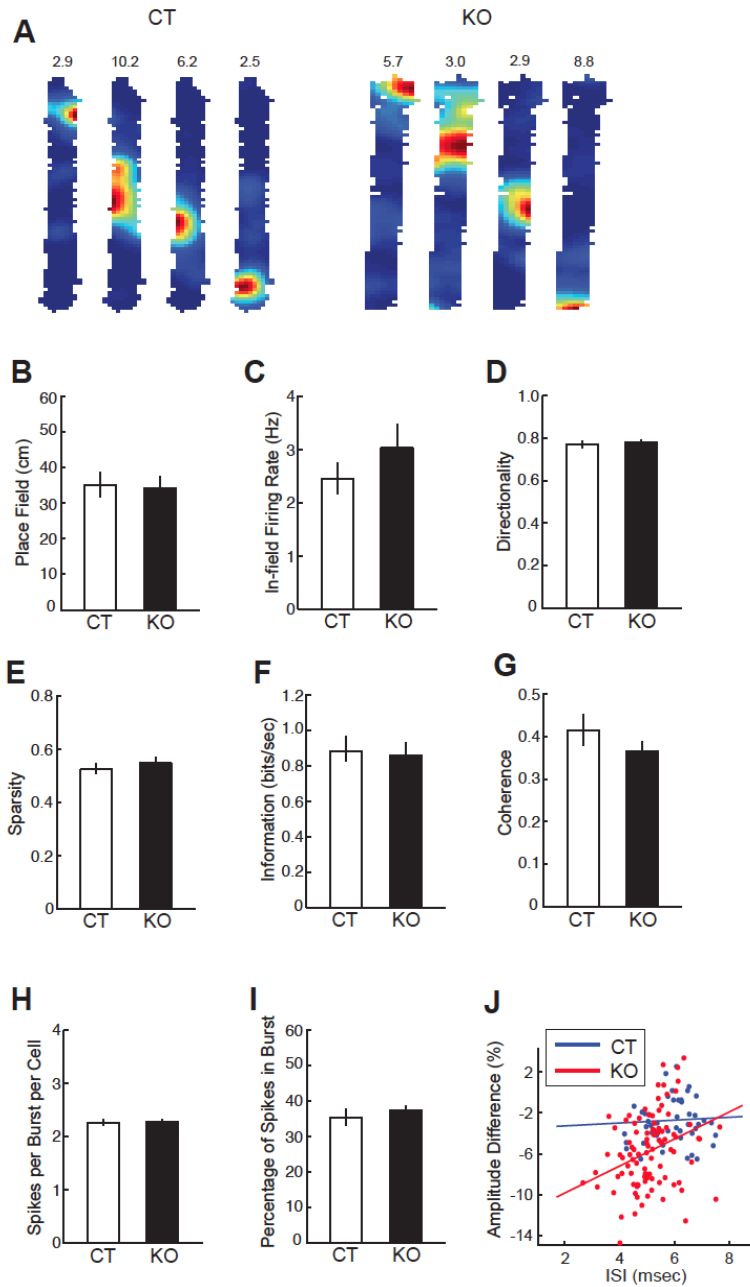


**Figure 4.3: Similar basic properties of place cells in CT and KO mice in run periods.**

(A) Examples of color-coded firing rate maps of CA1 place cells during run on a 10 x 76 cm linear track. Peak firing rates in Hz are shown above each rate map. (B-G) Quantitative description of place fields of CT and KO mice: (B) size of place field, (C)

mean in-field firing rate, (D) directionality, (E) sparsity, (F) spatial information, and (G) spatial coherence. (H-J) Quantification of spike activity during burst: (H) number spikes per burst per cell, and (I) the proportion of spikes, which were burst spikes, per cell. (J) The percentage of attenuation in spike amplitude within bursts as a function of in-burst inter-spike interval (ISI) for each cell (CT: 48 cells; KO: 97 cells).

Specifically, single units in KO exhibited normal place field sizes ( $F(1,138) = 0.01$ , NS; Figure 4.3B), normal firing rates within place fields ( $F(1,138) = 0.56$ , NS; Figure 4.3C), no difference in the normal tendency of units to fire more in one direction than another ( $F(1,138) = 0.19$ , NS; Figure 4.3D), and no difference in sparsity ( $F(1,138) = 0.85$ , NS; Figure 4.3E), which is a measure of the localization of place fields (Jung et al., 1994). In addition, no difference was observed in spatial information index ( $F(1,138) = 0.02$ , NS; Figure 4.3F), which measures how informative a spike from a place cell is (Markus et al., 1994), and spatial coherence ( $F(1,138) = 0.92$ , NS; Figure 4.3G), which measures the local smoothness of a firing rate pattern of spikes (Muller and Kubie, 1989).

Next, to determine whether excitability might be evident in the precise timing of single spikes, we further examined run-time unit activity on a finer timescale. Since hippocampal single units exhibit complex spikes, made up of a burst of several spikes occurring between 2-10 ms apart (Quirk and Wilson, 1999), we first measured the number of spikes during bursts. Both KO and CT units



exhibited similar numbers of spikes per burst ( $F(1,142) = 0.01$ , NS; Figure 4.3H) and a similar percentage of burst spikes ( $F(1,142) = 0.40$ , NS; Figure 4.3I). Interestingly, however, we found that bursts in KO tended to be faster, as measured by burst inter-spike interval (CT:  $5.70 \pm 0.70$  ms; KO:  $4.99 \pm 0.78$  ms;  $F(1,142) = 29.16$ ,  $p < 10^{-6}$ ; Figure 4.3J), and extracellular spike amplitude attenuation, which is associated with complex spikes (Quirk and Wilson, 1999; Harris et al., 2001), was also increased in KO (CT:  $2.84 \pm 0.39$  %; KO:  $5.93 \pm 0.38$  %;  $F(1,142) = 31.36$ ,  $p < 10^{-6}$ ; Figure 4.3J). Taken together, these results indicated that the spatial representation at the level of single cells in KO appears to be preserved during exploratory behavior, in spite of the bias toward enhanced synaptic strength and little change in spike timing during bursts.

### **Overactivity of place cells in calcineurin KO during SWRs**

Since the place responses of single units in calcineurin KO were largely normal during run, we next examined whether unit activity during immobile periods, specifically SWRs, was also unaltered. In both KO and CT mice, single units exhibited spikes during SWR events (Figure 4.4A). Place cells in KO, however, fired more than double the number of spikes during each SWR event as compared to those in CT (CT:  $1.11 \pm 0.14$  spikes per SWR; KO:  $2.56 \pm 0.54$  spikes per SWR;  $F(1,81)=4.84$ ,  $p < 0.05$ ; Figure 4.4B). Given that SWR events were also

more abundant in KO mice (Figure 4.1E), the compounded effect of both increased abundance of SWR events and increased spikes within each event could be illustrated as the firing rate of in-SWR spikes per each second of SWR events. Indeed, KO displayed a six-fold increase in the firing rate during SWR events compared to CT (CT:  $0.10 \pm 0.02$  spikes/s; KO:  $0.62 \pm 0.13$  spikes/s,  $F(1,78)=13.40$ ,  $p < 0.0005$ ; Figure 4.4C).

In principle, this increase in spiking activity may not by itself imply an alteration in the organization of information during each SWR. For example, the patterns of spikes associated with SWRs might be preserved, while being both enhanced and more frequent. However, such a possibility requires that the identity of cells participating in SWRs would not be altered. Alternatively, overexcitability during SWRs might lead to a degradation of SWR-associated information. To address this issue, we further analyzed the participation of single units across different SWRs. We found that single units in KO participated in a significantly greater fraction of SWR events than CT, increasing from around a third of SWRs to over half (CT:  $35.39 \pm 3.44$  %; KO:  $54.47 \pm 4.00$  %;  $F(1,86)=11.63$ ,  $p < 0.001$ ; Figure 4.4D). This finding indicates that neurons in KO were active during more than the normal number of SWR events, raising the possibility that spikes in KO may add noise rather than signal to SWR events. Therefore we

analyzed the coactivity of simultaneously recorded units during SWRs and determined whether and how the information content of SWRs was affected in calcineurin KO.

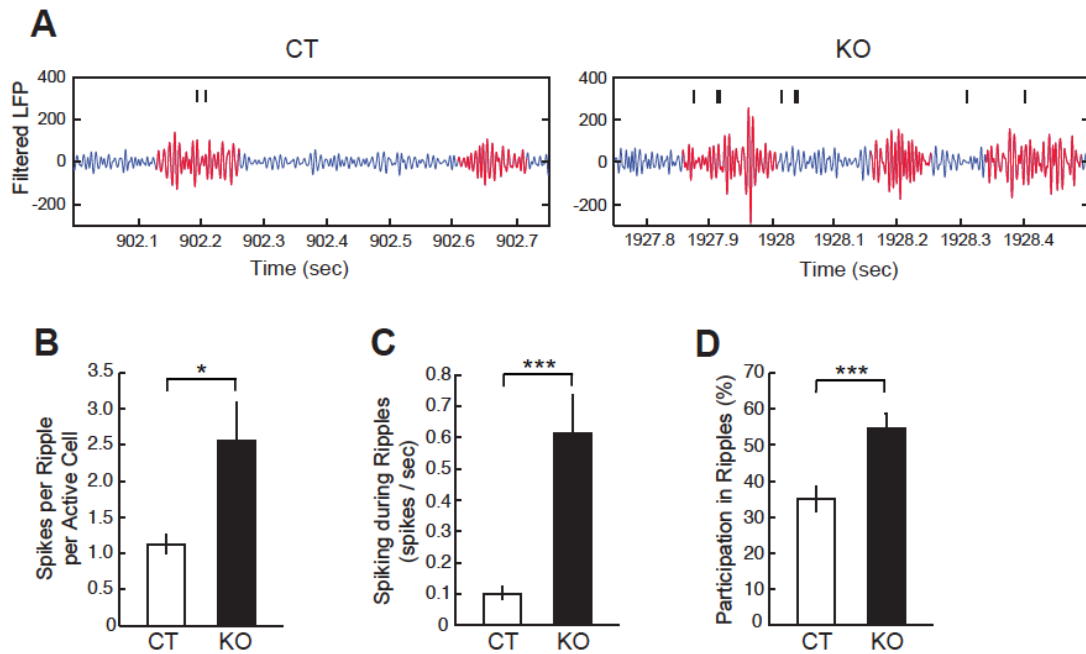


**Figure 4.4: Increased spike activity of place cells in calcineurin KO mice during ripple events.**

(A) A representative train of spikes is displayed with simultaneously recorded EEG filtered in ripple frequency range, for CT and KO. Ripple events are highlighted in red. (B) The number of spikes per ripple event per participating cell, *ie* for cells that fired at least one spike during the ripple event. (C) The number of average in-SWR spikes per per cell, per each second of awake resting period. (D) The fractional participation in ripples *ie* the fraction of ripple events for which a cell fired at least one spike, averaged across all cells.

## **Abolished spatial information content of reactivation events in calcineurin KO**

It has been demonstrated that awake SWR events are associated with temporally sequenced activity patterns of hippocampal place cells, referred to as “replay” due to the resemblance to spatial activity patterns in prior behavioral experience (Foster and Wilson, 2006; Diba and Buzsáki, 2007; Davidson et al., 2009; Karlsson and Frank, 2009; Gupta et al., 2010). It has also been shown that SWR events are associated with consolidation of previously encoded memory (Girardeau et al., 2009; Nakashiba et al., 2009; Ego-Stengel and Wilson, 2010), with encoding of a novel experience (Dragoi and Tonegawa, 2012, 2013) and, more interestingly, with spatial working memory (Jadhav et al., 2012). Therefore, we hypothesized that temporal sequences of place cells associated with SWRs in KO may be affected. Since the sequential replay suggests a distinct relationship between pairs of simultaneously recorded place cells, in which the distance between the cells’ place fields (measured using their peaks) should correlate with the temporal spike separation between cells during SWRs (Karlsson and Frank, 2009), we applied this analysis to pairs of simultaneously recorded place cells in KO and CT mice. We first noted that mean inter-spike intervals between pairs of cells were significantly shorter in KO than CT (CT:  $82.58 \pm 7.32$  ms; KO:  $29.3 \pm 2.03$  ms;  $F(1,428)=80.46$ ,  $p < 10^{-17}$ ). This result is in accordance with the general

increase in spike rates during SWRs noted earlier. We then considered the relationship between place field distance and temporal spike separation for pairs of cells. We created a representation of activity across the population by generating cross correlograms of spike trains during SWRs for each pair of cells, and then imaging each correlogram as a colorized row vector positioned on the y axis at a height corresponding to the distance between the place fields of those cells. When two or more correlograms occupied the same distance value, they were averaged together. In CT, this analysis revealed a distributed “V”-like pattern indicative of a replay-like relationship, as has been reported in rats (Karlsson and Frank, 2009) (Figure 4.5A, left). Strikingly, in contrast, the pattern was very different for KO, with a tight concentration around the null relative spike timing at all distances (Figure 4.5A, right).

Next, to verify whether the abnormal pattern in the correlogram in KO mice indicated a fundamentally disordered organization at the level of pairs of cells, we measured the mean temporal spike separation for each pair of cells, thus illustrating each pair of cells as a tuple of place field distance and mean spike separation (Figure 4.5B). There was a clear and significant positive correlation between place field distance and temporal spike separation in SWRs among cell pairs in CT ( $r = 0.21$ ,  $F=6.65$ ,  $p < 0.01$ ), indicating that hippocampal unit activity

during SWRs conveyed temporally structured information about the spatial distance of place fields. By contrast, the relationship between cell pairs in KO was completely abolished ( $r = -0.007$ ,  $F=0.015$ , NS). We also further quantified these pairwise effects by binning the data into “close” and “far” categories on the basis of the distance between place fields in a pair. Specifically, pairs of cells with place field peaks less than 10 cm apart were categorized as “close”, whereas pairs of cells with place field peaks more than 40 cm apart were categorized as “far”. CT exhibited a strong difference between these categories ( $F(1,76)=8.94$ ,  $p < 0.01$ ; Figure 4.5C, left), whereas KO exhibited no difference at all ( $F(1,194)=0.22$ , NS; Figure 4.5C, right). Furthermore, within-group comparison of “far” and “close” pairs also showed a significant decrease with this measure in KO (3-way ANOVA,  $F(1)=7.36$ ,  $p < 0.05$ ), and the mean of correlation coefficients is also significantly different between the genotype (z-test,  $Z=2.15$ ,  $p < 0.05$ ).

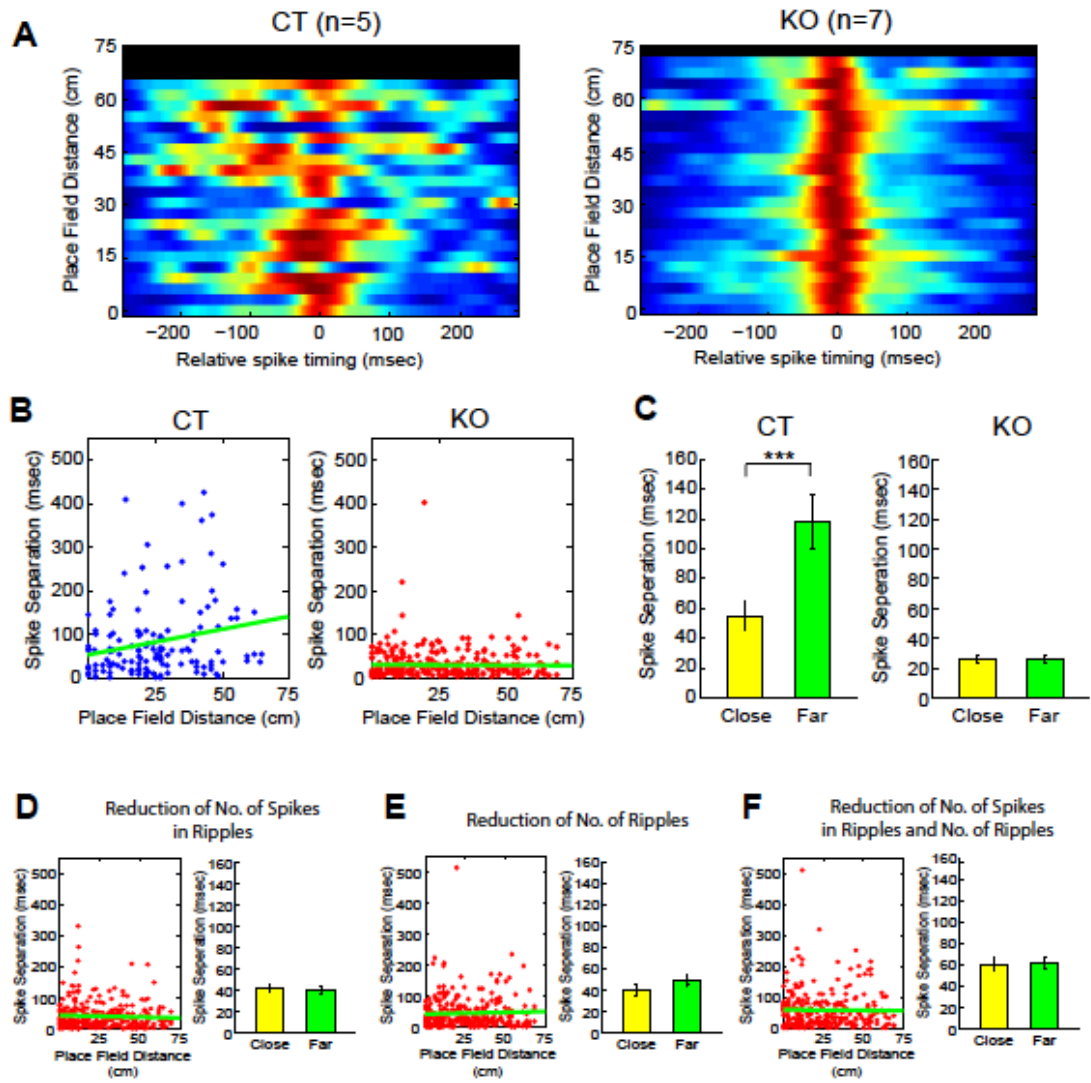


**Figure 4.5: Impaired reactivation of spatial experience on the linear track during awake resting periods on the linear track in calcineurin KO mice.**

(a) For each pair of neurons, the pair-wise cross-correlogram of the two spike trains around ripple events ( $\pm 300$  ms) is plotted at a y position given by the linear distance between the corresponding two place field peaks. Wherever more than one pair occupies the same y position (*ie* has the same inter-peak spatial distance), the cross-correlograms have been averaged. Pairwise data from all sessions are shown together on the left for CT and on the right for KO. (b) Distribution of temporal spike separations during ripples of all pairs of neurons is plotted as a function of the distance between

place field peaks on the track. (c) Comparison of the average spike separation for pairs of cells with place field peaks less than 10 cm apart (close cells) and pairs of cells with place field peaks more than 40 cm apart (far cells). (d-f) For KO mice, the reactivation assessment shown in (b) was reanalyzed while only extra spikes (d), only extra ripples (e), or both extra spikes and ripples (f) were randomly decimated.

Since the increased abundance of SWRs and increased number of spikes during SWRs can contribute to the abolished spatial information content in KO, we further analyzed the data under three conditions. First, to exclude the possibility of the effect of the increase in spike numbers in KO having an effect, we randomly decimated spike numbers from spike trains to match their average quantity equal to CT spikes (Figure 4.5D; 3-way nested ANOVA,  $F(1)=5.21$ ,  $p < 0.05$  and  $z$ -test,  $Z=2.66$ ,  $p < 0.01$ ). Second, to exclude a possibility of the effect of the increase in SWR abundance in KO having an effect on abolished spatial information content, we randomly decimated the number of SWR events (Figure 4.5E; 3-way nested ANOVA,  $F(1)=7.74$ ,  $p < 0.05$  and  $z$ -test,  $Z=2.53$ ,  $p < 0.05$ ). Finally, we combined both decimations to analyze cell pairs in KO under the same SWR abundance and spike rates as CT (Figure 4.5F; 3-way nested ANOVA,  $F(1)=11.14$ ,  $p < 0.01$ , and  $z$ -test,  $Z=2.33$ ,  $p < 0.05$ ). Under any condition, the flat relationship between place field distance and mean spike separation was still unaffected in KO. Therefore, neither increased abundance nor increased



spike rate by themselves account for the failure of cell pairs in KO to exhibit normally structured coactivity, but rather the fundamental relationship between spike times during SWRs and represented place fields during run has been completely abolished in KO.

## **Discussion**

We applied high-density electrophysiology recording to a mouse model of schizophrenia, in which functional calcineurin protein is deleted specifically in excitatory neurons from the forebrain. Our primary aim was to detect disruption of information processing in the hippocampus, which may underlie the schizophrenia-like behavioral impairments of the model mice. We demonstrated that calcineurin KO mice displayed a selective disruption in rest-related neural information processing. Hippocampal EEG in KO exhibited enhanced power in the ripple band, but not gamma or theta, and a 2.5-fold increase in the abundance of SWR events during awake resting periods. This abnormality was strikingly selective, since CA1 neurons in KO exhibited normal place fields during active exploratory behavior. By contrast, the same neurons were profoundly overactive during SWRs and participated in a greater fraction of SWR events. Furthermore, pairwise measures of unit activity during SWRs revealed that a normal linear relationship between spatial separation of place fields during run and temporal

separation of spikes during resting periods was completely abolished in KO. The spared place cell activity during run and degraded SWR-based trajectory events during rest have also been found in rats with blocked NMDA receptors (Silva et al., 2015). Therefore, specific impairments in synaptic plasticity result in state-dependent disruptions in hippocampal circuit activity. Moreover, we present a selective form of disruption of neural information processing in an animal model of schizophrenia.

What mechanism might underlie the increase in SWRs in KO mice? The shift in plasticity away from LTD and toward LTP (Zeng et al., 2001) would suggest an increase in excitability, which may produce an increase in the SWR number. In support, an electrophysiological study of CA1-CA3 slices producing spontaneous SWRs demonstrated that SWR abundance increases after LTP induction, and that this effect is dependent on NMDA receptors (Behrens et al., 2005). Next, how can the lack of LTD affect the temporal organization of place cell activity during ripple? It has been shown that the reactivation of hippocampal firing patterns reflects a recent experience in the environment the animal explored. Since the animal visited several places in space, the replay of place cell sequence could be resulted from the formation of asymmetric associations between place cells during exploration. Experimental results and

computational models suggested that place fields expand backwards relative to the direction in which the animal is running as an experience- and synaptic plasticity-dependent manner (Mehta et al., 1997; Ekstrom et al., 2001), and this asymmetry strengthens the association between cells with neighboring place fields. Since the calcineurin KO showed the abnormality in synaptic plasticity, neighboring place cells in KO could not make a proper association by synaptic weight. In addition, the increased excitability in KO hippocampus during ripples events drives the abnormal association more, therefore, consequently leads to the excessive temporal binding without direction.

Our results suggest that information processing during awake resting periods may play a critical role in normal brain function. Recently, there has been increasing interest in resting-state brain function and a related set of brain regions known as the “default mode network” (DMN), including the hippocampal formation as well as posterior cingulate cortex, retrosplenial cortex and prefrontal cortex (Raichle et al., 2001; Buckner and Carroll, 2007; Buckner et al., 2008; Broyd et al., 2009). It has also been proposed that the complex symptoms of schizophrenia could arise from an overactive or inappropriately active DMN (Buckner et al., 2008). For example, within schizophrenia patients, increased DMN activity during rest periods was correlated with the positive

symptoms of the disorder (*e.g.* hallucinations, delusions, and thought confusions) (Garrity et al., 2007). In addition, another study reported that DMN regions were correlated with each other to a significantly higher degree in schizophrenia patients compared to controls (Zhou et al., 2007). Here we demonstrated that the offline activity in the hippocampus, one of the DMN regions, is disrupted in calcineurin KO mice, thus providing the first evidence for DMN dysfunction in an animal model of schizophrenia.

Our finding that the basic physiological properties of place cells are normal in KO, despite their displaying a range of spatial learning impairments reinforces the conclusion drawn in many previous studies that place fields *per se* may not provide a robust indicator of spatial learning and memory (McHugh et al., 2007; Nakashiba et al., 2008; Suh et al., 2011). For instance, mice in which the projection from the layer III principal cells of the MEC to hippocampal area CA1 was specifically blocked by transgenic tetanus toxin displayed normal basic properties of CA1 place fields including field size, mean firing rate, and spatial information, and yet these mice exhibited impairments in spatial working memory (Suh et al., 2011). On the other hand, the precise and complete blockade of CA3 input to CA1 by transgenic tetanus toxin resulted in specific deficits both in the SWR frequency and SWR-associated co-reactivation of CA1 cells during

sleep, which correlate with a deficit in memory consolidation at the behavioral level (Nakashiba et al., 2009). Likewise, disruption of neural activity during SWRs by electrical micro-stimulation causes learning impairment (Girardeau et al., 2009; Ego-Stengel and Wilson, 2010). These and our present findings add to the growing evidence that more complex aspects of place cell activity, such as SWR-associated features, may be necessary elements of hippocampal information processing for learning and memory (Wilson and McNaughton, 1994; Foster and Wilson, 2006; Diba and Buzsáki, 2007; Nakashiba et al., 2009; Jadhav et al., 2012). Therefore, disruption of the temporal order of hippocampal place cell spikes during SWRs in KO mice suggests a novel mechanism underlying the cognitive impairments observed in schizophrenia.

The increase in SWR events provide a model that might unify several disparate aspects of schizophrenia: (1) the role of NMDA receptors in schizophrenia (the “glutamate hypothesis” (Olney and Farber, 1995) which is consistent with altered SWR abundance resulting from an imbalance in NMDA-receptor dependent synaptic plasticity mechanisms; (2) the cognitive symptoms of schizophrenia, which may be accounted for by SWR-mediated disruption of DMN function; (3) the presence of psychosis and disordered thinking in schizophrenia, which may result from abnormal memory reactivation in cortical

areas caused by abnormal memory reactivation in the hippocampus; and (4) abnormalities in dopaminergic signaling (the “dopamine hypothesis” (Carlsson, 1977), which may result from the effect of increased SWR abundance on downstream dopaminergic circuits (Pennartz et al., 2004; Lansink et al., 2009). Therefore, our findings provide a novel link that SWR activity may constitute a point of convergence across disparate schizophrenia models, and a new insight into the neural basis of the cognitive disorder.

## Chapter 5 : General Discussion

The hippocampus translates our life experiences into episodic memories, a process impaired during some psychiatric and neurological disorders. Cortical inputs to the hippocampus and computations within its different subregions perform this memory encoding and later memory retrieval during preparatory and consummatory behavioral states. However, the state-dependent contributions of subregions of the cortico-hippocampal network at the single neuron and the neural ensemble level are not yet completely understood. In particular, EC spatial information reaches CA1 through a “direct” monosynaptic pathway and an “indirect” CA3/CA2-mediated multisynaptic pathway. However, it is not clear how these direct and indirect pathways communicate with CA1 for spatial information processing.

Rats usually demonstrate either preparatory behaviors, such exploration, ambulation, etc., or consummatory behavioral, such as immobility, eating, grooming, etc., and this behavioral distinction maps well onto the dichotomy of theta—SPW-R hippocampal states (Buzsáki, 2015). I have shown that during preparatory behavior, the highly recurrent network of CA3 is necessary for the expression of place fields in CA1. The potential effect of CA2 was ruled out by

both careful injection of virus to CA3 and by placing optical fibers, which were attached with one readout tetrode, either in CA1 pyramidal layer or the lower part of CA1 stratum oriens for not illuminating CA2 projections by light (van Strien et al., 2009; Dudek et al., 2016). I propose that while precise positional information for “where” a CA1 place cell to fire on a familiar environment comes from EC, the extent of “how” to fire around that position comes from concurrently-active place cells in CA3. SC silencing therefore decimates place fields, but does not result in major global remapping, although some shift in place field location yet within the range of original place field may occur under light. I also proposed that CA3 competes with EC over CA1 ensemble activity to shift it from a theta-dominated rhythm to SWR-dominated offline brain state. Indeed, suppressing CA3 input to CA1 enhances theta power and theta locking strength, emphasizing the role of EC in CA1 theta entrainment. However, suppressing CA3 input to CA1 does not change theta phase precession, which proposes that other inputs such EC input are responsible for the temporal coding in CA1. I have also demonstrated that CA3, the essential component of indirect pathway from EC to CA1, is necessary for formation of SWRs during consummatory behavior. Silencing CA3 input to CA1 dramatically decreases occurrence rate of CA1 SWRs. Therefore, sequential reactivation of CA1



ensembles during SWRs, which is a proposed mechanism for memory consolidation and navigational planning, is also dependent on excitatory input from CA3. Overall, the indirect pathway and especially the self-organizing network of CA3 are indispensable for normal hippocampal output during both preparatory and consummatory behavioral states.

The calcineurin mouse model of schizophrenia with its impaired synaptic plasticity shows state-dependent deficits in hippocampal ensemble activity. While place cells are expressed normally during preparatory behavior, SWR incidence rate increases and SWR-associated replay degrades during consummatory behavior. In these mice, the calcineurin protein is selectively deleted from EC and CA1, while CA3 cell bodies and axons express this protein normally (Zeng et al., 2001). Therefore, synaptic plasticity is not only degraded in both the presynaptic and postsynaptic components of the MEC-CA1 monosynaptic pathway but also in the postsynaptic part of the CA3-to-CA1 projection. Although it is not yet studied in these mice, the direct pathway is thus expected to show an even stronger deficit in synaptic plasticity than the examined indirect pathway. Because these animals have normal SCs and impaired CA1 synapses, it is challenging to explain the selective deficit in CA1 place cell ensemble activity. In other words, it is not clear whether deficits in

plasticity at synaptic inputs from EC or CA3 induces more abnormal LTP/LTD ratio in CA1 place cells. Additionally, in this chronic adult-onset gene deletion study, compensatory mechanisms may play a critical role in rescuing hippocampal function.

Nevertheless, increased LTP/LTD ratio and subsequent increase in excitability may explain the increase in SWRs in calcineurin KO mice. In support of this hypothesis, an electrophysiological study of CA3-CA1 slices producing spontaneous SWRs demonstrated that SWR abundance increases after LTP induction (Behrens et al., 2005). However, how can the plasticity shift in KO mice degrade the temporal organization of place cell activity during SWRs? Several models have proposed that synaptic plasticity occurring during exploratory running behavior may drive associations between successively active place cells and sculpt the sequences that can be subsequently generated (Jensen and Lisman, 1996; Mehta et al., 2002). Synaptic plasticity that is excessive and unbalanced toward potentiation in calcineurin KO mice might cause excessive temporal binding between place cells during running behavior, despite the fact that the activity of the place cells during running is normal. Hence, this excessive temporal binding would then be inaccurately manifested during the information

retrieval process associated with SWRs and would degrade hippocampal replays.

By using these two complementary approaches, I probed how the fine temporal structure of activity in the integration region of the hippocampus, CA1, responds when the relative influence of its two major inputs, CA3 and MEC, is manipulated. I found several similarities and differences between the findings of these two optogenetic and genetic manipulations studies. First, while a balance interplay of both EC and CA3 pathways is essential for the expression of a spatial firing field in CA1 place cells, but the extent to which they fire in their field, or even in some cases if they fire at all, can be powerfully controlled by CA3. Second, CA3 input is necessary for the generation of SWRs, as virtually no SWRs occurred with SC silencing. Excessive potentiation in the CA3 and presumably EC pathways to CA1 actually increased the number of SWRs, but it is unclear whether silencing EC would have also abolished SWR incidence. Third, despite increasing the incidence of SWRs and the participation of individual place cells in firing during SWRs, perturbing information transfer from CA3 to CA1 substantially decreased the temporal ordering of spiking activity during replays. Therefore, CA3 pathway satisfactorily appears critical for the normal function of

SWRs, by being crucial for the generation of SWRs and the normal information content of replays.

However, numerous differences in the methods used here are worth noting. First, the calcineurin KO mice had impaired information transfer between EC and CA1, due to both increased potentiation and disruption of normal information processing in EC, and CA3 to CA1 due postsynaptic impairments in synaptic plasticity, while silencing the SC between CA3 and CA1 simply decreased the relative influence of CA3 input. Second, CA1 cell bodies and EC projections to CA1 are genetically aberrant in the calcineurin KO mice, but they are unaffected in SC silencing study. Third, SC silencing was applied in a temporally acute manner within each session, while calcineurin deletion was chronic and could induce long term homeostatic plasticity. Fourth, SC silencing was local in space and specifically targeted only the CA3 to CA1 projection, while the calcineurin deletion affected all CA1 and EC pyramidal cells. It is therefore important to keep these differences in mind when interpreting the different effects of manipulating CA3 and EC input to CA1.

With these considerations in mind, I can conclude that rats with silenced SCs, in contrast to calcineurin KO mice, show substantial impairments in their place

field expression during preparatory behavior. However, both of them show disrupted SWRs during consummatory behavior. One explanation for this is that during run, EC and CA3 are competing over CA1 place cell activity via excitatory and inhibitory projections modulating local pyramidal cells and interneurons. Because the CA1 synapses of calcineurin KO mice have abnormally higher potentiation to CA3 and EC inputs, an overall balance between these two excitatory inputs is still preserved. Therefore, place fields are normally expressed in these mice. However, during rest, where CA3 wins the competition with EC on dominion over CA1 neural activity, SWRs become more abundant than normal. This implies that during preparatory behavior both EC and CA3 are essential for normal hippocampal output while during consummatory behavior, CA3 is more indispensable.

## **Implications**

The findings discussed in this dissertation have broader implications. It has long been held that self-organized sequential activation of neuronal assemblies is the neural basis of cognition (Hebb, 1949). These sequential activities are found in cortical and hippocampal structures during preparatory and consummatory behaviors (Pastalkova et al., 2008; Foster and Knierim, 2012; Harvey et al., 2012).

Our findings affirm the distinct causal role of highly-recurrent brain areas such as CA3 in producing sequential ensemble activity.

SWR-associated sequential trajectory events, presumably initiated by the information-rich excitatory input from CA3 to CA1, are important for memory storage and recall as well as planning (Diba and Buzsáki, 2007; Davidson et al., 2009; Karlsson and Frank, 2009; Foster and Knierim, 2012; Jadhav et al., 2012; Pfeiffer and Foster, 2013, 2015). These prospective hippocampal ensemble activities during SWRs give diverse options to the brain for decision making and might be the neural basis for priming creative thoughts in humans (Buzsáki, 2015). Everyday we might experience tens of thousands of involuntary thoughts. The frequency of these “mind pops” increases in drowsiness between waking and sleep, the brain state with abundant SWRs (Gordon, 2013). Creative individuals have reported to come up with novel ideas and unexpected solutions to their challenges during this drowsy less externally-focused mental state (Bristol and Viskontas, 2006). Because we know SWRs are likely useful for consolidating and using newly acquired information, it is not too large of a logical jump to hypothesize they may be involved in these spontaneous and unexpected creative thoughts in humans. This intriguing idea would implicate

CA3, the potential SWR generator in the hippocampus, as a key primer of involuntary creative thought.

Involuntary episodic thoughts occur in intrusive forms of “racing” and “crowded” thoughts in many mental disorders, including bipolar disorder, depression, obsessive-compulsive disorder (OCD), attention deficit hyperactivity disorder (ADHD), anxiety, and schizophrenia (Brewin et al., 2010; Piguet et al., 2010). On the other hand, calcineurin KO mice and several mouse models of psychiatric diseases selectively show aberrant SWR activity (Boone et al., n.d.; Phillips et al., 2012; Suh et al., 2013; Ishikawa et al., 2014; Witton et al., 2014; Altimus et al., 2015; Gillespie et al., 2016; Nicole et al., 2016). Therefore, these intrusive thoughts in patients might be caused by SWRs that are abnormal either in incidence rate, information content, or both. CA3 as the potential generator of SWRs may therefore be specifically disrupted in these patients (Behrendt, 2010). For example, CA3 and CA2 are hyperactive in schizophrenia patients (Behrendt, 2010; Li et al., 2015). This accumulation of converging evidence might transform the definition of schizophrenia, and perhaps other mental disorders, to a disease of synaptic plasticity, with certain symptoms, such as intrusive thoughts, traced to specific aberrant circuits such as CA3 (Tamminga et al., 2012; McCullumsmith, 2015).

## **Future work**

Real-time SWR detection and manipulation is a potentially fruitful direction of future research. Although there is evidence that local optogenetic activation of CA1 neurons can produce sequential activity among them, whether this is distinct from mechanisms of normal replay generation in poorly-connected CA1 pyramidal cells is not yet clearly understood (Thomson and Radpour, 1991; Stark et al., 2015). In other words, it is not clear if CA3 only sends an initiation signal to CA1 via sharp waves, while the sequential activity itself is coordinated within CA1, or continuously instructs all steps of mental navigation to CA1. This can be examined by online detection of CA1 SWRs in conjunction with suppressing SCs for a short period of time (e.g. 10-20 ms) at the middle of SWRs. If CA3 only sends the “go” signal to CA1, this intermediate silencing might not affect decoded replays in CA1. In contrast, if continuous input from CA3 is needed, this suppression would interrupt completion of CA1 replay, possibly by causing abnormal leaps in trajectory events to new locations. While this idea is technically challenging, online replay decoding algorithm (ORDEAL) method, recently developed in our lab, may be an important step towards its feasibility (Ambrose, 2016).



For examining the effect of CA3 input on well-established and stable CA1 place fields, the experiments described in this dissertation were all performed on familiar linear tracks. However, the auto-associative network of CA3 needs positional information from MEC, either directly or via DG, to form its own de novo place cell response and influence spatial tunings in CA1 place cells (Nakazawa et al., 2004). Therefore, CA3 may contribute differently to CA1 place fields in a novel environment, when a new episodic memory will require the encoding of new spatial information. Transgenic mice with disrupted synaptic plasticity in CA3 show larger CA1 place fields compared to control mice in a novel linear track but these fields are not significantly different from control fields in later re-exposures to track (Nakazawa et al., 2003). On the other hand, because behavior on a linear track does not require decision making about where to explore, it is not an appropriate setting for examining navigational planning. Therefore, more complex spatial environments, such as the W-maze and open field, could be used to study the contribution of CA3 on CA1 ensemble activity during navigational planning and decision making. For example, it is important to investigate if prospective and retrospective SWR-associated trajectory events depend differently on CA3 input (Jadhav et al., 2012; Pfeiffer and Foster, 2013).

Overall, novel and complex environments may shed further light on the selective contributions of CA3 to CA1 place cell and SWR activity.

Other complementary questions about hippocampal function can be addressed by this novel optetrode. While some optogenetic studies showed the effect of MEC on hippocampal place cell responses, the contribution of EC input in CA1 SWRs and replays are not yet investigated (Miao et al., 2015; Rueckemann et al., 2016). Therefore, temporoammonic pathway (TA) silencing with a similar experimental design would shed light on the direct contribution of either MEC or LEC in CA1 place fields, SWRs, and replays. I hypothesize that such an experiment would uncover no major effect on SWRs and replays but global remapping in CA1 place fields. Also, according to the previously-described competition between EC and CA3 over CA1 activity, TA silencing may result in shifting the hippocampus away from the theta-dominated state by causing a decrease in theta power and disrupting theta phase precession. Indeed, some MEC lesion studies have found remapped place fields and impaired theta phase precession in some CA1 place cells and a decrease in CA1 theta power (Brun et al., 2008; Zhang et al., 2013; Hales et al., 2014; Miao et al., 2015; Schlesiger et al., 2015; Rueckemann et al., 2016). Therefore, a transient

optogenetic silencing may reveal intricate contributions of the major components of EC on hippocampal output.

Gain of function studies may also further clarify the contribution of CA3 and EC to CA1 SWRs and place fields. It is quite informative to explore in what stimulation frequency ranges optogenetic activation of SCs and possibly TA induces ripples in CA1 circuitry. One may also examine if such induced ripples cause sequential activity in CA1 (Stark et al., 2014, 2015). Furthermore, previously-described theta versus SWR state competition model predicts that EC and CA3 are pivotal in inclining the hippocampus to these two states, respectively. This model can be tested by activating the input pathway in the CA1 state in which it is not usually active and examine if this stimulation can cause a state transition. For example, I predict activating TA during quiet wakefulness abolishes SWRs and causes a sustained increase in theta power. Oppositely, it might be possible to generate SWR-like activity by stimulating SCs during run. Overall, these diverse experiments may further elucidate hippocampal circuit.

Emerging neural circuit recording and manipulation techniques are broadening the capability of neuroscientists to address more fundamental

questions about hippocampal circuitry. In vivo two-photon calcium imaging of place cells has revealed their location-dependent activity in physical and virtual environments (Dombeck et al., 2010; Ziv et al., 2013; Pfeiffer et al., 2014; Rickgauer et al., 2014; Sheffield and Dombeck, 2015; Villette et al., 2015; Danielson et al., 2016; Malvache et al., 2016). Although the time course of calcium transients in synapses is orders of magnitudes slower than actual action potentials, the subcellular spatial resolution of this technique, capability to simultaneously monitor hundreds of neurons, ability to distinguishably screen neurons in different planes of pyramidal layer, and weeks-long imaging stability make it a compelling method to study place cells.

High-resolution two photon calcium imaging combined with axon photometry could resolve whether there are different activity properties at dendritic spines receiving EC input and spines receiving CA3 input in CA1 stratum oriens and stratum radiatum. Moreover, just as replay itself was only discoverable when the number of simultaneously recorded neurons was large enough new hippocampal network phenomena may be observed. In addition, a combination of calcium imaging and optogenetic stimulation may reveal the contribution of CA3 and EC inputs to a vast number of place cells (Rickgauer et al., 2014). Simultaneous multi-plane imaging of CA1 stratum pyramidale may

not only reveal functional specificity of superficial and deep place cells but also differences in the extent of inputs they receive (Danielson et al., 2016).

Furthermore, long-term imaging stability allows for monitoring changes in the amount of EC and CA3 inputs that dendritic spines in CA1 place cells receive in a novel environment and re-exposures to the same environment in next days.

Therefore, calcium imaging is an important method to study the formation mechanisms of place cells, SWRs, and SWR-associated neural sequences.

These ideas are just a few of the potential directions for future research on neural mechanisms for spatial information processing. This dissertation describes my work to better understand hippocampal circuit, how it function in health and disease and its critical role in the neural basis of episodic memory and the cognitive map.

## References

- Altimus C, Harrold J, Jaaro-Peled H, Sawa A, Foster DJ (2015) Disordered Ripples Are a Common Feature of Genetically Distinct Mouse Models Relevant to Schizophrenia. *Mol Neuropsychiatry* 1:52–59.
- Ambrose RE (2016) Hippocampal replay and learning from reward. Baltimore, MD: Johns Hopkins University.
- Ambrose RE, Pfeiffer BE, Correspondence DJF, Foster DJ (2016) Reverse Replay of Hippocampal Place Cells Is Uniquely Modulated by Changing Reward. *Neuron* 91:1–13.
- Andersen P, Morris R, Amaral D, Bliss T, O'Keefe J (2009) *The Hippocampus Book*. Oxford University Press.
- Anderson MI, Jeffery KJ (2003) Heterogeneous modulation of place cell firing by changes in context. *J Neurosci* 23:8827–8835.
- Anikeeva P, Andalman AS, Witten I, Warden M, Goshen I, Grosenick L, Gunaydin LA, Frank LM, Deisseroth K (2012) Optetrode: a multichannel readout for optogenetic control in freely moving mice. *Nat Neurosci* 15:163–170.
- Arguello PA, Gogos JA (2006) Modeling Madness in Mice: One Piece at a Time. *Neuron* 52:179–196.
- Bäckman L, Jones S, Berger AK, Laukka EJ, Small BJ (2004) Multiple cognitive deficits during the transition to Alzheimer's disease. *J Intern Med* 256:195–204.
- Bannerman DM, Sprengel R, Sanderson DJ, McHugh SB, Rawlins JNP, Monyer H, Seeburg PH (2014) Hippocampal synaptic plasticity, spatial memory and anxiety. *Nat Rev Neurosci* 15:181–192.

- Barch DM, Ceaser A (2012) Cognition in schizophrenia: Core psychological and neural mechanisms. *Trends Cogn Sci* 16:27–34.
- Behrendt RP (2010) Contribution of hippocampal region CA3 to consciousness and schizophrenic hallucinations. *Neurosci Biobehav Rev* 34:1121–1136.
- Behrens CJ, van den Boom LP, de Hoz L, Friedman A, Heinemann U (2005) Induction of sharp wave-ripple complexes in vitro and reorganization of hippocampal networks. *Nat Neurosci* 8:1560–1567.
- Bieri KW, Bobbitt KN, Colgin LL (2014) Slow and Fast Gamma Rhythms Coordinate Different Spatial Coding Modes in Hippocampal Place Cells. *Neuron* 82:670–681.
- Bonner-Jackson A, Yodkovik N, Csernansky JG, Barch DM (2008) Episodic memory in schizophrenia: The influence of strategy use on behavior and brain activation. *Psychiatry Res - Neuroimaging* 164:1–15.
- Boone C, Davoudi H, Harrold J, Foster D (n.d.) Abnormal sleep architecture and hippocampal circuit dysfunction in mouse Fragile X model. Submitted.
- Bostock E, Muller RU, Kubie JL (1991) Experience-dependent modifications of hippocampal place cell firing. *Hippocampus* 1:193–205.
- Boyden ES, Zhang F, Bamberg E, Nagel G, Deisseroth K (2005) Millisecond-timescale, genetically targeted optical control of neural activity. *Nat Neurosci* 8:1263–1268.
- Boyer P, Phillips JL, Rousseau FL, Ilivitsky S (2007) Hippocampal abnormalities and memory deficits: New evidence of a strong pathophysiological link in schizophrenia. *Brain Res Rev* 54:92–112.
- Bragin A, Jandó G, Nádasdy Z, van Landeghem M, Buzsáki G (1995) Dentate EEG spikes and associated interneuronal population bursts in the hippocampal hilar region of the rat. *J Neurophysiol* 73:1691–1705.
- Brandon MP, Koenig J, Leutgeb JK, Leutgeb S (2014) New and Distinct

- Hippocampal Place Codes Are Generated in a New Environment during Septal Inactivation. *Neuron* 82:789–796.
- Brewin CR, Gregory JD, Lipton M, Burgess N (2010) Intrusive images in psychological disorders: characteristics, neural mechanisms, and treatment implications. *Psychol Rev* 117:210–232.
- Bristol AS, Viskontas I V. (2006) The Creating Brain: The Neuroscience of Genius. *Psychol Aesthetics, Creat Arts* 5:51–52.
- Broyd SJ, Demanuele C, Debener S, Helps SK, James CJ, Sonuga-Barke EJS (2009) Default-mode brain dysfunction in mental disorders: A systematic review. *Neurosci Biobehav Rev* 33:279–296.
- Brun VH, Leutgeb S, Wu HQ, Schwarcz R, Witter MP, Moser EI, Moser MB (2008) Impaired Spatial Representation in CA1 after Lesion of Direct Input from Entorhinal Cortex. *Neuron* 57:290–302.
- Brun VH, Otnass MK, Molden S, Steffenach H-A, Witter MP, Moser M-B, Moser EI (2002) Place cells and place recognition maintained by direct entorhinal-hippocampal circuitry. *Science* 296:2243–2246.
- Buckner RL (2010) The Role of the Hippocampus in Prediction and Imagination. *Annu Rev Psychol* 61:27–48.
- Buckner RL (2013) The brain's default network: Origins and implications for the study of psychosis. *Dialogues Clin Neurosci* 15:351–358.
- Buckner RL, Andrews-Hanna JR, Schacter DL (2008) The brain's default network: Anatomy, function, and relevance to disease. *Ann N Y Acad Sci* 1124:1–38.
- Buckner RL, Carroll DC (2007) Self-projection and the brain. *Trends Cogn Sci* 11:49–57.
- Bush D, Barry C, Burgess N (2014) What do grid cells contribute to place cell firing? *Trends Neurosci* 37:136–145.



- Buzsáki G (1984) Long-term changes of hippocampal sharp-waves following high frequency afferent activation. *Brain Res* 300:179–182.
- Buzsáki G (1986) Hippocampal sharp waves: Their origin and significance. *Brain Res* 398:242–252.
- Buzsáki G (1989) Two-stage model of memory trace formation: A role for “noisy” brain states. *Neuroscience* 31:551–570.
- Buzsáki G (2015) Hippocampal sharp wave-ripple: A cognitive biomarker for episodic memory and planning. *Hippocampus* 25:1073–1188.
- Buzsáki G, Lai-Wo S. L, Vanderwolf CH (1983) Cellular bases of hippocampal EEG in the behaving rat. *Brain Res Rev* 6:139–171.
- Buzsáki G, Moser EI (2013) Memory, navigation and theta rhythm in the hippocampal-entorhinal system. *Nat Neurosci* 16:130–138.
- Carlsson a (1977) Does dopamine play a role in schizophrenia? *Psychol Med* 7:583–597.
- Carr MF, Jadhav SP, Frank LM (2011) Hippocampal replay in the awake state: a potential substrate for memory consolidation and retrieval. *Nat Neurosci* 14:147–153.
- Carr MF, Karlsson MP, Frank LM (2012) Transient Slow Gamma Synchrony Underlies Hippocampal Memory Replay. *Neuron* 75:700–713.
- Cenquizca LA, Swanson LW (2007) Spatial organization of direct hippocampal field CA1 axonal projections to the rest of the cerebral cortex. *Brain Res Rev* 56:1–26.
- Chrobak JJ, Buzsáki G (1994) Selective activation of deep layer (V-VI) retrohippocampal cortical neurons during hippocampal sharp waves in the behaving rat. *J Neurosci* 14:6160–6170.
- Chrobak JJ, Buzsáki G (1996) High-frequency oscillations in the output networks

- of the hippocampal-entorhinal axis of the freely behaving rat. *J Neurosci* 16:3056–3066.
- Cobb SR, Buhl EH, Halasy K, Paulsen O, Somogyi P (1995) Synchronization of neuronal activity in hippocampus by individual GABAergic interneurons. *Nature* 378:75–78.
- Colgin LL, Denninger T, Fyhn M, Hafting T, Bonnevie T, Jensen O, Moser M-B, Moser EI (2009) Frequency of gamma oscillations routes flow of information in the hippocampus. *Nature* 462:353–357.
- Colgin LL, Kubota D, Jia Y, Rex CS, Lynch G (2004) Long-term potentiation is impaired in rat hippocampal slices that produce spontaneous sharp waves. *J Physiol* 558:953–961.
- Corkin S (2002) What's new with the amnesic patient H.M.? *Nat Rev Neurosci* 3:153–160.
- Csicsvari J, Hirase H, Czurkó a, Mamiya a, Buzsáki G (1999) Oscillatory coupling of hippocampal pyramidal cells and interneurons in the behaving Rat. *J Neurosci* 19:274–287.
- Csicsvari J, Hirase H, Mamiya a, Buzsáki G (2000) Ensemble patterns of hippocampal CA3-CA1 neurons during sharp wave-associated population events. *Neuron* 28:585–594.
- Danielson NB, Zaremba JD, Kaifosh P, Bowler J, Ladow M, Losonczy A (2016) Sublayer-specific coding dynamics during spatial navigation and learning in hippocampal area CA1. *Neuron* 91:1–14.
- Davidson TJ, Kloosterman F, Wilson MA (2009) Hippocampal Replay of Extended Experience. *Neuron* 63:497–507.
- Diba K, Buzsáki G (2007) Forward and reverse hippocampal place-cell sequences during ripples. *Nat Neurosci* 10:1241–1242.
- Dombeck DA, Harvey CD, Tian L, Looger LL, Tank DW (2010) Functional

imaging of hippocampal place cells at cellular resolution during virtual navigation. *Nat Neurosci* 13:1433–1440.

Dragoi G, Buzsáki G (2006) Temporal Encoding of Place Sequences by Hippocampal Cell Assemblies. *Neuron* 50:145–157.

Dragoi G, Tonegawa S (2012) Preplay of future place cell sequences by hippocampal cellular assemblies. *Nature* 469:397–401.

Dragoi G, Tonegawa S (2013) Distinct preplay of multiple novel spatial experiences in the rat. *Proc Natl Acad Sci U S A* 110:9100–9105.

Dudek SM, Alexander GM, Farris S (2016) Rediscovering area CA2: unique properties and functions. *Nat Rev Neurosci* 17:89–102.

Dudek SM, Bear MF (1992) Homosynaptic long-term depression in area CA1 of hippocampus and effects of N-methyl-D-aspartate receptor blockade. *Proc Natl Acad Sci U S A* 89:4363–4367.

Eastwood SL, Burnet PWJ, Harrison PJ (2005) Decreased hippocampal expression of the susceptibility gene PPP3CC and other calcineurin subunits in schizophrenia. *Biol Psychiatry* 57:702–710.

Ego-Stengel V, Wilson MA (2010) Disruption of ripple-associated hippocampal activity during rest impairs spatial learning in the rat. *Hippocampus* 20:1–10.

Ekstrom a D, Kahana MJ, Caplan JB, Fields T a, Isham E a, Newman EL, Fried I (2003) Cellular networks underlying human spatial navigation. *Nature* 425:184–188.

Ekstrom AD, Meltzer J, McNaughton BL, Barnes CA (2001) NMDA receptor antagonism blocks experience-dependent expansion of hippocampal “place fields.” *Neuron* 31:631–638.

Ellender TJ, Nissen W, Colgin LL, Mann EO, Paulsen O (2010) Priming of hippocampal population bursts by individual perisomatic-targeting

- interneurons. *J Neurosci* 30:5979–5991.
- Elvevåg B, Goldberg TE (2000) Cognitive impairment in schizophrenia is the core of the disorder. *Crit Rev Neurobiol* 14:1–21.
- Fatemi SH, Folsom TD (2009) The neurodevelopmental hypothesis of Schizophrenia, revisited. *Schizophr Bull* 35:528–548.
- Feng T, Silva D, Foster DJ (2015) Dissociation between the experience-dependent development of hippocampal theta sequences and single-trial phase precession. *J Neurosci* 35:4890–4902.
- Fernando ABP, Robbins TW (2011) Animal models of neuropsychiatric disorders. *Annu Rev Clin Psychol* 7:39–61.
- Foster DJ, Knierim JJ (2012) Sequence learning and the role of the hippocampus in rodent navigation. *Curr Opin Neurobiol* 22:294–300.
- Foster DJ, Wilson MA (2007) Hippocampal theta sequences. *Hippocampus* 17:1093–1099.
- Foster DJ, Wilson M a (2006) Reverse replay of behavioural sequences in hippocampal place cells during the awake state. *Nature* 440:680–683.
- Fyhn M, Hafting T, Treves A, Moser M-B, Moser EI (2007) Hippocampal remapping and grid realignment in entorhinal cortex. *Nature* 446:190–194.
- Fyhn M, Molden S, Witter MP (2004) Spatial Representation in the Entorhinal Cortex. *Science* 305:1258–1265.
- Gaffan D (1994) Scene-Specific Memory for Objects: A Model of Episodic Memory Impairment in Monkeys with Fornix Transection. *J Cogn Neurosci* 6:305–320.
- Garrity AG, Pearlson GD, McKiernan K, Lloyd D, Kiehl KA, Calhoun VD (2007) Aberrant “default mode” functional connectivity in schizophrenia. *Am J Psychiatry* 164:450–457.

- Gerber DJ, Hall D, Miyakawa T, Demars S, Gogos JA, Karayiorgou M, Tonegawa S (2003) Evidence for association of schizophrenia with genetic variation in the 8p21.3 gene, PPP3CC, encoding the calcineurin gamma subunit. *Proc Natl Acad Sci U S A* 100:8993–8998.
- Gerber DJ, Tonegawa S (2004) Psychotomimetic Effects of Drugs — A Common Pathway to Schizophrenia? *N Engl J Med* 350:1047–1048.
- Gillespie AK, Jones EA, Lin YH, Karlsson MP, Kay K, Yoon SY, Tong LM, Nova P, Carr JS, Frank LM, Huang Y (2016) Apolipoprotein E4 Causes Age-Dependent Disruption of Slow Gamma Oscillations during Hippocampal Sharp-Wave Ripples. *Neuron* 90:740–751.
- Girardeau G, Benchenane K, Wiener SI, Buzsáki G, Zugaro MB (2009) Selective suppression of hippocampal ripples impairs spatial memory. *Nat Neurosci* 12:1222–1223.
- Girardeau G, Zugaro M (2011) Hippocampal ripples and memory consolidation. *Curr Opin Neurobiol* 21:452–459.
- Gold AE, Kesner RP (2005) The role of the CA3 subregion of the dorsal hippocampus in spatial pattern completion in the rat. *Hippocampus* 15:808–814.
- Goldman-Rakic PS (1994) Working memory dysfunction in schizophrenia. *J Neuropsychiatry Clin Neurosci* 6:348–357.
- Gomperts SN, Kloosterman F, Wilson MA (2015) VTA neurons coordinate with the hippocampal reactivation of spatial experience. *Elife* 4:e05360.
- Gordon B (2013) Can we control our thoughts? Why do thoughts pop into my head as I'm trying to fall asleep? *Sci Am Mind* 24:72–72.
- Gradinaru V, Zhang F, Ramakrishnan C, Mattis J, Prakash R, Diester I, Goshen I, Thompson KR, Deisseroth K (2010) Molecular and Cellular Approaches for Diversifying and Extending Optogenetics. *Cell* 141:154–165.

- Gupta AS, van der Meer MAA, Touretzky DS, Redish AD (2010) Hippocampal Replay Is Not a Simple Function of Experience. *Neuron* 65:695–705.
- Gupta AS, van der Meer MA, Touretzky DS, Redish AD (2012) Segmentation of spatial experience by hippocampal  $\theta$  sequences. *Nat Neurosci* 15:1032–1039.
- Hafting T, Fyhn M, Molden S, Moser M, Moser EI (2005) Microstructure of a spatial map in the entorhinal cortex. *Nature* 436:801–806.
- Halassa MM, Siegle JH, Ritt JT, Ting JT, Feng G, Moore CI (2011) Selective optical drive of thalamic reticular nucleus generates thalamic bursts and cortical spindles. *Nat Neurosci* 14:1118–1120.
- Hales JB, Schlesiger MI, Leutgeb JK, Squire LR, Leutgeb S, Clark RE (2014) Medial entorhinal cortex lesions only partially disrupt hippocampal place cells and hippocampus- dependent place memory. *Cell Rep* 9:893–901.
- Harris KD, Hirase H, Leinekugel X, Henze DA, Buzsáki G (2001) Temporal interaction between single spikes and complex spike bursts in hippocampal pyramidal cells. *Neuron* 32:141–149.
- Harrison BJ, Yücel M, Pujol J, Pantelis C (2007) Task-induced deactivation of midline cortical regions in schizophrenia assessed with fMRI. *Schizophr Res* 91:82–86.
- Harvey CD, Coen P, Tank DW (2012) Choice-specific sequences in parietal cortex during a virtual-navigation decision task. *Nature* 484:62–68.
- Hassabis D, Kumaran D, Vann SD, Maguire E a (2007) Patients with hippocampal amnesia cannot imagine new experiences. *Proc Natl Acad Sci U S A* 104:1726–1731.
- Hasselmo ME (1999) Neuromodulation: Acetylcholine and memory consolidation. *Trends Cogn Sci* 3:351–359.
- Hasselmo ME (2006) The role of acetylcholine in learning and memory. *Curr Opin Neurobiol* 16:710–715.

- Hasselmo ME (2012) *How We Remember: Brain Mechanisms of Episodic Memory*. Boston: MIT press.
- Hebb DO (1949) The Organization of Behavior. *Organ Behav* 911:335.
- Heckers S (2010) Hippocampal pathology in schizophrenia. *Behav Neurobiol Schizophr Its Treat*:529–553.
- Hitti FL, Siegelbaum SA (2014) The hippocampal CA2 region is essential for social memory. *Nature* 508:88–92.
- Hofer KT, Kandrás Á, Ulbert I, Pál I, Szabó C, Héja L, Wittner L (2015) The hippocampal CA3 region can generate two distinct types of sharp wave-ripple complexes, in vitro. *Hippocampus* 25:169–186.
- Ishikawa D, Matsumoto N, Sakaguchi T, Matsuki N, Ikegaya Y (2014) Operant Conditioning of Synaptic and Spiking Activity Patterns in Single Hippocampal Neurons. *J Neurosci* 34:5044–5053.
- Ishizuka N, Weber J, Amaral DG (1990) Organization of intrahippocampal projections originating from CA3 pyramidal cells in the rat. *J Comp Neurol* 295:580–623.
- Jadhav SP, Kemere C, German PW, Frank LM (2012) Awake Hippocampal Sharp-Wave Ripples Support Spatial Memory. *Science* (80- ) 336:1454–1458.
- Jensen O, Lisman JE (1996) Hippocampal CA3 region predicts memory sequences: accounting for the phase precession of place cells. *Learn Mem* 3:279–287.
- Johnson A, Redish a D (2007) Neural ensembles in CA3 transiently encode paths forward of the animal at a decision point. *J Neurosci* 27:12176–12189.
- Jones C, Watson D, Fone K (2011) Animal models of schizophrenia. *Br J Pharmacol* 164:1162–1194.
- Jones MW, Mchugh TJ (2011) Updating hippocampal representations: CA2 joins

- the circuit. *Trends Neurosci* 34:526–535.
- Jouvet M, Michel F, Courjon J (1959) L'activité électrique du rhinencéphale au cours du sommeil chez le chat. *CRSocBiol(Paris)* 153:101–105.
- Karlsson MP, Frank LM (2009) Awake replay of remote experiences in the hippocampus. *Nat Neurosci* 12:913–918.
- Kay K, Sosa M, Chung JE, Karlsson MP, Larkin MC, Frank LM (2016) A hippocampal network for spatial coding during immobility and sleep. *Nature* 531:185–190.
- Keck T, Toyozumi T, Chen L, Doiron B, Feldman DE, Fox K, Gerstner W, Haydon PG, Hübener M, Lee H-K, Lisman JE, Rose T, Sengpiel F, Stellwagen D, Stryker MP, Turrigiano GG, van Rossum MC (2017) Integrating Hebbian and homeostatic plasticity: the current state of the field and future research directions. *Philos Trans R Soc London B Biol Sci* 372.
- Kempter R, Leibold C, Buzsáki G, Diba K, Schmidt R (2012) Quantifying circular-linear associations: Hippocampal phase precession. *J Neurosci Methods* 207:113–124.
- Kinoshita Y, Suzuki T, Ikeda M, Kitajima T, Yamanouchi Y, Inada T, Yoneda H, Iwata N, Ozaki N (2005) No association with the calcineurin a gamma subunit gene (PPP3CC) haplotype to Japanese schizophrenia. *J Neural Transm* 112:1255–1262.
- Klausberger T, Somogyi P (2008) Neuronal diversity and temporal dynamics: the unity of hippocampal circuit operations. *Science* 321:53–57.
- Knierim JJ, Neunuebel JP (2016) Tracking the flow of hippocampal computation: Pattern separation, pattern completion, and attractor dynamics. *Neurobiol Learn Mem* 129:38–49.
- Knierim JJ, Neunuebel JP, Deshmukh SS (2013) Functional correlates of the lateral and medial entorhinal cortex: objects, path integration and local–global reference frames. *Philos Trans R Soc B Biol Sci* 369.



- Koenig J, Linder AN, Leutgeb JK, Leutgeb S (2011) The Spatial Periodicity of Grid Cells Is Not Sustained During Reduced Theta Oscillations. *Science* (80- ) 332:592–595.
- Kropff E, Carmichael JE, Moser M-B, Moser EI (2015) Speed cells in the medial entorhinal cortex. *Nature* 523:419–424.
- Kvajo M, McKellar H, Gogos JA (2012) Avoiding mouse traps in schizophrenia genetics: Lessons and promises from current and emerging mouse models. *Neuroscience* 211:136–164.
- Kyogoku C, Yanagi M, Nishimura K, Sugiyama D, Morinobu A, Fukutake M, Maeda K, Shirakawa O, Kuno T, Kumagai S (2011) Association of calcineurin A gamma subunit (PPP3CC) and early growth response 3 (EGR3) gene polymorphisms with susceptibility to schizophrenia in a Japanese population. *Psychiatry Res* 185:16–19.
- Langston RF, Ainge JA, Couey JJ, Canto CB, Bjerknes TL, Witter MP, Moser EI, Moser M-B (2010) Development of the Spatial Representation System in the Rat. *Science* (80- ) 328:1576–1580.
- Lansink CS, Goltstein PM, Lankelma J V., McNaughton BL, Pennartz CMA (2009) Hippocampus leads ventral striatum in replay of place-reward information. *PLoS Biol* 7.
- Leavitt VM, Goldberg TE (2009) Episodic memory in schizophrenia. *Neuropsychol Rev* 19:312–323.
- Lee AK, Wilson MA (2002) Memory of sequential experience in the hippocampus during slow wave sleep. *Neuron* 36:1183–1194.
- Lee MG, Chrobak JJ, Sik A, Wiley RG, Buzsáki G (1994) Hippocampal theta activity following selective lesion of the septal cholinergic system. *Neuroscience* 62:1033–1047.
- Leutgeb JK, Leutgeb S, Moser M, Moser EI, Moser I (2007) Pattern Separation in the Dentate Gyrus and CA3 of the Hippocampus. *Science* (80- ) 315:961–966.

- Leutgeb JK, Leutgeb S, Treves A, Meyer R, Barnes CA, McNaughton BL, Moser MB, Moser EI (2005a) Progressive transformation of hippocampal neuronal representations in “morphed” environments. *Neuron* 48:345–348.
- Leutgeb S, Leutgeb JK (2007) Pattern separation, pattern completion, and new neuronal codes within a continuous CA3 map. *Learn Mem* 14:745–757.
- Leutgeb S, Leutgeb JK, Barnes CA, Moser EI, McNaughton BL, Moser M-B (2005b) Independent codes for spatial and episodic memory in hippocampal neuronal ensembles. *Science* 309:619–623.
- Leutgeb S, Leutgeb JK, Moser EI, Moser MB (2006) Fast rate coding in hippocampal CA3 cell ensembles. *Hippocampus* 16:765–774.
- Li W, Ghose S, Gleason K, Begovic A, Perez J, Bartko J, Russo S, Wagner AD, Selemon L, Tamminga CA (2015) Synaptic proteins in the hippocampus indicative of increased neuronal activity in CA3 in schizophrenia. *Am J Psychiatry* 172:373–382.
- Li XG, Somogyi P, Ylinen A, Buzsaki G (1994) The hippocampal CA3 network: An in vivo intracellular labeling study. *J Comp Neurol* 339:181–208.
- Lisman JE, Talamini LM, Raffone A (2005) Recall of memory sequences by interaction of the dentate and CA3: A revised model of the phase precession. *Neural Networks* 18:1191–1201.
- Liu CH, Coleman JE, Davoudi H, Zhang K, Hussaina Shuler MG (2015) Selective Activation of a Putative Reinforcement Signal Conditions Cued Interval Timing in Primary Visual Cortex. *Curr Biol* 25:1551–1561.
- Liu X, Ramirez S, Pang PT, Puryear CB, Govindarajan A, Deisseroth K, Tonegawa S (2012) Optogenetic stimulation of a hippocampal engram activates fear memory recall. *Nature* 484:381–385.
- Liu YL, Fann CSJ, Liu CM, Chang CC, Yang WC, Hung SI, Yu SL, Hwang TJ, Hsieh MH, Liu CC, Tsuang MM, Wu JY, Jou YS, Faraone S V, Tsuang MT, Chen WJ, Hwu H-G (2007) More evidence supports the association of

PPP3CC with schizophrenia. *Mol Psychiatry* 12:966–974.

Logothetis NK, Eschenko O, Murayama Y, Augath M, Steudel T, Evrard HC, Besserve M, Oeltermann A (2012) Hippocampal-cortical interaction during periods of subcortical silence. *Nature* 491:547–553.

Louie K, Wilson MA (2001) Temporally structured replay of awake hippocampal ensemble activity during rapid eye movement sleep. *Neuron* 29:145–156.

Lu L, Leutgeb JK, Tsao A, Henriksen EJ, Leutgeb S, Barnes C a, Witter MP, Moser M-B, Moser EI (2013) Impaired hippocampal rate coding after lesions of the lateral entorhinal cortex. *Nat Neurosci* 16:1085–1093.

MacDonald CJ, Lepage KQ, Eden UT, Eichenbaum H (2011) Hippocampal “time cells” bridge the gap in memory for discontinuous events. *Neuron* 71:737–749.

Malenka RC, Bear MF (2004) LTP and LTD: An embarrassment of riches. *Neuron* 44:5–21.

Malvache A, Reichinnek S, Villette V, Haimerl C, Cossart R (2016) Awake hippocampal reactivations project onto orthogonal neuronal assemblies. *Science* (80- ) 353.

Marr D (1971) Simple Memory: A Theory for Archicortex. *Source Philos Trans R Soc London Ser B, Biol Sci* 262:23–81.

Matsumura N, Nishijo H, Tamura R, Eifuku S, Endo S, Ono T (1999) Spatial- and Task-Dependent Neuronal Responses during Real and Virtual Translocation in the Monkey Hippocampal Formation. *J Neurosci* 19:2381–2393.

McCullumsmith RE (2015) Evidence for Schizophrenia as a Disorder of Neuroplasticity. *Am J Psychiatry* 172:312–313.

McHugh TJ, Blum KI, Tsien JZ, Tonegawa S, Wilson A (1996a) Impaired hippocampal representation of space in CA1-Specific NMDAR1 Knockout Mice. *Cell* 87:1339–1349.

- McHugh TJ, Blum KI, Tsien JZ, Tonegawa S, Wilson MA (1996b) Impaired hippocampal representation of space in CA1-specific NMDAR1 knockout mice. *Cell* 87:1339–1349.
- McHugh TJ, Jones MW, Quinn JJ, Balthasar N, Coppari R, Elmquist JK, Lowell BB, Fanselow MS, Wilson MA, Tonegawa S (2007) Dentate gyrus NMDA receptors mediate rapid pattern separation in the hippocampal network. *Science* 317:94–99.
- McNaughton BL, Barnes CA, Meltzer J, Sutherland RJ (1989) Hippocampal granule cells are necessary for normal spatial learning but not for spatially-selective pyramidal cell discharge. *Exp Brain Res* 76:485–496.
- Mehta MR, Barnes C a, McNaughton BL (1997) Experience-dependent, asymmetric expansion of hippocampal place fields. *Proc Natl Acad Sci U S A* 94:8918–8921.
- Mehta MR, Lee a K, Wilson M a (2002) Role of experience and oscillations in transforming a rate code into a temporal code. *Nature* 417:741–746.
- Mesholam-Gately RI, Giuliano AJ, Goff KP, Faraone S V., Seidman LJ (2009) Neurocognition in first-episode schizophrenia: A meta-analytic review. *Neuropsychology* 23:315–336.
- Miao C, Cao Q, Ito HT, Yamahachi H, Witter MP, Moser MB, Moser EI (2015) Hippocampal Remapping after Partial Inactivation of the Medial Entorhinal Cortex. *Neuron* 88:590–603.
- Middleton SJ, McHugh TJ (2016) Silencing CA3 disrupts temporal coding in the CA1 ensemble. *Nat Neurosci* 19:945–951.
- Miller VM, Best PJ (1980) Spatial correlates of hippocampal unit activity are altered by lesions of the fornix and entorhinal cortex. *Brain Res* 194:311–323.
- Miyakawa T, Leiter LM, Gerber DJ, Gainetdinov RR, Sotnikova TD, Zeng H, Caron MG, Tonegawa S (2003) Conditional calcineurin knockout mice exhibit multiple abnormal behaviors related to schizophrenia. *Proc Natl*

Acad Sci U S A 100:8987–8992.

- Mizumori SJ, McNaughton BL, Barnes CA, Fox KB (1989) Preserved spatial coding in hippocampal CA1 pyramidal cells during reversible suppression of CA3c output: evidence for pattern completion in hippocampus. *J Neurosci* 9:3915–3928.
- Mizuseki K, Royer S, Diba K, Buzsáki G (2012) Activity dynamics and behavioral correlates of CA3 and CA1 hippocampal pyramidal neurons. *Hippocampus* 22:1659–1680.
- Mizuseki K, Sirota A, Pastalkova E, Buzsáki G (2009) Theta Oscillations Provide Temporal Windows for Local Circuit Computation in the Entorhinal-Hippocampal Loop. *Neuron* 64:267–280.
- Morris RG, Garrud P, Rawlins JN, O'Keefe J (1982) Place navigation impaired in rats with hippocampal lesions. *Nature* 297:681–683.
- Moser EI, Kropff E, Moser M-B (2008) Place cells, grid cells, and the brain's spatial representation system. *Annu Rev Neurosci* 31:69–89.
- Moser EI, Moser MB, Andersen P (1993) Spatial learning impairment parallels the magnitude of dorsal hippocampal lesions, but is hardly present following ventral lesions. *J Neurosci* 13:3916–3925.
- Muller RU, Kubie JL (1987) The effects of changes in the environment on the spatial firing of hippocampal complex-spike cells. *J Neurosci* 7:1951–1968.
- Muller RU, Kubie JL, Muller RU (1989) The firing of hippocampal place cells predicts the future position of freely moving rats. *J Neurosci* 9:4101–4110.
- Murata M, Tsunoda M, Sumiyoshi T, Sumiyoshi C, Matsuoka T, Suzuki M, Ito M, Kurachi M (2008) Calcineurin A gamma and B gene expressions in the whole blood in Japanese patients with schizophrenia. *Prog Neuro-Psychopharmacology Biol Psychiatry* 32:1000–1004.
- Nádasy Z, Hirase H, Czurkó A, Csicsvari J, Buzsáki G (1999) Replay and time

- compression of recurring spike sequences in the hippocampus. *J Neurosci* 19:9497–9507.
- Nakashiba T, Buhl DL, McHugh TJ, Tonegawa S (2009) Hippocampal CA3 Output Is Crucial for Ripple-Associated Reactivation and Consolidation of Memory. *Neuron* 62:781–787.
- Nakashiba T, Young JZ, McHugh TJ, Derek L. Buhl, Tonegawa S (2008) Transgenic Inhibition of Synaptic Transmission Reveals Role of CA3 Output in Hippocampal Learning. *Science* (80- ) 1260:1260–1264.
- Nakazawa K, McHugh TJ, Wilson MA, Tonegawa S (2004) NMDA receptors, place cells and hippocampal spatial memory. *Nat Rev Neurosci* 5:361–372.
- Nakazawa K, Quirk, M.C., Chitwood RA, Watanabe M, Yeckel MF, Sun LD, Kato A, Carr CA, Johnstone D, Wilson MA, Tonegawa S (2002) Requirement for Hippocampal CA3 NMDA Receptors in Associative Memory Recall. *Science* 297:211–218.
- Nakazawa K, Sun LD, Quirk MC, Rondi-Reig L, Wilson MA, Tonegawa S (2003) Hippocampal CA3 NMDA receptors are crucial for memory acquisition of one-time experience. *Neuron* 38:305–315.
- Nestler EJ, Hyman SE (2010) Animal models of neuropsychiatric disorders. *Nat Neurosci* 13:1161–1169.
- Nestor PG, Kubicki M, Kuroki N, Gurrera RJ, Niznikiewicz M, Shenton ME, McCarley RW (2007) Episodic memory and neuroimaging of hippocampus and fornix in chronic schizophrenia. *Psychiatry Res - Neuroimaging* 155:21–28.
- Nicole O, Hadzibegovic S, Gajda J, Bontempi B, Bem T, Meyrand P (2016) Soluble amyloid beta oligomers block the learning-induced increase in hippocampal sharp wave-ripple rate and impair spatial memory formation. *Sci Rep* 6:22728.
- Norimoto H, Matsumoto N, Miyawaki T, Matsuki N, Ikegaya Y (2013) Subicular

- activation preceding hippocampal ripples in vitro. *Sci Rep* 3:2696.
- O'Keefe J (1976) Place units in the hippocampus of the freely moving rat. *Exp Neurol* 51:78–109.
- O'Keefe J, Dostrovsky J (1971) The hippocampus as a spatial map. Preliminary evidence from unit activity in the freely-moving rat.
- O'Keefe J, Nadel L (1978) *The hippocampus as a cognitive map*. Oxford Univ Press.
- O'Keefe J, Recce ML (1993) Phase relationship between hippocampal place units and the EEG theta rhythm. *Hippocampus* 3:317–330.
- Oliva A, Fernández-Ruiz A, Buzsáki G, Berényi A (2016) Role of Hippocampal CA2 Region in Triggering Sharp-Wave Ripples. *Neuron* 91:1–14.
- Olney JW, Farber NB (1995) Glutamate receptor dysfunction and schizophrenia. *Arch Gen Psychiatry* 52:998–1007.
- Olton DS, Samuelson RJ (1976) Remembrance of places passed: Spatial memory in rats. *J Exp Psychol Anim Behav Process* 2:97–116.
- Ormond J, McNaughton BL (2015) Place field expansion after focal MEC inactivations is consistent with loss of Fourier components and path integrator gain reduction. *Proc Natl Acad Sci U S A* 112:4116–4121.
- Papatheodoropoulos C (2010) Patterned activation of hippocampal network (~10 Hz) during in vitro sharp wave-ripples. *Neuroscience* 168:429–442.
- Pastalkova E, Itskov V, Amarasingham A, Buzsaki G (2008) Internally Generated Cell Assembly Sequences in the Rat Hippocampus. *Science* (80- ) 321:1322–1327.
- Paul EW, Harrison J (2004) The hippocampus in schizophrenia: a review of the neuropathological evidence and its pathophysiological implications. *Psychopharmacology (Berl)* 174:151–162.

- Paxinos G, Watson C (2007) *The Rat Brain in Stereotaxic Coordinates* Sixth Edition.
- Pennartz CM a, Lee E, Verheul J, Lipa P, Barnes CA, McNaughton BL (2004) The Ventral Striatum in Off-Line Processing: Ensemble Reactivation during Sleep and Modulation by Hippocampal Ripples. *J Neurosci* 24:6446–6456.
- Pfeiffer BE, Foster DJ (2013) Hippocampal place-cell sequences depict future paths to remembered goals. *Nature* 497:1–8.
- Pfeiffer BE, Foster DJ (2015) Autoassociative dynamics in the generation of sequences of hippocampal place cells. *Science* 349:180–183.
- Pfeiffer T, Draguhn A, Reichinnek S, Both M (2014) Optimized temporally deconvolved Ca<sup>2+</sup> imaging allows identification of spatiotemporal activity patterns of CA1 hippocampal ensembles. *Neuroimage* 94:239–249.
- Phillips KG, Bartsch U, McCarthy AP, Edgar DM, Tricklebank MD, Wafford KA, Jones MW (2012) Decoupling of Sleep-Dependent Cortical and Hippocampal Interactions in a Neurodevelopmental Model of Schizophrenia. *Neuron* 76:526–533.
- Piguet C, Dayer A, Kosel M, Desseilles M, Vuilleumier P, Bertschy G (2010) Phenomenology of racing and crowded thoughts in mood disorders: A theoretical reappraisal. *J Affect Disord* 121:189–198.
- Pothuizen HHJ, Zhang WN, Jongen-Rêlo AL, Feldon J, Yee BK (2004) Dissociation of function between the dorsal and the ventral hippocampus in spatial learning abilities of the rat: A within-subject, within-task comparison of reference and working spatial memory. *Eur J Neurosci* 19:705–712.
- Quirk MC, Wilson MA (1999) Interaction between spike waveform classification and temporal sequence detection. In: *Journal of Neuroscience Methods*, pp 41–52.
- Raichle ME, MacLeod AM, Snyder AZ, Powers WJ, Gusnard DA, Shulman GL (2001) A default mode of brain function. *Proc Natl Acad Sci U S A* 98:676–



682.

Ramirez S, Liu X, Lin P-A, Suh J, Pignatelli M, Redondo RL, Ryan TJ, Tonegawa S (2013) Creating a false memory in the hippocampus. *Sci (New York, NY)* 341:387–391.

Redish AD, Battaglia FP, Chawla MK, Ekstrom AD, Gerrard JL, Lipa P, Rosenzweig ES, Worley PF, Guzowski JF, McNaughton BL, Barnes C a (2001) Independence of firing correlates of anatomically proximate hippocampal pyramidal cells. *J Neurosci* 21:RC134.

Remondes M, Schuman EM (2004) Role for a cortical input to hippocampal area CA1 in the consolidation of a long-term memory. *Nature* 431:699–703.

Rickgauer JP, Deisseroth K, Tank DW (2014) Simultaneous cellular-resolution optical perturbation and imaging of place cell firing fields. *Nat Neurosci* 17:1816–1824.

Robbe D, Montgomery SM, Thome A, Rueda-Orozco PE, McNaughton BL, Buzsaki G (2006) Cannabinoids reveal importance of spike timing coordination in hippocampal function. *Nat Neurosci* 9:1526–1533.

Rubin DC, Schrauf RW, Greenberg DL (2003) Belief and recollection of autobiographical memories. *Mem Cognit* 31:887–901.

Rueckemann JW, Dimauro AJ, Rangel LM, Han X, Boyden ES, Eichenbaum H (2016) Transient optogenetic inactivation of the medial entorhinal cortex biases the active population of hippocampal neurons. *Hippocampus* 26:246–260.

Rugg MD, Vilberg KL (2012) Brain networks underlying episodic memory retrieval. *Curr Opin Neurobiol* 23.

Sanders AR et al. (2008) No Significant Association of 14 Candidate Genes With Schizophrenia in a Large European Ancestry Sample: Implications for Psychiatric Genetics. *Am J Psychiatry* 165:497–506.

- Sargolini F, Fyhn M, Hafting T, McNaughton BL, Witter MP, Moser M-B, Moser EI (2006) Conjunctive Representation of Position, Direction, and Velocity in Entorhinal Cortex. *Science* (80- ) 312:758–763.
- Schacter DL (1996) *Searching for memory: the brain, the mind, and the past*. New York: Basic Books.
- Schlesiger MI, Cannova CC, Boubilil BL, Hales JB, Mankin EA, Brandon MP, Leutgeb JK, Leibold C, Leutgeb S (2015) The medial entorhinal cortex is necessary for temporal organization of hippocampal neuronal activity. *Nat Neurosci* 18:1123–1132.
- Schlingloff D, Kali S, Freund TF, Hajos N, Gulyas AI (2014) Mechanisms of Sharp Wave Initiation and Ripple Generation. *J Neurosci* 34:11385–11398.
- Schmitzer-Torbert N, Jackson J, Henze D, Harris K, Redish AD (2005) Quantitative measures of cluster quality for use in extracellular recordings. *Neuroscience* 131:1–11.
- Scoville WB, Milner B (1957) Loss of Recent Memory After Bilateral Hippocampal Lesions. *J Neurol Neurosurg Psychiatry* 20:11–21.
- Sheffield MEJ, Dombeck DA (2015) Calcium transient prevalence across the dendritic arbour predicts place field properties. *Nature* 517:200–204.
- Siapas AG, Wilson MA (1998) Coordinated interactions between hippocampal ripples and cortical spindles during slow-wave sleep. *Neuron* 21:1123–1128.
- Siegle JH, Carlen M, Meletis K, Tsai LH, Moore CI, Ritt J (2011) Chronically implanted hyperdrive for cortical recording and optogenetic control in behaving mice. *Proc Annu Int Conf IEEE Eng Med Biol Soc EMBS*:7529–7532.
- Sigurdsson T (2016) Neural circuit dysfunction in schizophrenia: Insights from animal models. *Neuroscience* 321:42–65.
- Sigurdsson T, Stark KL, Karayiorgou M, Gogos JA, Gordon JA (2010) Impaired

- hippocampal–prefrontal synchrony in a genetic mouse model of schizophrenia. *Nature* 464:763–767.
- Silva D, Feng T, Foster DJ (2015) Trajectory events across hippocampal place cells require previous experience. *Nat Neurosci* 18:1772–1779.
- Skaggs WE, McNaughton BL, Wilson MA, Barnes CA (1996) Theta phase precession in hippocampal neuronal populations and the compression of temporal sequences. *Hippocampus* 6:149–172.
- Small SA, Schobel SA, Buxton RB, Witter MP, Barnes CA (2011) A pathophysiological framework of hippocampal dysfunction in ageing and disease. *Nat Rev Neurosci* 12:585–601.
- Smith SL, Häusser M (2010) Parallel processing of visual space by neighboring neurons in mouse visual cortex. *Nat Neurosci* 13:1144–1149.
- Solstad T, Solstad T, Boccara CN, Boccara CN, Kropff E, Kropff E, Moser M-B, Moser M-B, Moser EI, Moser EI (2008) Representation of geometric borders in the entorhinal cortex. *Science* (80- ) 322:1865–1868.
- Song J, Sun J, Moss J, Wen Z, Sun GJ, Hsu D, Zhong C, Davoudi H, Christian KM, Toni N, Ming G-L, Song H (2013) Parvalbumin interneurons mediate neuronal circuitry-neurogenesis coupling in the adult hippocampus. *Nat Neurosci* 16:1728–1730.
- Squire LR, Zola-Morgan M (2011) The cognitive neuroscience of human memory since H.M. *Annu Rev Neurosci* 34:259–288.
- Stark E, Eichler R, Roux L, Fujisawa S, Rotstein HG, Buzsáki G (2013) Inhibition-Induced theta resonance in cortical circuits. *Neuron* 80:1263–1276.
- Stark E, Roux L, Eichler R, Buzsáki G (2015) Local generation of multineuronal spike sequences in the hippocampal CA1 region. *Proc Natl Acad Sci U S A* 112:10521–10526.
- Stark E, Roux L, Eichler R, Senzai Y, Royer S, Buzsáki G (2014) Pyramidal cell-

- interneuron interactions underlie hippocampal ripple oscillations. *Neuron* 83:467–480.
- Steele RJ, Morris RGM (1999) Delay-dependent impairment of a matching-to-place task with chronic and intrahippocampal infusion of the NMDA-antagonist D-AP5. *Hippocampus* 9:118–136.
- Strange B a, Witter MP, Lein ES, Moser EI (2014) Functional organization of the hippocampal longitudinal axis. *Nat Rev Neurosci* 15:655–669.
- Stujenske JM, Spellman T, Gordon JA (2015) Modeling the Spatiotemporal Dynamics of Light and Heat Propagation for In Vivo Optogenetics. *Cell Rep* 12:525–534.
- Suh J, Foster DJ, Davoudi H, Wilson MA, Tonegawa S (2013) Impaired Hippocampal Ripple-Associated Replay in a Mouse Model of Schizophrenia. *Neuron* 80:484–493.
- Suh J, Rivest AJ, Nakashiba T, Tominaga T, Tonegawa S (2011) Entorhinal cortex layer III input to the hippocampus is crucial for temporal association memory. *Science* (80- ) 334:1415–1420.
- Sullivan D, Csicsvari J, Mizuseki K, Montgomery S, Diba K, Buzsáki G (2011) Relationships between hippocampal sharp waves, ripples, and fast gamma oscillation: influence of dentate and entorhinal cortical activity. *J Neurosci* 31:8605–8616.
- Suzuki SS, Smith GK (1988a) Spontaneous EEG spikes in the normal hippocampus. IV. Effects of medial septum and entorhinal cortex lesions. *Electroencephalogr Clin Neurophysiol* 70:73–83.
- Suzuki SS, Smith GK (1988b) Spontaneous EEG spikes in the normal hippocampus II. Relations to synchronous burst discharges. *Electroencephalogr Clin Neurophysiol* 69:532–540.
- Tammaing CA, Southcott S, Sacco C, Wagner AD, Ghose S (2012) Glutamate dysfunction in hippocampus: Relevance of dentate gyrus and CA3 signaling.

- Schizophr Bull 38:927–935.
- Thomas SA (2015) Neuromodulatory signaling in hippocampus-dependent memory retrieval. *Hippocampus* 25:415–431.
- Thomson AM, Radpour S (1991) Excitatory Connections Between CA1 Pyramidal Cells Revealed by Spike Triggered Averaging in Slices of Rat Hippocampus are Partially NMDA Receptor Mediated. *Eur J Neurosci* 3:587–601.
- Tolman EC (1948) Cognitive maps in rats and men. *Psychol Rev* 55:189–208.
- Toulopoulou T, Rabe-Hesketh S, King H, Murray RM, Morris RG (2003) Episodic memory in schizophrenic patients and their relatives. *Schizophr Res* 63:261–271.
- Traub RD, Wong RKS (1982) Cellular mechanism of neuronal synchronization in epilepsy. *Science* (80- ) 216:745–747.
- Tulving E (1972) Episodic and semantic memory. In: *Organization and Memory*, pp 382–402.
- Turrigiano GG (2017) The dialectic of Hebb and homeostasis. *Philos Trans R Soc London B Biol Sci* 372.
- Turrigiano GG, Leslie KR, Desai NS, Rutherford LC, Nelson SB (1998) Activity-dependent scaling of quantal amplitude in neocortical neurons. *Nature* 391:892–896.
- Tye KM, Deisseroth K (2012) Optogenetic investigation of neural circuits underlying brain disease in animal models. *Nat Rev Neurosci* 13:251–266.
- Van Cauter T, Camon J, Alvernhe A, Elduayen C, Sargolini F, Save E (2013) Distinct roles of medial and lateral entorhinal cortex in spatial cognition. *Cereb Cortex* 23:451–459.
- Van Cauter T, Poucet B, Save E (2008) Unstable CA1 place cell representation in rats with entorhinal cortex lesions. *Eur J Neurosci* 27:1933–1946.

- van Strien NM, Cappaert NLM, Witter MP (2009) The anatomy of memory: an interactive overview of the parahippocampal–hippocampal network. *Nat Rev Neurosci* 10:272–282.
- Vandecasteele M, Varga V, Berényi A, Papp E, Barthó P, Venance L, Freund TF, Buzsáki G (2014) Optogenetic activation of septal cholinergic neurons suppresses sharp wave ripples and enhances theta oscillations in the hippocampus. *Proc Natl Acad Sci U S A* 111:13535–13540.
- Vanderwolf CH (1969) Hippocampal electrical activity and voluntary movement in the rat. *Electroencephalogr Clin Neurophysiol* 26:407–418.
- Varga C, Golshani P, Soltesz I (2012) Frequency-invariant temporal ordering of interneuronal discharges during hippocampal oscillations in awake mice. *Proc Natl Acad Sci U S A* 109:E2726–34.
- Villette V, Malvache A, Tressard T, Dupuy N, Cossart R (2015) Internally Recurring Hippocampal Sequences as a Population Template of Spatiotemporal Information. *Neuron* 88:357–366.
- Vladimirov N, Tu Y, Traub RD (2013) Synaptic gating at axonal branches, and sharp-wave ripples with replay: A simulation study. *Eur J Neurosci* 38:3435–3447.
- Vogels TP, Sprekeler H, Zenke F, Clopath C, Gerstner W (2011) Inhibitory plasticity balances excitation and inhibition in sensory pathways and memory networks. *Science* 334:1569–1573.
- Voigts J, Siegle JH, Pritchett DL, Moore CI (2013) The flexDrive: an ultra-light implant for optical control and highly parallel chronic recording of neuronal ensembles in freely moving mice. *Front Syst Neurosci* 7:8.
- Wada A, Kunii Y, Ikemoto K, Yang Q, Hino M, Matsumoto J, Niwa S ichi (2012) Increased ratio of calcineurin immunoreactive neurons in the caudate nucleus of patients with schizophrenia. *Prog Neuro-Psychopharmacology Biol Psychiatry* 37:8–14.

- Wada A, Kunii Y, Matsumoto J, Hino M, Yang Q, Niwa S ichi, Yabe H (2017) Prominent increased calcineurin immunoreactivity in the superior temporal gyrus in schizophrenia: A postmortem study. *Psychiatry Res* 247:79–83.
- Wang Y, Romani S, Lustig B, Leonardo A, Pastalkova E (2014) Theta sequences are essential for internally generated hippocampal firing fields. *Nat Neurosci* 18:282–288.
- Wang D V, Yau H-J, Broker CJ, Tsou J-H, Bonci A, Ikemoto S (2015) Mesopontine median raphe regulates hippocampal ripple oscillation and memory consolidation. *Nat Neurosci* 18:728–735.
- Weinberger DR (1999) Cell biology of the hippocampal formation in schizophrenia. *Biol Psychiatry* 45:395–402.
- Wills TJ, Cacucci F, Burgess N, O'Keefe J (2010) Development of the hippocampal cognitive map in preweanling rats. *Science* (80- ) 328:1573–1576.
- Wilson M a, McNaughton BL (1994) Reactivation of Hippocampal Ensemble Memories During Sleep. *Science* (80- ) 265:676–679.
- Wilson MA, McNaughton BL (1993) Dynamics of the hippocampal ensemble code for space. *Science* (80- ) 261:1055–1058.
- Wittner L, Henze DA, Záborszky L, Buzsáki G (2007) Three-dimensional reconstruction of the axon arbor of a CA3 pyramidal cell recorded and filled in vivo. *Brain Struct Funct* 212:75–83.
- Witton J, Staniaszek LE, Bartsch U, Randall AD, Jones MW, Brown JT (2014) Disrupted hippocampal sharp-wave ripple-associated spike dynamics in a transgenic mouse model of dementia. *J Physiol* 0:1–16.
- XI Z, YU L, SHI Y, WEI Q, ZHENG Y, ZHANG J, HE G, YAO W, ZHANG K, GU N, Gu N, Feng G, Zhu S (2007) No association between PPP3CC and schizophrenia in the Chinese population. *Schizophr Res* 90:357–359.
- Yamada K, Gerber DJ, Iwayama Y, Ohnishi T, Ohba H, Toyota T, Aruga J,

- Minabe Y, Tonegawa S, Yoshikawa T (2007) Genetic analysis of the calcineurin pathway identifies members of the EGR gene family, specifically EGR3, as potential susceptibility candidates in schizophrenia. *Proc Natl Acad Sci* 104:2815–2820.
- Yizhar O, Fenno LE, Davidson TJ, Mogri M, Deisseroth K (2011) Optogenetics in Neural Systems. *Neuron* 71:9–34.
- Ylinen A, Bragin A, Nádasdy Z, Jandó G, Szabó I, Sik A, Buzsáki G (1995) Sharp wave-associated high-frequency oscillation (200 Hz) in the intact hippocampus: network and intracellular mechanisms. *J Neurosci* 15:30–46.
- Zeng H, Chattarji S, Barbarosie M, Rondi-Reig L, Philpot BD, Miyakawa T, Bear MF, Tonegawa S (2001) Forebrain-specific calcineurin knockout selectively impairs bidirectional synaptic plasticity and working/episodic-like memory. *Cell* 107:617–629.
- Zhang S-J, Ye J, Miao C, Tsao A, Cerniauskas I, Ledergerber D, Moser MB, Moser EI (2013) Optogenetic Dissection of Entorhinal-Hippocampal Functional Connectivity. *Science* (80- ) 340:1232627–1232627.
- Zheng C, Bieri KW, Hsiao YT, Colgin LL (2016) Spatial Sequence Coding Differs during Slow and Fast Gamma Rhythms in the Hippocampus. *Neuron* 89:398–408.
- Zhou Y, Liang M, Tian L, Wang K, Hao Y, Liu H, Liu Z, Jiang T (2007) Functional disintegration in paranoid schizophrenia using resting-state fMRI. *Schizophr Res* 97:194–205.
- Ziv Y, Burns LD, Cocker ED, Hamel EO, Ghosh KK, Kitch LJ, Gamal A El, Schnitzer MJ (2013) Long-term dynamics of CA1 hippocampal place codes. *Nat Neurosci* 16:264–266.



# Curriculum Vitae

Heydar Davoudi

March 6, 2017

## Education

Ph.D. 2017 Biomedical Engineering Johns Hopkins School of Medicine

Mentor: David J. Foster, Ph.D.

M.S. 2009 Electrical Engineering Sharif University of Technology

B.S. 2006 Electrical Engineering Iran University of Science and Technology

## Research Experience

Feb 2011– May 2011 Lab of Hongjun Song, Institute for Cell Engineering, Johns Hopkins School of Medicine

Oct 2010- Jan 2011 Lab of Xiaoqin Wang, Department of Biomedical Engineering, Johns Hopkins School of Medicine

Jul 2010- Oct 2010 Lab of Charles Della Santina, Departments of Otolaryngology, Johns Hopkins School of Medicine

Jan 2010- Jun 2010 Lab of Eugene Goldfield, Wyss Institute, Harvard Medical School

## Awards

Dec 2015 Best poster award Society for Neuroscience- Maryland chapter

## Publications

### Journal Papers

**Davoudi H** and Foster DJ, Hippocampal area CA3 is necessary for the formation of sharp-wave ripples and expression of place fields in area CA1, *submitted*.

Boone CE, **Davoudi H**, Harrold JO, Foster DJ, Abnormal sleep architecture and hippocampal circuit dysfunction in mouse Fragile X model, *submitted*.

Liu CH, Coleman JE, **Davoudi H**, Zhang K, and Shuler MGH, (2015) Selective activation of a putative reinforcement signal conditions cued interval timing in primary visual cortex. *Current Biology* 25:12, 1551–1561.

Song J, Wen Z, Moss J, Hsu D, Zhong C, Sun J, Sun G, **Davoudi H**, Christian K, Toni N, Ming GL, Song H. (2013) Parvalbumin interneuron-mediated neuronal circuitry-neurogenesis coupling in the adult hippocampus. *Nature Neuroscience* 16, 1728–1730.

Suh J, Foster DJ, **Davoudi H**, Wilson M, and Tonegawa S. (2013) Impaired Hippocampal Ripple-Associated Replay in a Mouse Model of Schizophrenia. *Neuron* 80, 484- 493.

### **Conference Papers and Abstracts**

**Davoudi H** and Foster DJ (2015) Hippocampal area CA3 is necessary for the induction of sharp-wave ripples in area CA1, Society for Neuroscience (SfN) Conference, Chicago, IL, 2015.

**Davoudi H** and Foster DJ (2016) Hippocampal area CA3 is necessary for the induction of sharp-wave ripples in area CA1, 2nd Annual Johns Hopkins Sleep & Circadian Research Day, Baltimore, MD, August, 2016.

Suh J, Foster DJ, **Davoudi H**, Wilson M, and Tonegawa S (2012) Selective impairment of hippocampal sharp wave ripple and memory reactivation in a mouse model of schizophrenia, Society for Neuroscience (SfN) Conference, New Orleans, 2012.

Liu CH, Coleman JE, **Davoudi H**, Bear MF, Zhang K, and Shuler MGH (2012) Conditioned interval timing in V1 neurons by optogenetically hijacking basal forebrain inputs, Society for Neuroscience (SfN) Conference, New Orleans, 2012.

**Davoudi H**, Taalimi A, Fatemizadeh E (2009) Extracting activated regions of fMRI data using unsupervised learning, The International Joint Conference on Neural Networks (IJCNN), Pages 641-645, Atlanta, USA, June 2009.

**Davoudi H, Vosoughi-Vahdat B (2009)** A biologically plausible learning method for neuro-robotic systems, The 4th International IEEE EMBS Conference on Neural Engineering (EMBS NER), Pages 128-132, Antalia, Turkey, April 2009.

Bayati H, **Davoudi H**, Fatemizadeh E (2008) A heuristic method for finding the optimal number of clusters with application in medical data, The 30th IEEE Conference on Engineering in Medicine and Biology Society (IEEE EMBC), Pages 4684-4687, Vancouver, Canada, August 2008.

**Davoudi H, Oraizi H (2007)** A novel quad-band antenna for vehicular application, The 15th Iranian Conference on Electrical Engineering (ICEE), Tehran, Iran, May 2007.

### **Dissertations**

**Davoudi H (2017)** On the origin of hippocampal ensemble activity: neural mechanisms for sharp-wave ripples and place cell responses. Ph.D. dissertation, Johns Hopkins University.

**Davoudi H (2009)** A statistical learning method inspired by the human motor learning. M.S. thesis, Sharif University of Technology.

**Davoudi H (2006)** Design, analysis, and fabrication of a quad-band vehicular antenna. B.S. thesis, Iran University of Science and Technology.

### **Service and Leadership Experience**

#### **Teaching Assistantship**

Fall 2015	Cell physiology	First-year course for medical students, School of Medicine
Spring 2014	Systems bioengineering II lab	Undergraduate/graduate course, Department of Biomedical Engineering
Fall 2012	Models of the neuron	Graduate course, Department of Biomedical Engineering

#### **Leadership**

Spring 2015- Winter      Managing eight JHU undergraduate students and one

- 2015 high school student toward their required research credits.
- Spring 2013- Spring 2015 Representative of School of Medicine in the Student Representative Committee of Johns Hopkins Student Assistance Program (JHSAP)
- Spring 2013 Co-organizing Persian New Year celebration with Biomedical Engineering PhD Council.